Calhoun: The NPS Institutional Archive
DSpace Repository

Theses and Dissertations 1. Thesis and Dissertation Collection, all items

1970

Energy loss of high energy electrons in tin, lead, and gadolinium

Mosbrooker, Michael Lee; Sandquist, David Lee

Monterey, California ; Naval Postgraduate School

http://hdl.handle.net/10945/14987

Downloaded from NPS Archive: Calhoun

Calhoun is the Naval Postgraduate School's public access digital repository for research materials and institutional publications created by the NPS community. Calhoun is named for Professor of Mathematics Guy K. Calhoun, NPS's first appointed -- and published -- scholarly author.

Dudley Knox Library / Naval Postgraduate School
411 Dyer Road / 1 University Circle
Monterey, California USA 93943

http://www.nps.edu/library

ENERGY LOSS OF HIGH ENERGY ELECTRONS IN TIN, LEAD, AND GADOLINIUM

by

Michael Lee Mosbrooker

United States
Naval Postgraduate School

THESIS

ENERGY LOSS OF HIGH ENERGY ELECTRONS IN TIN, LEAD, AND GADOLINIUM

by

Michael Lee Mosbrooker

and

David Lee Sandquist

June 1970

This document has been approved for public release and sale; its distribution is unlimited.

T136107

Energy Loss of High Energy Electrons
in Tin, Lead, and Gadolinium

by

Michael Lee Mosbrooker
Major, United States Army
B.S., California State Polytechnic College, 1960

and

David Lee Sandquist
Major, United States Army
B.S., Iowa State University, 1961

Submitted in partial fulfillment of the
requirements for the degree of

MASTER OF SCIENCE IN PHYSICS

from the

NAVAL POSTGRADUATE SCHOOL
June 1970

Thesis M8405
c.1

ABSTRACT

The LINAC at the Naval Postgraduate School, Monterey, was used to accelerate electrons to energies ranging from 52 to 92 MeV in order to study the energy distributions of high energy electrons before and after passing through layers of tin, gadolinium, and lead. The thickness of these materials ranged from 0.8 to 5.9 g/cm^2.

The most probable energy losses agreed with the theory of Blunck and Westphal for all materials used, while distribution half-widths agreed only for absorbers of thickness less than 3.0 g/cm^2. The thickness at which theory and experiment began to exhibit a noticeable discrepancy was found to be dependent on the atomic number of the material.

Where comparison was possible, results of this experiment generally agreed with the findings of similar works concluded previously.

LIBRARY
NAVAL POSTGRADUATE SCHOOL
MONTEREY, CALIF. 93940

TABLE OF CONTENTS

Page

I. INTRODUCTION -- 11

II. THEORETICAL CONSIDERATIONS ------------------------------ 13

III. EXPERIMENTAL PROCEDURE --------------------------------- 17

IV. TREATMENT OF DATA --------------------------------------- 19

V. RESULTS AND OBSERVATIONS --------------------------------- 21

APPENDIX A. Tables -- 23

APPENDIX B. Figures --- 26

APPENDIX C. Beam Folding Technique -------------------------- 64

APPENDIX D. Computer Program -------------------------------- 68

BIBLIOGRAPHY -- 81

INITIAL DISTRIBUTION LIST ----------------------------------- 82

FORM DD 1473 -- 83

LIST OF TABLES

Table	Title	Page
I.	Energy Loss Distribution Characteristics of Tin ----------	23
II.	Energy Loss Distribution Characteristics of Gadolinium ---	24
III.	Energy Loss Distribution Characteristics of Lead ---------	25

LIST OF FIGURES

Appendix B

Figure	Title	Page
1	Most Probable Energy Loss Vs. Tin Absorber Thickness	26
2	Half-Widths Vs. Tin Absorber Thickness	27
3	Most Probable Energy Loss Vs. Gadolinium Absorber Thickness	28
4	Half-Widths Vs. Gadolinium Absorber Thickness	29
5	Most Probable Energy Loss Vs. Lead Absorber Thickness	30
6	Half-Widths Vs. Lead Absorber Thickness	31
7	Energy Distribution, Tin Absorber, $T = 1.485$ g/cm^2 $E_i = 52.51$ MeV	32
8	Energy Distribution, Tin Absorber, $T = 2.970$ g/cm^2 $E_i = 52.51$ MeV	33
9	Energy Distribution, Tin Absorber, $T = 4.455$ g/cm^2 $E_i = 52.51$ MeV	34
10	Energy Distribution, Tin Absorber, $T = 5.940$ g/cm^2 $E_i = 52.51$ MeV	35
11	Energy Distribution, Tin Absorber, $T = 1.485$ g/cm^2 $E_i = 74.95$ MeV	36
12	Energy Distribution, Tin Absorber, $T = 2.970$ g/cm^2 $E_i = 74.95$ MeV	37
13	Energy Distribution, Tin Absorber, $T = 4.455$ g/cm^2 $E_i = 74.95$ MeV	38
14	Energy Distribution, Tin Absorber, $T = 5.940$ g/cm^2 $E_i = 74.95$ MeV	39
15	Energy Distribution, Tin Absorber, $T = 1.485$ g/cm^2 $E_i = 94.32$ MeV	40
16	Energy Distribution, Tin Absorber, $T = 2.970$ g/cm^2 $E_i = 94.32$ MeV	41

Figure	Title	Page
17	Energy Distribution, Tin Absorber, $T = 4.455$ g/cm^2 $E_i = 94.32$ MeV	42
18	Energy Distribution, Tin Absorber, $T = 5.940$ g/cm^2 $E_i = 94.32$ MeV	43
19	Energy Distribution, Gadolinium Absorber, $T = 0.814$ g/cm^2 $E_i = 53.16$ MeV	44
20	Energy Distribution, Gadolinium Absorber, $T = 1.610$ g/cm^2 $E_i = 52.78$ MeV	45
21	Energy Distribution, Gadolinium Absorber, $T = 3.221$ g/cm^2 $E_i = 52.78$ MeV	46
22	Energy Distribution, Gadolinium Absorber, $T = 4.026$ g/cm^2 $E_i = 53.16$ MeV	47
23	Energy Distribution, Gadolinium Absorber, $T = 4.831$ g/cm^2 $E_i = 53.16$ MeV	48
24	Energy Distribution, Gadolinium Absorber, $T = 0.814$ g/cm^2 $E_i = 74.96$ MeV	49
25	Energy Distribution, Gadolinium Absorber, $T = 1.610$ g/cm^2 $E_i = 74.96$ MeV	50
26	Energy Distribution, Gadolinium Absorber, $T = 3.221$ g/cm^2 $E_i = 74.96$ MeV	51
27	Energy Distribution, Gadolinium Absorber, $T = 4.026$ g/cm^2 $E_i = 74.96$ MeV	52
28	Energy Distribution, Gadolinium Absorber, $T = 4.831$ g/cm^2 $E_i = 74.96$ MeV	53
29	Energy Distribution, Gadolinium Absorber, $T = 0.814$ g/cm^2 $E_i = 91.74$ MeV	54
30	Energy Distribution, Gadolinium Absorber, $T = 1.610$ g/cm^2 $E_i = 91.74$ MeV	55
31	Energy Distribution, Gadolinium Absorber, $T = 3.221$ g/cm^2 $E_i = 91.74$ MeV	56
32	Energy Distribution, Gadolinium Absorber, $T = 4.026$ g/cm^2 $E_i = 91.74$ MeV	57
33	Energy Distribution, Gadolinium Absorber, $T = 4.880$ g/cm^2 $E_i = 91.74$ MeV	58

Figure Title Page

34 Energy Distribution, Lead Absorber, $T = 2.825$ g/cm^2 $E_i = 53.17$ MeV 59

35 Energy Distribution, Lead Absorber, $T = 4.236$ g/cm^2 $E_i = 53.17$ MeV 60

36 Energy Distribution, Lead Absorber, $T = 2.825$ g/cm^2 $E_i = 74.97$ MeV 61

37 Energy Distribution, Lead Absorber, $T = 4.236$ g/cm^2 $E_i = 74.97$ MeV 62

38 Energy Distribution, Lead Absorber, $T = 2.854$ g/cm^2 $E_i = 91.76$ MeV 63

Appendix C

1 Beam Folding Technique 65

I. INTRODUCTION

The theoretical energy distribution for an initially monoenergetic electron beam which has passed through an absorbing material was determined by Blunck and Westphal [1]. Their work modified previous theoretical calculations of Landau [2], Eyges [3], Bethe and Heitler [4], and Blunck and Leisegang [5] by adding radiation losses to the previous predictions of ionization losses for electrons when passing through thin absorbing layers. The distribution assumes energy losses small compared to the incident beam energy. The theoretical treatment is presented in Section II.

Several measurements of energy losses by high energy electrons passing through various materials have been performed in the 10 MeV to 150 MeV range. Of note are the works of Breuer on aluminium [6]; Bumiller, Buskirk, Dyer, and Miller on aluminum [7,8]; Goodwin on copper [9]; and DeLeuil and Raynis on aluminum, copper, and lead [10]. Except for Breuer's work on the Darmstadt linear accelerator, the experiments were performed on the LINAC at the Naval Postgraduate School. These experimental results are in general agreement with theory for thin absorbers (≤ 2 g/cm^2), but discrepancies with theoretical predictions are reported for the thicker absorbers. Such discrepancies are expected for the thicker absorbers since the energy loss is no longer small compared to the initial beam energy.

In this thesis the energy loss measurements are extended to include tin (Z = 50) and gadolinium (Z = 64). These metals were chosen to provide experimental results for materials with atomic numbers between copper (Z = 29) and lead (Z = 82). It was thought that analysis of these materials would provide more conclusive information on the effects of atomic number on the agreement between experimental and theoretical half-widths as reported by DeLeuil and Raynis [10]. Thicknesses used ranged from 1.485 to 5.940 g/cm^2 for tin and from 0.814 to 4.831 g/cm^2 for gadolinium; nominal beam energies were 52, 75, and 92 MeV. Thick lead absorbers (2.825 and 4.236 g/cm^2) were investigated as an extension of the work of DeLeuil and Raynis, and, in addition, their thickest aluminum absorber (5.574 g/cm^2) was investigated as a continuity check between the two experiments.

The energy loss distributions are characterized by the most probable energy loss and the half-width. The half-width is the full width of the distribution curve at half maximum. These quantities, obtained from experiment and theory, are the basis for comparison between experimental and theoretical results.

II. THEORETICAL CONSIDERATIONS

The Blunck and Westphal theory of the distribution for the energy loss of a beam of monoenergetic electrons in passing through a layer of absorbing material assumes that the energy loss Q is small compared to the initial beam energy, E_i. Let W(Q)dQ be the probability of energy loss between Q and Q + dQ, and X be that portion of the loss Q due to radiation. Hence, the ionization loss is Q - X. Considering these two loss processes, the probability of energy loss is

$$W(Q)dQ = \int_o^Q W_I(Q-X)W_S(X)dXdQ \qquad (1)$$

where W_I and W_S are the energy loss distributions for ionization and radiation respectively.

The Landau equation [2], as modified by Blunck and Leisegang, is used for the energy loss distribution due to ionization. The distribution is expressed as a function of Landau's dimensionless parameter λ as follows:

$$W_I(Q)dQ = \Phi(\lambda)\ d\lambda = \sum_n \frac{C_n\gamma_n}{\sqrt{b^2 + \gamma_n^2}} \exp\left[-\frac{(\lambda - \lambda_n)^2}{b^2 + \gamma_n^2}\right] d\lambda \qquad (2)$$

$$\text{where} \quad \lambda = \frac{Q-\overline{Q}}{aR} + \ln \frac{E_i}{aR} - 1.116 \qquad (3)$$

The terms used in equations (2) and (3) are defined as follows:

C_n, γ_n, and λ_n are constants given by Blunck and Leisegang [5] and are used to fit Landau's distribution to a sum of gaussian functions.

R is the absorber thickness in cm.

The quantity "a" is a function of the atomic number Z, the atomic weight A, and the density ρ of the absorber; and $\beta(=v/c)$ of the electrons:

$$a = \frac{0.154\ Z\ \rho}{A\ \beta^2}\ \text{MeV/cm.} \qquad (4)$$

The quantity b^2 is a correction to Landau's theory given by Blunck and Leisegang [5]:

$$b^2 = \frac{3.0}{aR} \sum_m \frac{I_m N_m}{Z} \ln \left[\frac{2\ E_i}{I_m(1 - \beta^2)} \right], \qquad (5)$$

where the summation is over the ionization potentials of the atomic electrons, and N_m is the number of electrons with ionization potential I_m.

$\overline{Q}$ is the average energy loss due to ionization (no radiation) for electrons of incident energy E_i, and is given by Sternheimer [11,12, and 13] as follows:

$$\overline{Q} = \frac{A_s t}{\beta^2} \left[B + 0.43 + \ln E_i - \beta^2 - C - a_s(X_1 - \log_{10} p/mc)^{m_s} \right] \text{MeV} \qquad (6)$$

where t is the thickness in g/cm^2, and the constants A_s, B, C, X_1, a_s, and m_s are parameters of the absorber material. These parameters for tin, lead, and various other material are listed in reference [13]. The parameters for gadolinium are not listed but were determined by the following method.

A_s for gadolinium was obtained by extrapolating from a plot of A_s vs. Z/A for the absorber materials listed in reference 13. The result was $A_s = 0.0624$. B for gadolinium was found in a similar manner from a B vs. I^2 (ionization potential) plot where I was determined from a Z vs. I graph. The result was B = 13.3. C was determined from a semi-log plot of $I^2A/\rho Z$ vs. -C, and the result was C = -6.80. The values for a_s, X_1, and m_s were more difficult to determine, but fortunately they contribute little in determining $\overline{Q}$. These constants were numerically determined. The values for the term $a_s(X_1 - \log_{10}(p/mc))^{m_s}$ were calculated for tin (Z = 50) and tungsten (Z = 74) in the p/mc range (p is momentum, and m is the rest mass of the electron) of the energies used in the experiment. Using Z as a basis of interpolation, the corresponding values for gadolinium (Z = 64) were estimated for two representative p/mc values (100 and 150). The value for X_1 was arbitrarily set to be 3.0, and the a_s and m_s values were determined from a simultaneous algebraic solution based on the interpolated values. The results were $a_s = 0.418$ and $m_s = 2.10$. The error in the determination of $\overline{Q}$ using these values was estimated to be 1% or less.

For W_S, the energy loss distribution due to radiation, Blunck and Westphal [1] give:

$$W_S(Q)dQ = B\alpha R(Q/E_i)^{\alpha R} \frac{dQ}{Q} \tag{7}$$

where

$$\alpha = 1.4 \times 10^{-3} \frac{\rho Z}{A} \left[4/3 \ln \frac{183}{Z^{1/3}} + 1/9 \right] \text{cm}^{-1} \tag{8}$$

and B is a normalizing factor $= \frac{1}{\Gamma(\alpha R + 1)}$.

The distribution of total energy loss according to Blunck and Westphal is obtained by putting equations (7) and (2) into equation (1) and performing the required integration. The result is the energy loss distribution for a single electron of incident energy E_i. For comparison of theoretical and experimental values, this distribution function was used, with corrections to account for the finite energy width of the incident electron beam. This treatment is described in Section IV and Appendix C.

III. EXPERIMENTAL PROCEDURE

The LINAC of the Naval Postgraduate School was used to obtain electron beam energies from 52 MeV to 92 MeV. This beam was elastically scattered at 90° from a thin (3.5 mil) aluminum scattering foil, passed through the absorber, and finally analyzed by a 120° magnetic spectrometer described by Kenaston, Luke, and Sones [14].

This general experimental arrangement was similar to that used by Miller [7,8] and DeLeuil and Raynis [10] with the exception of the removal of a 3.5 mil aluminum window and the installation of a ten channel coincidence counting system. These changes are discussed below.

The aluminum window removed was located just before the scattering chamber. Since the presence of the window caused a broadening of the incident electron beam distribution, its removal decreased the energy width of the incident beam for this experiment, as compared to previous works done at the NPS.

The ten channel counting system consists of ten front counters and a single backing counter operated in coincidence with the front counters. The entire ten channel system has an energy spread of about 3%.

The absorbers were positioned approximately 3 cm. from the scattering foil as recommended by DeLeuil and Raynis [10]. Absorber thicknesses for tin were 1.485, 2.970, 4.455, and 5.940 g/cm^2; thicknesses for gadolinium were 0.814, 1.610, 3.221, 4.026, and 4.831 g/cm^2; absorber thicknesses for lead were 2.825 and 4.236 g/cm^2.

A thick aluminum absorber (5.574 g/cm^2) was used to correlate the results of this experiment to the results of DeLeuil and Raynis [10], which were obtained before the ten channel counting system was installed. The results agreed within experimental accuracy.

Since the electron beam scattered into the absorbing material was not monoenergetic, the energy distribution was determined both before and after passing through the absorber. Various thicknesses of absorber material, including no absorber, were positioned on a remotely controlled ladder device. For measurement of the distribution before passing through the absorbers (called a zero peak), the ladder was positioned such that the beam passed only through the scattering foil. After measuring the zero peak spectrum, the various absorbers were moved into the beam to determine the energy distribution of the beam after passing through each absorber.

In the case of tin and lead all absorber thicknesses could be measured without turning off the accelerator and thus possibly altering the character of the beam. This was not possible for gadolinium. Because of its cost, only a small quantity was purchased. Hence, only two gadolinium absorbers could be run without turning off the accelerator and rearranging the gadolinium on the ladder. Since the beam character could change, a zero peak measurement was made whenever absorbers were replaced.

The data represented the number of electrons detected by the coincidence counting system at the exit of the magnetic spectrometer. A downstream Secondary Emission Monitor was used as a standard for normalization purposes, in that each data point corresponded to a given integration current, i.e., a certain number of electrons passing through the absorbing material.

IV. TREATMENT OF DATA

The data reduction for the ten channel counting system is standard for multi-channel systems and is on file in the NPS LINAC computer library. In this reduction process, three characteristics of the counting system are required. The characteristics are:

(1) the energy spread of the counting system,

(2) the energy seen by each front counter,

(3) the relative efficiencies of the front counters.

With this information the actual energy corresponding to the front counter data is calculated. Counting rate and background corrections are also performed during this computerized process.

In the lower energy regions of the spectrum, where all counter readings should be nearly equal, a counting discrepancy was noted in that the lower energy front counters read consistently higher than those on the higher energy portion of the counting spectrum. This effect occurred at energies lower than required to obtain distribution half-widths and thus did not affect the data reported. However, it made confirmation of the shape of the distributions at very low energy (< 20 MeV) impossible.

The electron beam energy is not monoenergetic as required by Blunck and Westphal theory. To compare experimental and theoretical results, the zero peak data must be used to modify the theoretical predictions. With no data treatment, the theory will predict half-widths which are too small and, in the case of asymmetric zero peaks, erroneous most probable energy losses. Removal of the aluminum window noted in Section III narrowed the zero peak to the extent that it could be treated as a symmetrical gaussian distribution. The IBM 360 computer of the NPS was used to unfold the zero peak energy distribution into the theory. A histogram method described in Appendix C was used for this unfolding. The computer program used to accomplish the unfolding is Appendix D.

In the comparison of experiment with theory, the measured incident energy distribution was unfolded as previously described, properly normalized to the experimental data, and plotted. From these plots the theoretical half-widths and most probable energy losses were determined. The experimental data were plotted along with the corresponding theoretical curve, and measurable parameters were compared. The curves are shown in figures 1 through 38 of Appendix B.

V. RESULTS AND OBSERVATIONS

The values predicted by theory and the experimental results for the most probable energy loss and half-width for tin, gadolinium, and lead are shown in Tables I, II, and III respectively. In these tables, BW refers to Blunck and Westphal theoretical predictions, Q_p represents the most probable energy loss, and HW is the half-width. Data are given for predictions with and without beam folding.

On comparing the theoretical predictions with beam folding and the experimental results, it is seen that good agreement exists for target thicknesses less than about 3.0 g/cm^2 for both half-width and most probable energy loss. At thicknesses greater than this, the agreement in most probable energy loss is still reasonably good, but there is poor agreement in half-width. The greatest variation in most probable energy loss is 8% while the average variation is 3%. These percentages, while averaged over all material, are typical and not material dependent. The average half-width variation is 9% where half-widths were obtained. As can be seen from Appendix B, figures 2, 4, and 6, the theory does not predict a half-width for a certain target thickness for each element. This cutoff thickness is smaller as the atomic number increases. For example, the theory would predict a half-width for 5.6 g/cm^2 aluminum, but not for 4.2 g/cm^2 lead.

It is concluded from these results that the Blunck and Westphal theory predicts correctly the most probable energy loss for all targets used and predicts satisfactorily the half-widths for the thinner targets. Thin targets can be defined empirically as those satisfying the relation $T(Z)^{1/3} \leq 13.5$, where T is the absorber thickness (g/cm^2) and Z is the absorber atomic number.

APPENDIX A - TABLES

TABLE I. Energy Loss Distribution Characteristics of Tin

		Q_p (MeV)			HW (MeV)		
E_i (MeV)	$t(g/cm^2)$	BW	BW Folded	Experimental	BW	BW Folded	Experimental
52.53	1.485	1.79	1.83	1.78 ± .05	.65	.75	.78 ± .10
	2.970	3.84	3.84	3.86 ± .15	2.48	3.03	3.02 ± .40
	4.455	6.56	6.56	6.35 ± .30	16.65	16.70	11.3 ± 2.0
	5.940	12.67	12.67	13.00 ± 1.0	*	*	18.6 ± 6.0
75.0	1.485	1.81	1.81	1.77 ± .07	.66	.73	.83 ± .10
	2.970	3.84	3.93	3.86 ± .15	2.99	2.56	2.96 ± .42
	4.455	6.56	6.56	6.65 ± .30	16.61	16.69	15.50 ± 2.0
	5.940	12.67	12.67	12.10 ± 2.0	*	*	28.9 ± 15.0
94.4	1.485	1.83	1.88	1.87 ± .10	.66	.83	.88 ± .15
	2.970	3.84	3.93	3.96 ± .20	2.50	2.63	2.72 ± .45
	4.455	6.56	6.56	7.00 ± 1.0	16.57	16.75	16.20 ± 4.0
	5.940	12.67	12.67	11.72 ± 3.0	*	*	*

* Half width not obtained

TABLE II. Energy Loss Distribution Characteristics of Gadolinium

		Q_p (MeV)			HW (MeV)		
E_i (MeV)	t(g/cm^2)	BW	BW Folded	Experimental	BW	BW Folded	Experimental
52.80	1.610	1.93	1.94	1.92 ± .10	.84	.91	1.00 ± .15
	3.221	4.24	4.24	4.16 ± .30	5.47	5.52	5.75 ± .72
53.18	.814	.92	.97	.92 ± .08	.35	.46	.52 ± .07
	4.026	5.90	5.90	5.76 ± .50	*	*	10.60 ± 1.50
	4.831	9.26	9.26	9.16 ± 1.1	*	*	14.2 ± 3.0
75.00	.814	.92	.97	.97 ± .05	.36	.51	.59 ± .08
	1.610	1.93	1.97	1.92 ± .10	.84	.96	1.00 ± .15
	3.221	4.24	4.24	4.09 ± .30	5.47	5.55	5.80 ± .80
	4.026	5.90	5.90	6.00 ± .60	*	*	15.4 ± 1.50
	4.831	9.40	9.40	9.26 ± 2.5	*	*	36.1 ±13.0
91.80	.814	.92	.97	.97 ± .05	.36	.60	.64 ± .08
	1.610	1.93	1.97	1.90 ± .10	.84	.96	1.10 ± .18
	3.221	4.20	4.20	4.13 ± .40	5.47	5.56	8.1 ± .95
	4.026	5.90	5.90	5.9 ± .50	*	*	12.0 ± 2.0
	4.88**	9.79	9.79	17.60 ± 5.0	*	*	45.00 ±20.0

* Half width not obtained

** Effective thickness used due to 8° error in target angle.

TABLE III. Energy Loss Distribution Characteristics of Lead

		Q_p(MeV)			HW (MeV)		
E_i(MeV	t(g/cm^2)	BW	BW Folded	Experimental	BW	BW Folded	Experimental
53.18	2.825 4.236	3.57 8.87	3.57 9.07	3.60 ± .10 8.97 ± 2.0	6.38 *	6.45 *	6.50 ± .70 22.6 ± 5.0
75.00	2.825 4.236	3.57 9.07	3.66 9.07	3.69 ± .10 8.87 ± 2.5	6.39 *	6.52 *	6.48 ± .70 31.6 ± 8.0
91.80	2.854 **	3.69	3.69	3.80 ± .25	6.85	6.95	8.8 ± .70

* Half width not obtained

** Effective thickness used due to 8° error in target angle.

APPENDIX B. Figures

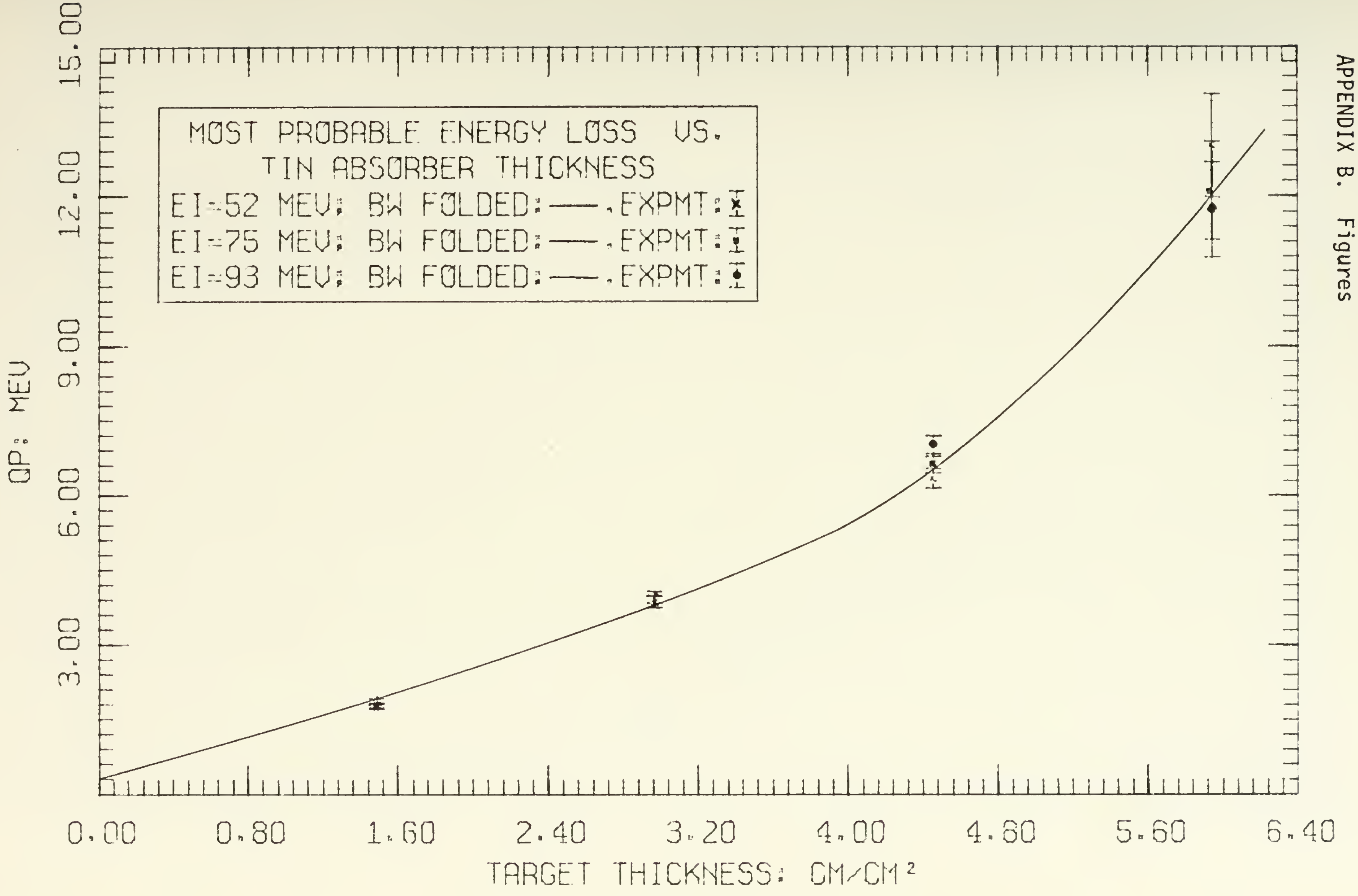

Figure 1

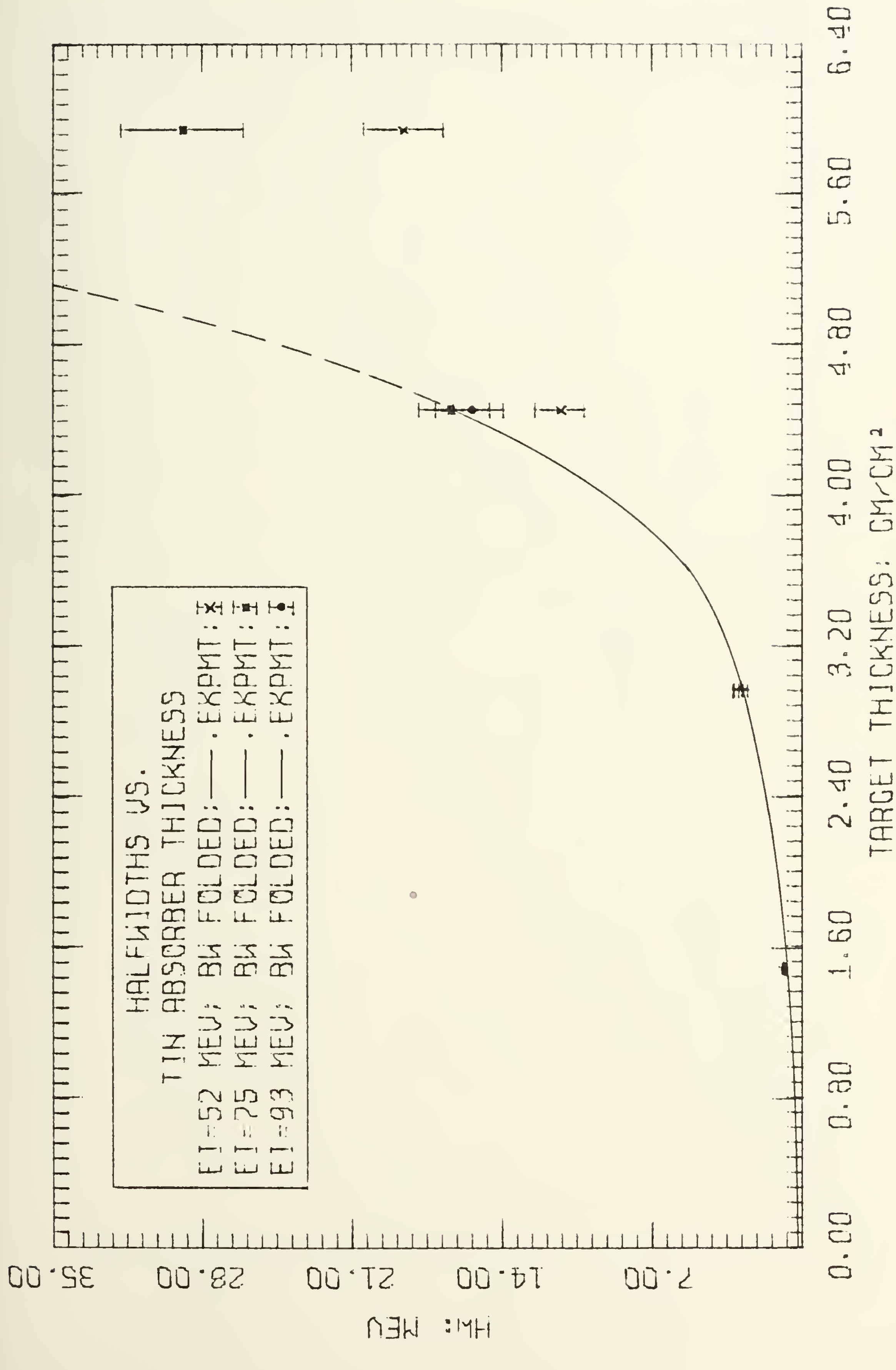
HALFWIDTHS VS.
TIN ABSORBER THICKNESS
E1=52 MEV; BW FOLDED:——.EXPMT: ⌶
E1=75 MEV; BW FOLDED:——.EXPMT: ⌶
E1=93 MEV; BW FOLDED:——.EXPMT: ⌶
HW: MEV
0.00
7.00
14.00
21.00
28.00
35.00
TARGET THICKNESS: GM/CM²
0.00
0.80
1.60
2.40
3.20
4.00
4.80
5.60
6.40

Figure 2

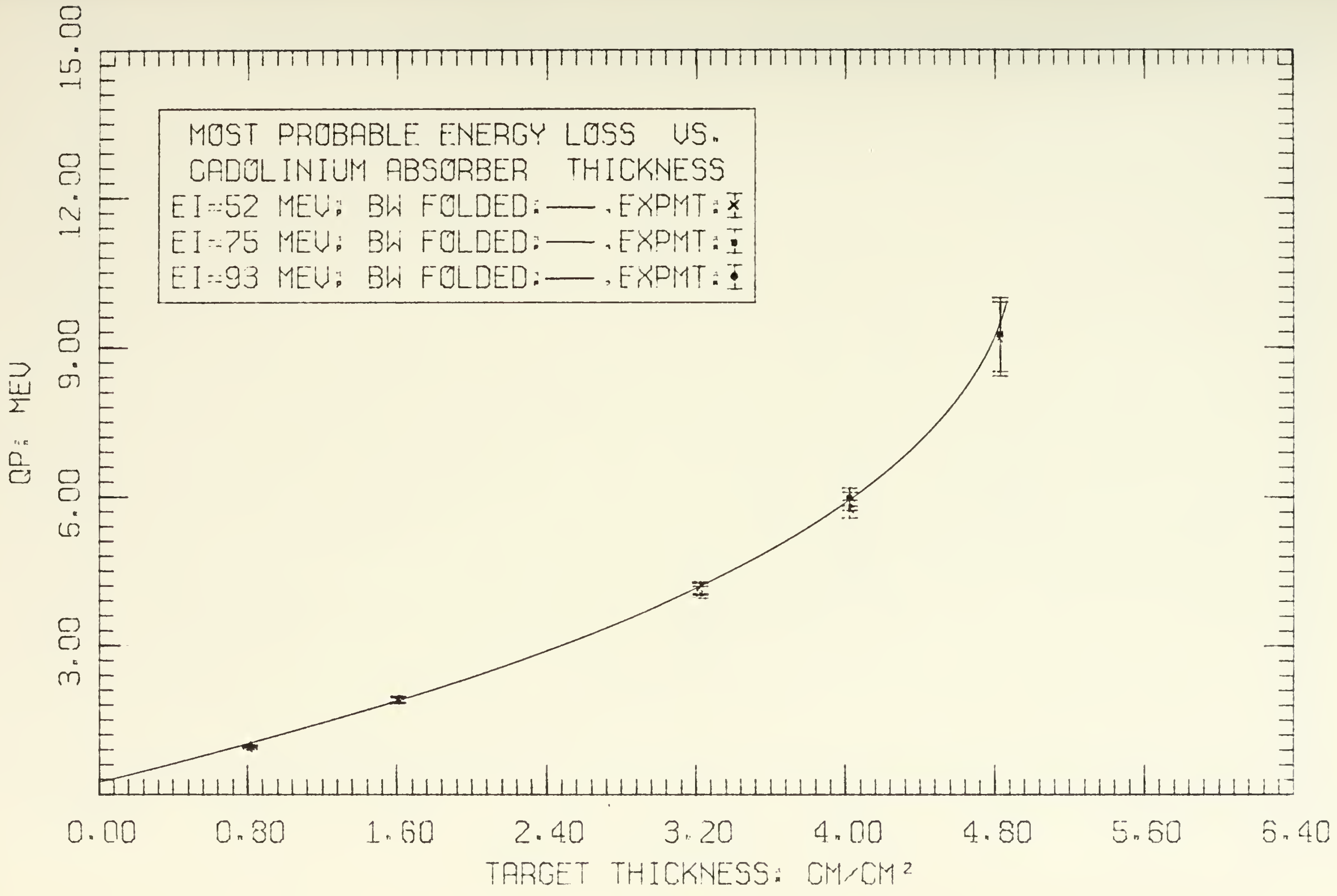MØST PRØBABLE ENERGY LØSS VS.
GADØLINIUM ABSØRBER THICKNESS
EI=52 MEV; BW FØLDED:——, EXPMT: ×
EI=75 MEV; BW FØLDED:——, EXPMT: ■
EI=93 MEV; BW FØLDED:——, EXPMT: ●
QP: MEV
15.00
12.00
9.00
6.00
3.00
0.00
0.80
1.60
2.40
3.20
4.00
4.80
5.60
6.40
TARGET THICKNESS: CM/CM²

Figure 3

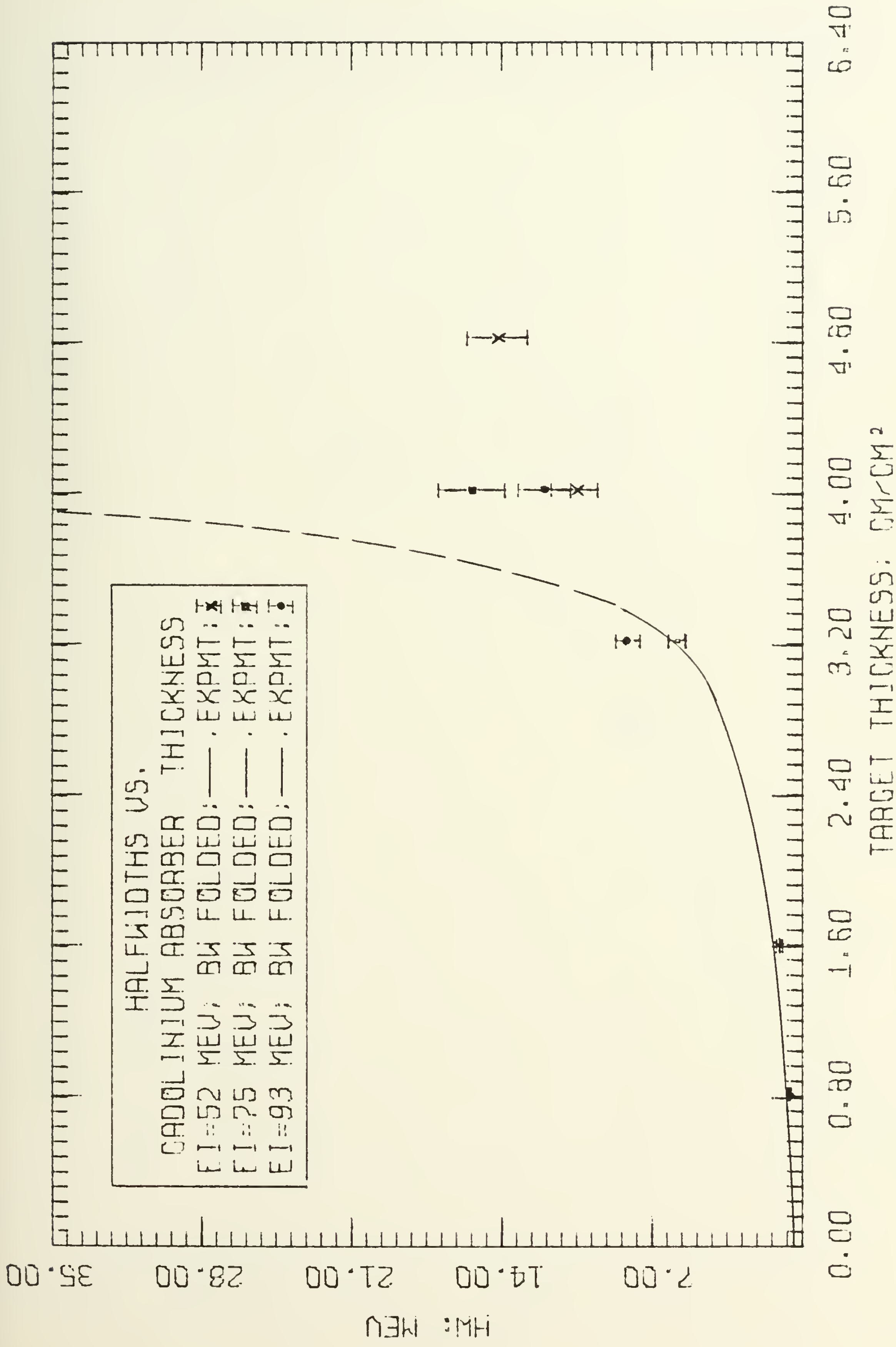
HALFWIDTHS VS.
GADOLINIUM ABSORBER THICKNESS
EI=52 MEV; BW FOLDED:——. EXPMT: ×
EI=75 MEV; BW FOLDED:——. EXPMT: ■
EI=93 MEV; BW FOLDED:——. EXPMT: ●
HW: MEV
TARGET THICKNESS: GM/CM²
0.00
7.00
14.00
21.00
28.00
35.00
0.00
0.80
1.60
2.40
3.20
4.00
4.80
5.60
6.40

Figure 4

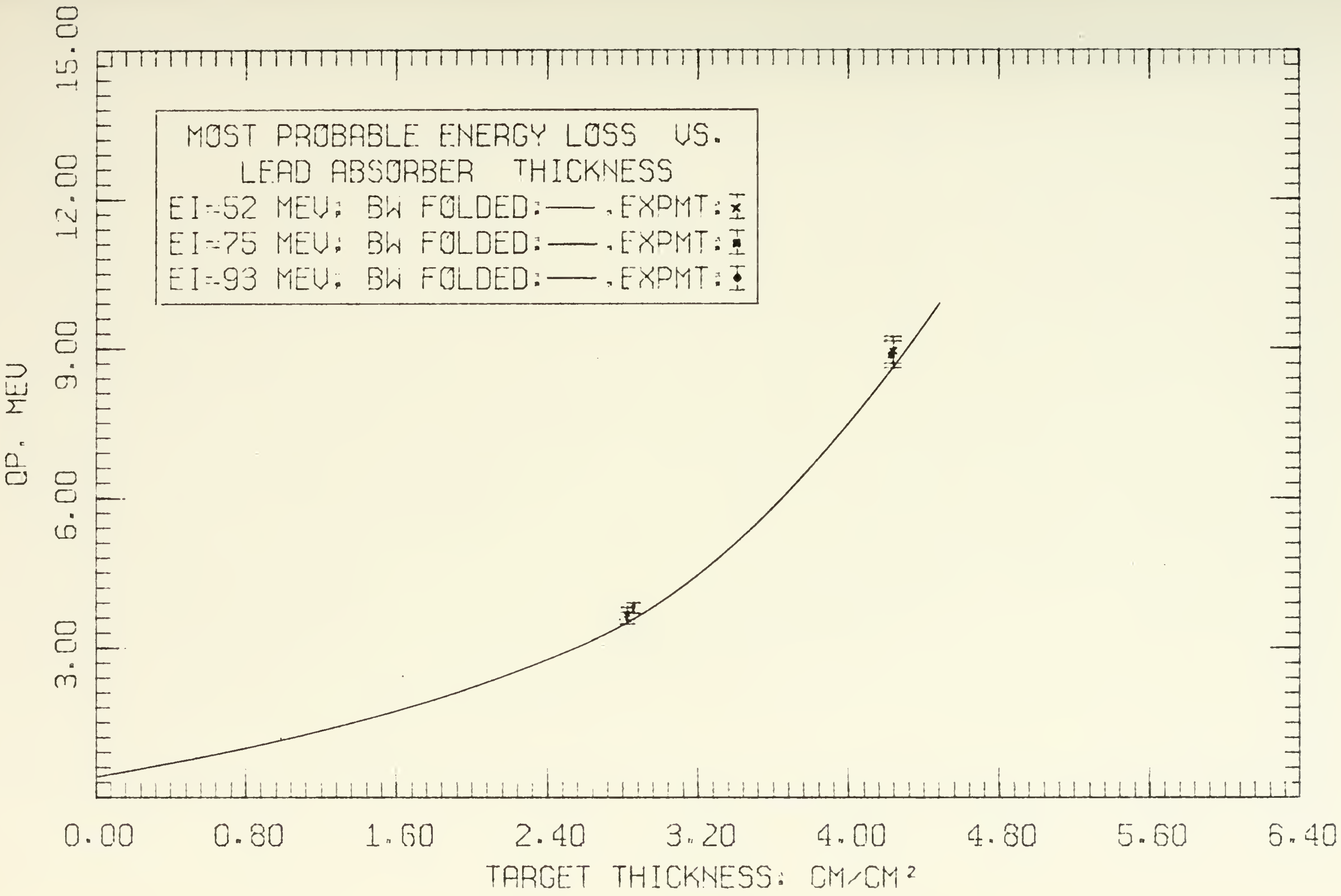
MØST PRØBABLE ENERGY LØSS VS.
LEAD ABSØRBER THICKNESS
EI=52 MEV; BW FØLDED:——, EXPMT: ×
EI=75 MEV; BW FØLDED:——, EXPMT: ■
EI=93 MEV; BW FØLDED:——, EXPMT: ●
QP. MEV
15.00
12.00
9.00
6.00
3.00
0.00
0.80
1.60
2.40
3.20
4.00
4.80
5.60
6.40
TARGET THICKNESS: CM/CM²

Figure 5

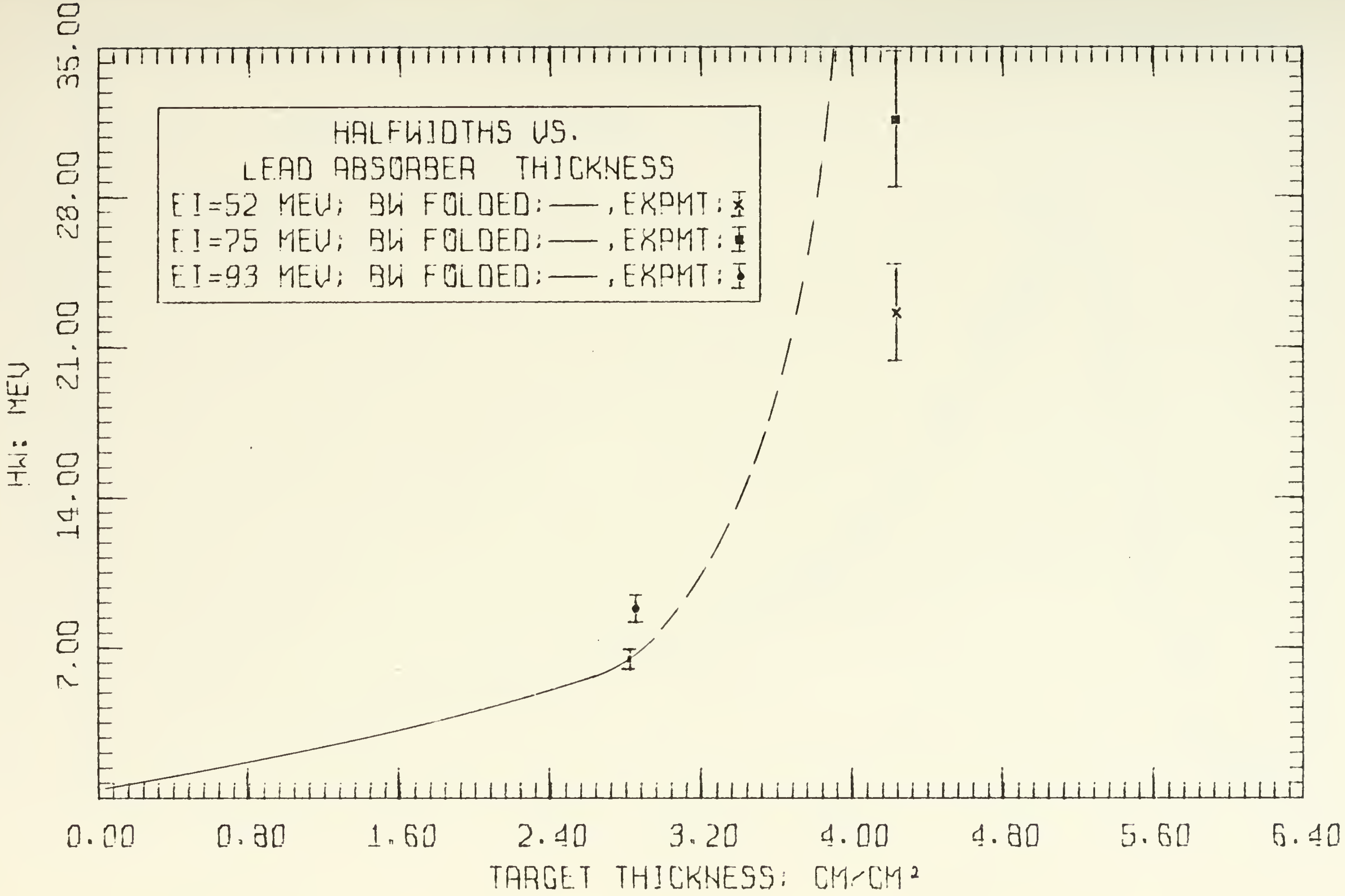
HALFWIDTHS VS.
LEAD ABSORBER THICKNESS
EI=52 MEV; BW FOLDED:——,EXPMT:
EI=75 MEV; BW FOLDED:——,EXPMT:
EI=93 MEV; BW FOLDED:——,EXPMT:
HW: MEV
35.00
28.00
21.00
14.00
7.00
0.00
0.80
1.60
2.40
3.20
4.00
4.80
5.60
6.40
TARGET THICKNESS: CM/CM²

Figure 6

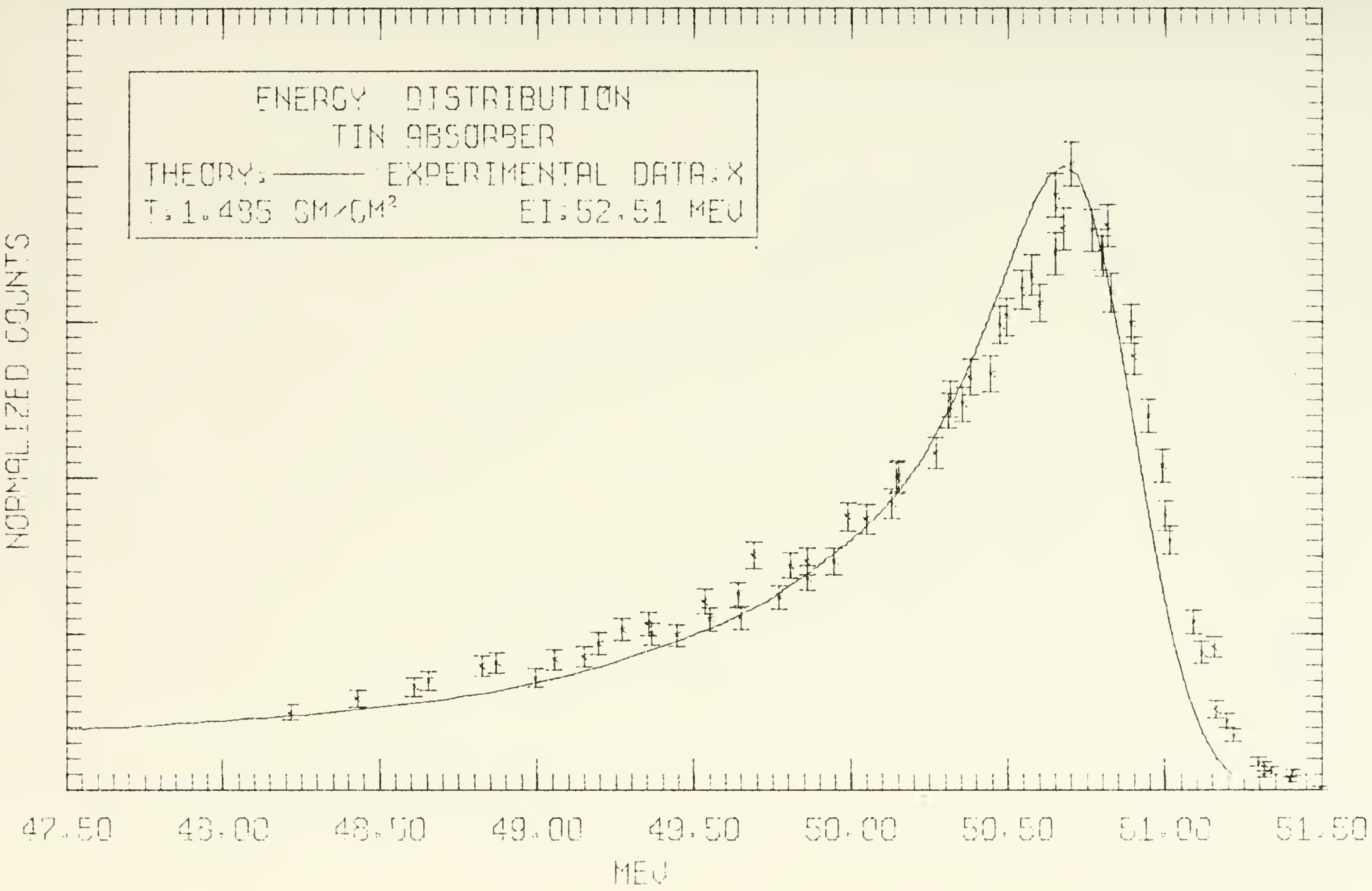
ENERGY DISTRIBUTION
TIN ABSORBER
THEORY: ——— EXPERIMENTAL DATA: X
T: 1.485 GM/CM²
EI: 52.51 MEV
NORMALIZED COUNTS
47.50
48.00
48.50
49.00
49.50
50.00
50.50
51.00
51.50
MEV

Figure 7

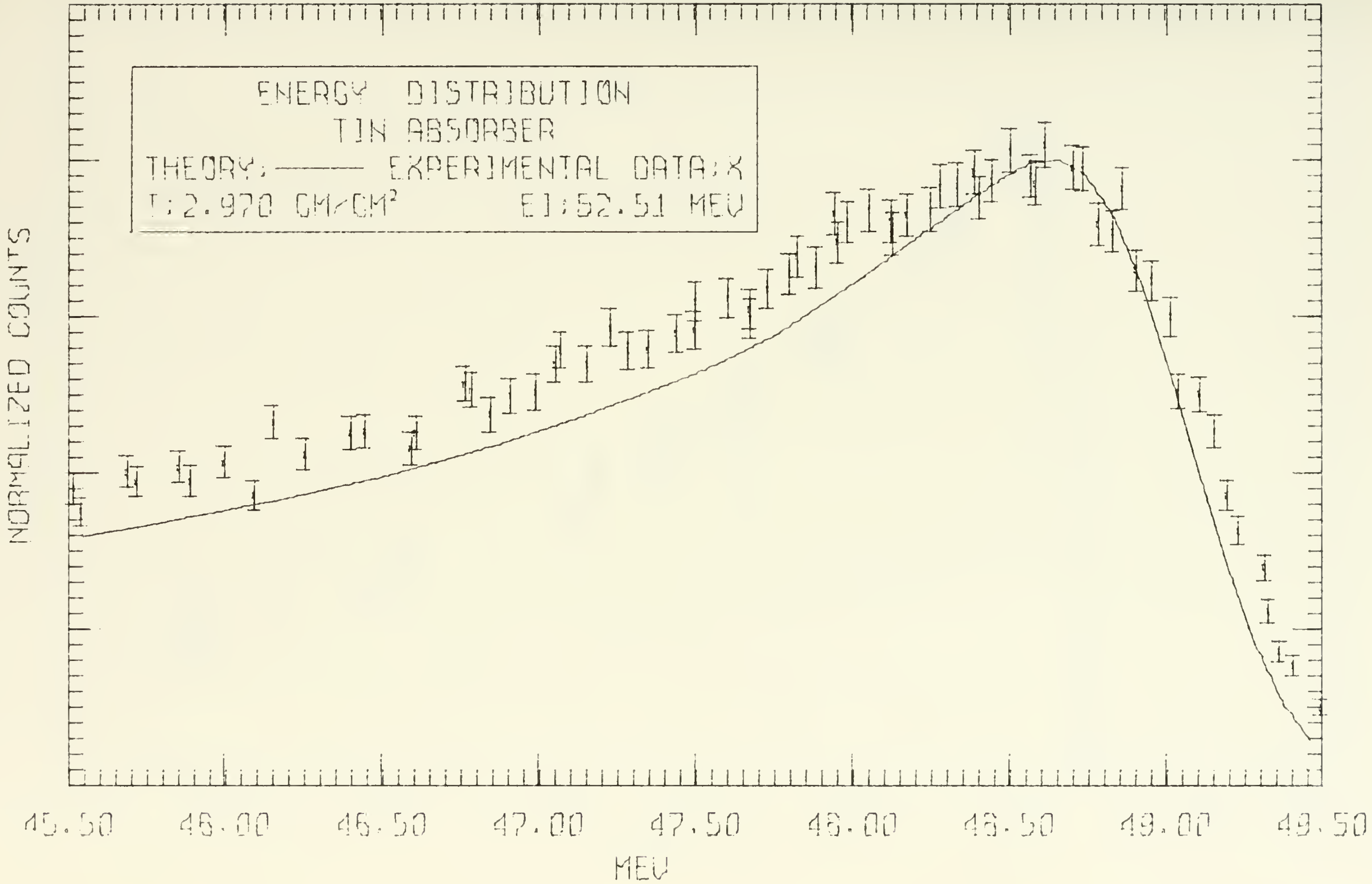
ENERGY DISTRIBUTION
TIN ABSORBER
THEORY: ——— EXPERIMENTAL DATA: X
T: 2.970 GM/CM²
E1: 52.51 MEV
NORMALIZED COUNTS
45.50
46.00
46.50
47.00
47.50
48.00
48.50
49.00
49.50
MEV

Figure 8

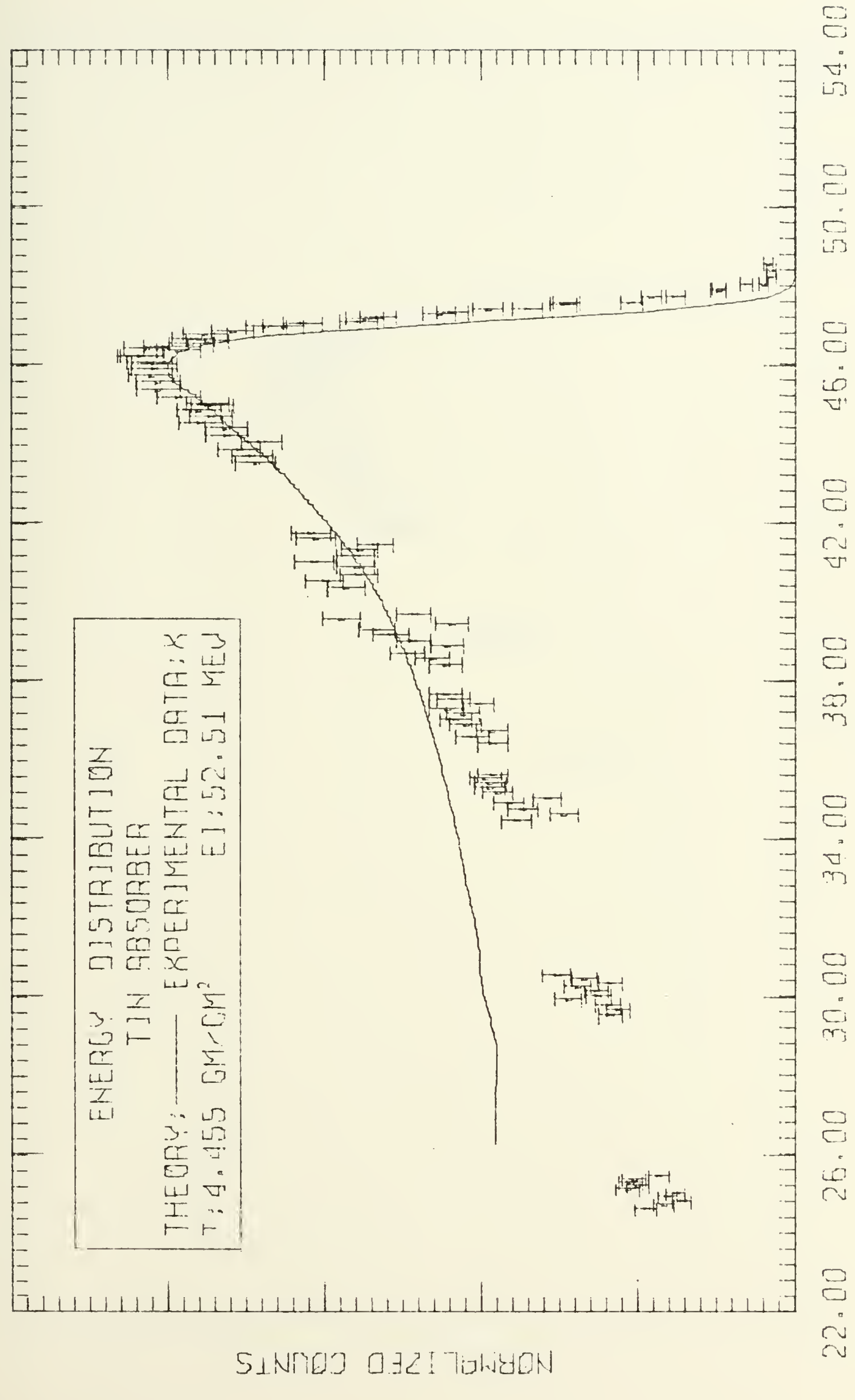
ENERGY DISTRIBUTION
TIN ABSORBER
THEORY; —— EXPERIMENTAL DATA; X
T; 4.455 GM/CM²
E1; 52.51 MEV
22.00
26.00
30.00
34.00
38.00
42.00
46.00
50.00
54.00
MEV
NORMALIZED COUNTS

Figure 9

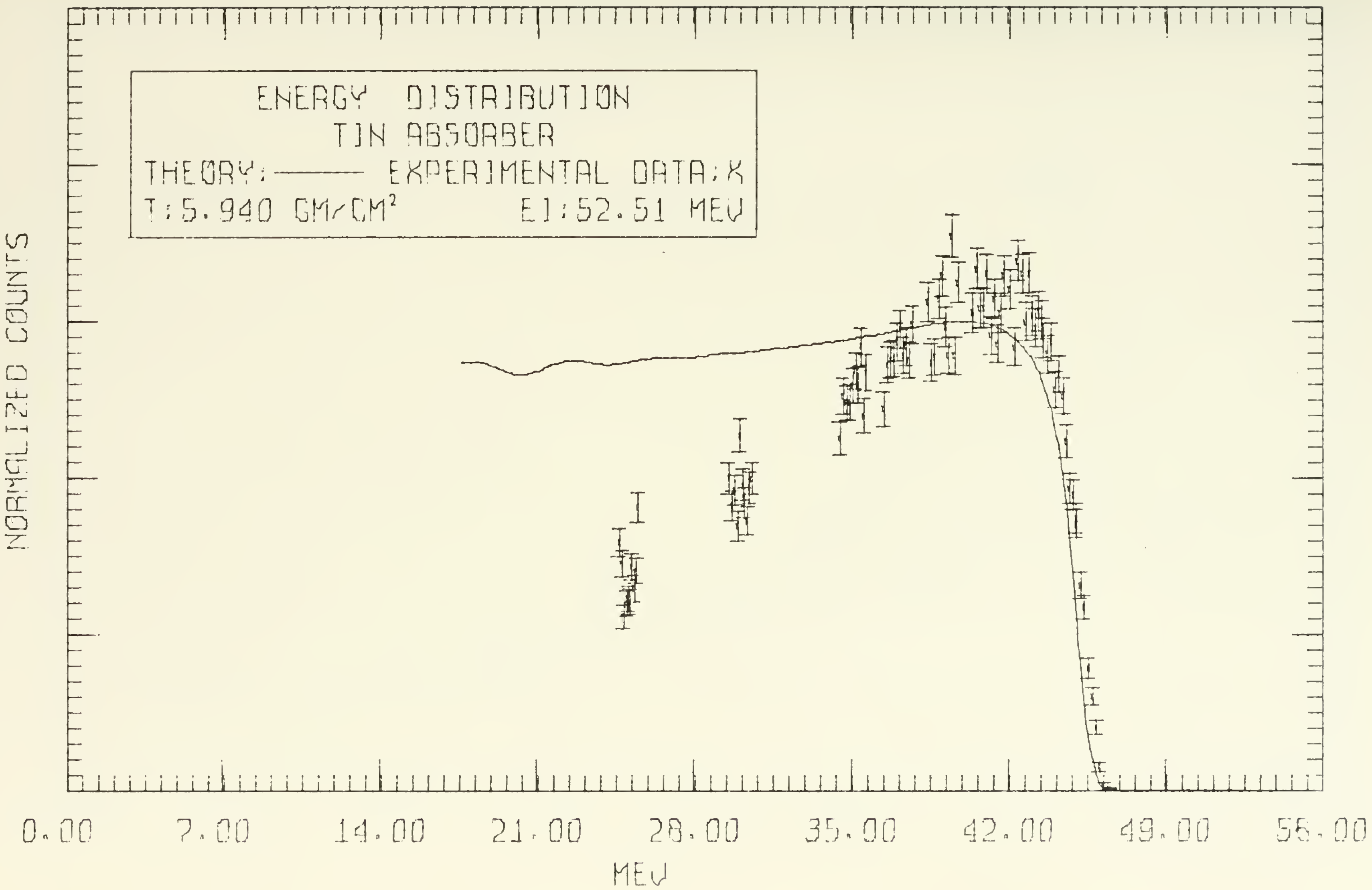
ENERGY DISTRIBUTION
TIN ABSORBER
THEORY: ——— EXPERIMENTAL DATA: K
T: 5.940 GM/CM²
E1: 52.51 MEV
NORMALIZED COUNTS
0.00
7.00
14.00
21.00
28.00
35.00
42.00
49.00
56.00
MEV

Figure 10

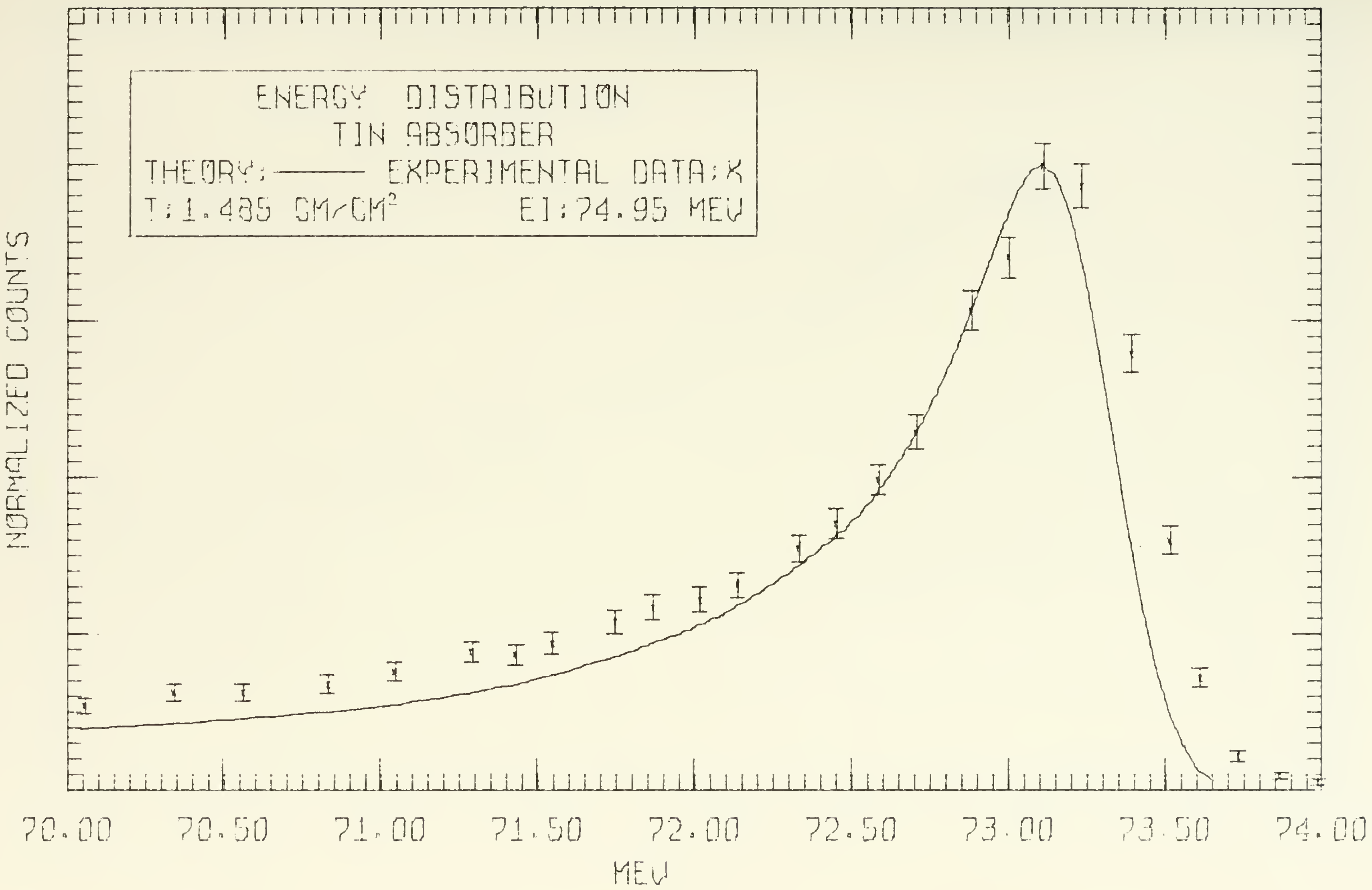
ENERGY DISTRIBUTION
TIN ABSORBER
THEORY; ——— EXPERIMENTAL DATA; X
T; 1.485 GM/CM²
EI; 74.95 MEV
NORMALIZED COUNTS
70.00
70.50
71.00
71.50
72.00
72.50
73.00
73.50
74.00
MEV

Figure 11

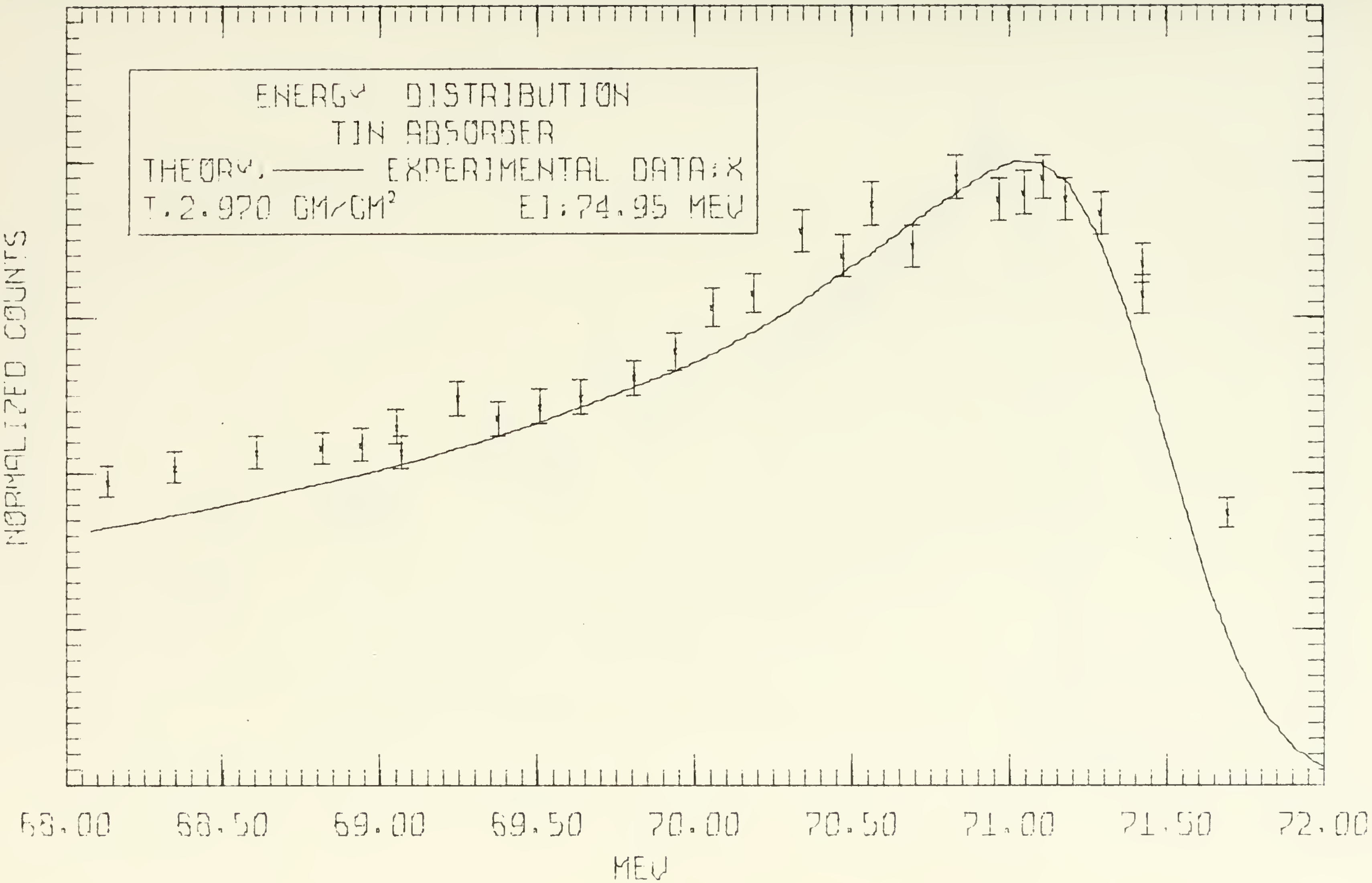
ENERGY DISTRIBUTION
TIN ABSORBER
THEORY, ——— EXPERIMENTAL DATA: X
T. 2.970 GM/CM²
EI: 74.95 MEV
NORMALIZED COUNTS
68.00
68.50
69.00
69.50
70.00
70.50
71.00
71.50
72.00
MEV

Figure 12

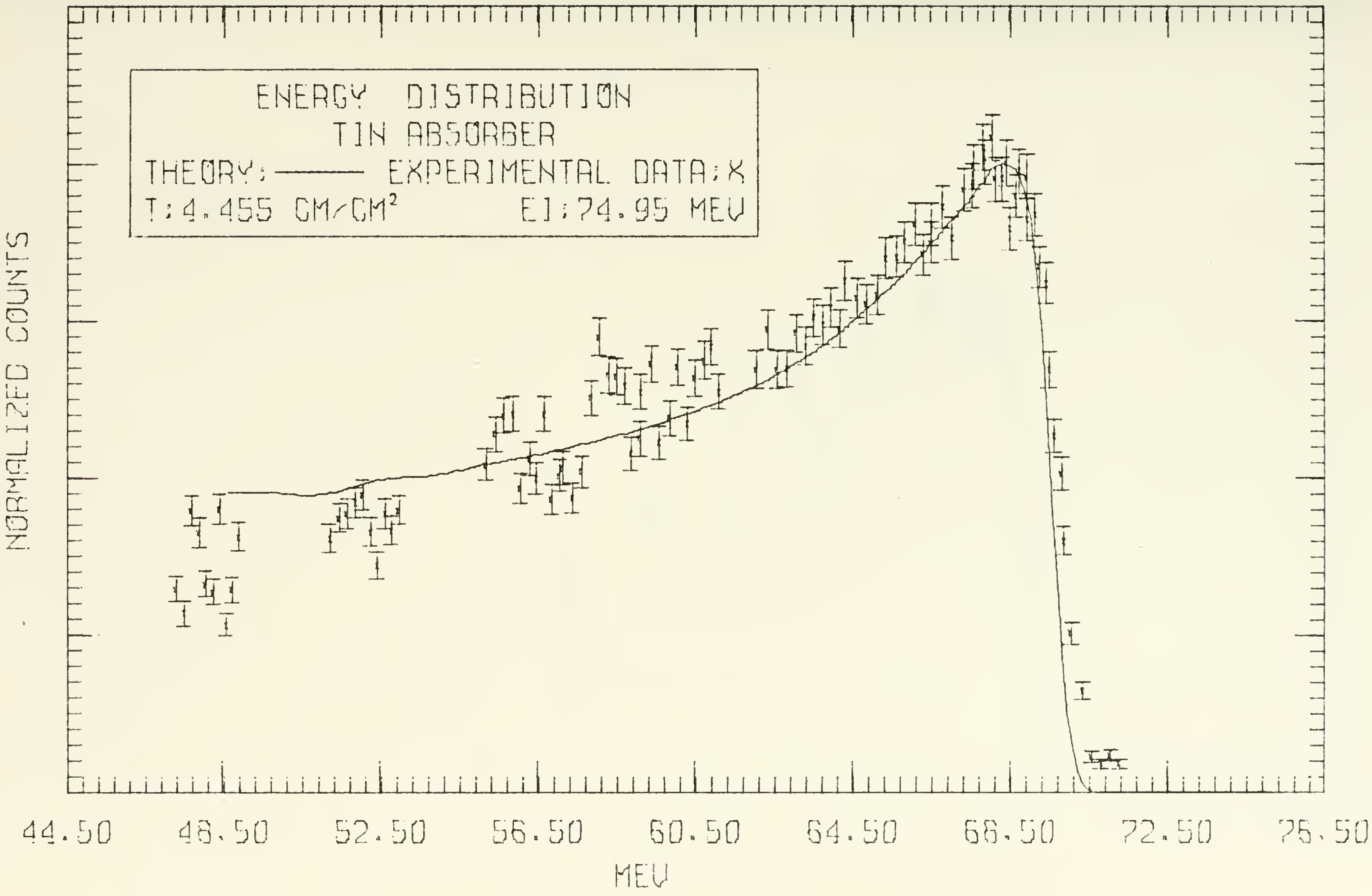
ENERGY DISTRIBUTION
TIN ABSORBER
THEORY: ——— EXPERIMENTAL DATA: X
T: 4.455 GM/CM²
EI: 74.95 MEV
NORMALIZED COUNTS
44.50
48.50
52.50
56.50
60.50
64.50
68.50
72.50
76.50
MEV

Figure 13

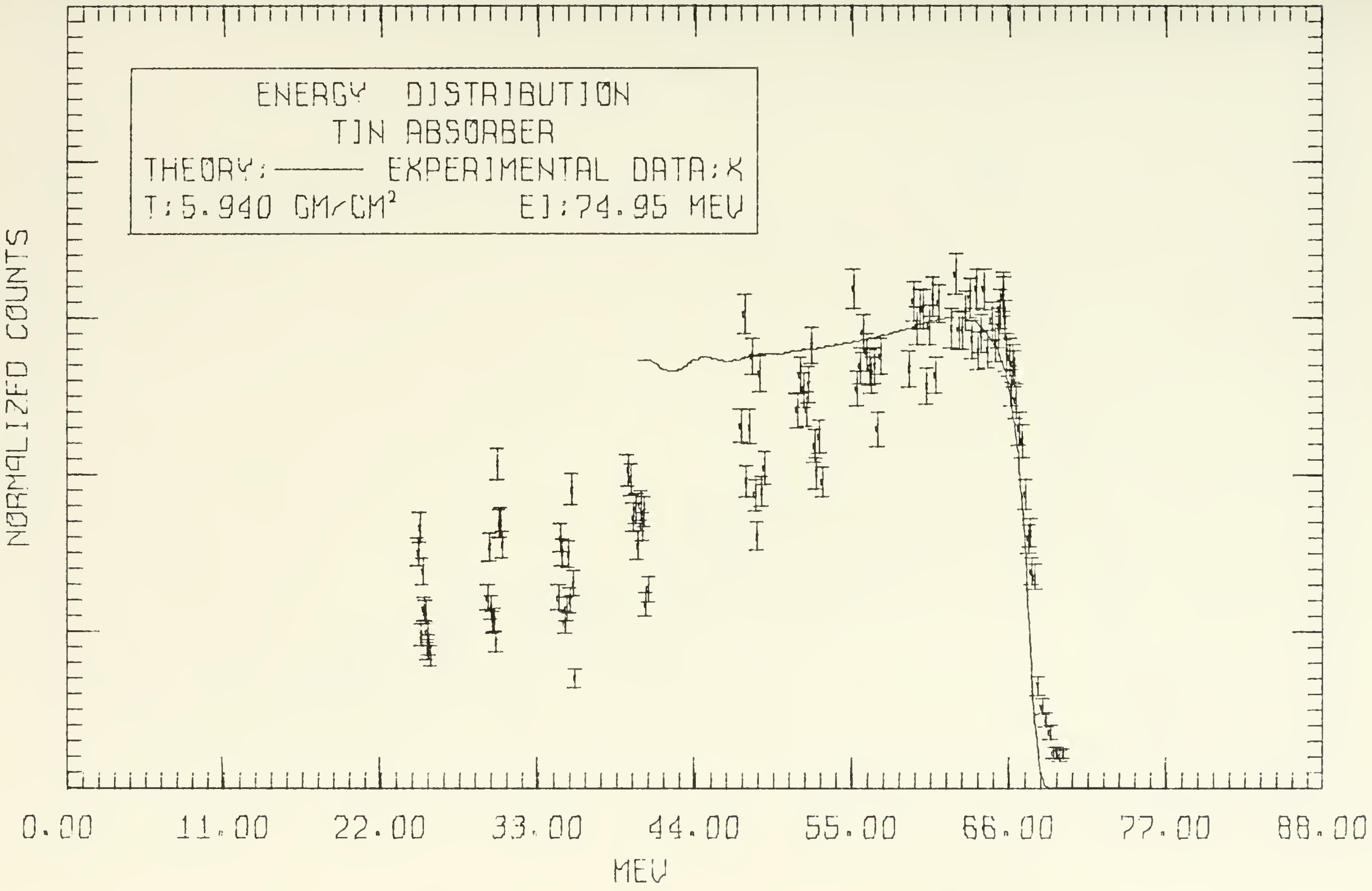
ENERGY DISTRIBUTION
TIN ABSORBER
THEORY: ——— EXPERIMENTAL DATA: X
T: 5.940 GM/CM²
EI: 74.95 MEV
NORMALIZED COUNTS
0.00
11.00
22.00
33.00
44.00
55.00
66.00
77.00
88.00
MEV

Figure 14

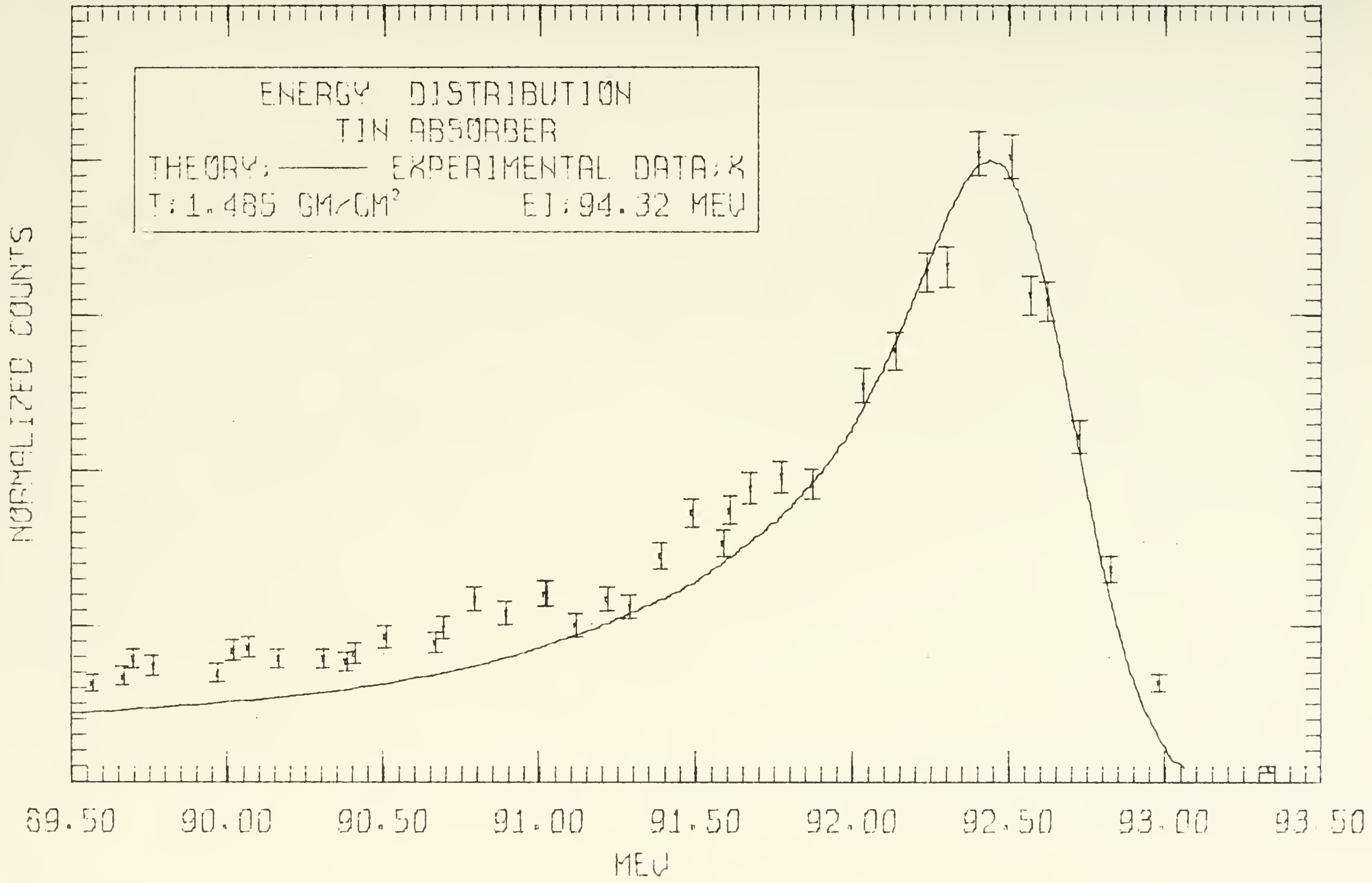
ENERGY DISTRIBUTION
TIN ABSORBER
THEORY; ——— EXPERIMENTAL DATA; X
T; 1.485 GM/CM²
EI; 94.32 MEV
NORMALIZED COUNTS
89.50
90.00
90.50
91.00
91.50
92.00
92.50
93.00
93.50
MEV

Figure 15

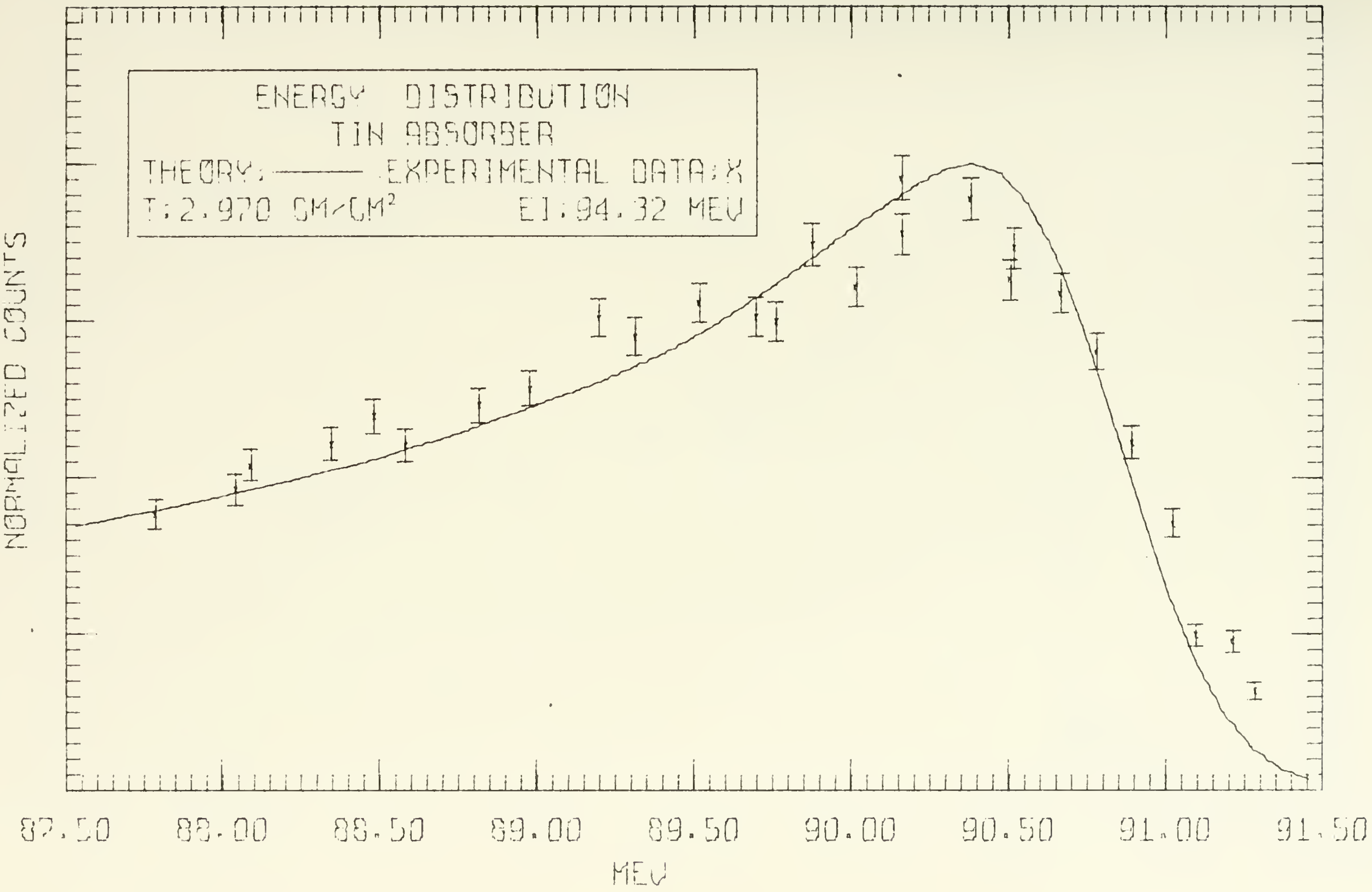
ENERGY DISTRIBUTION
TIN ABSORBER
THEORY: ——— EXPERIMENTAL DATA: X
T: 2.970 GM/CM²
EI: 94.32 MEV
NORMALIZED COUNTS
87.50
88.00
88.50
89.00
89.50
90.00
90.50
91.00
91.50
MEV

Figure 16

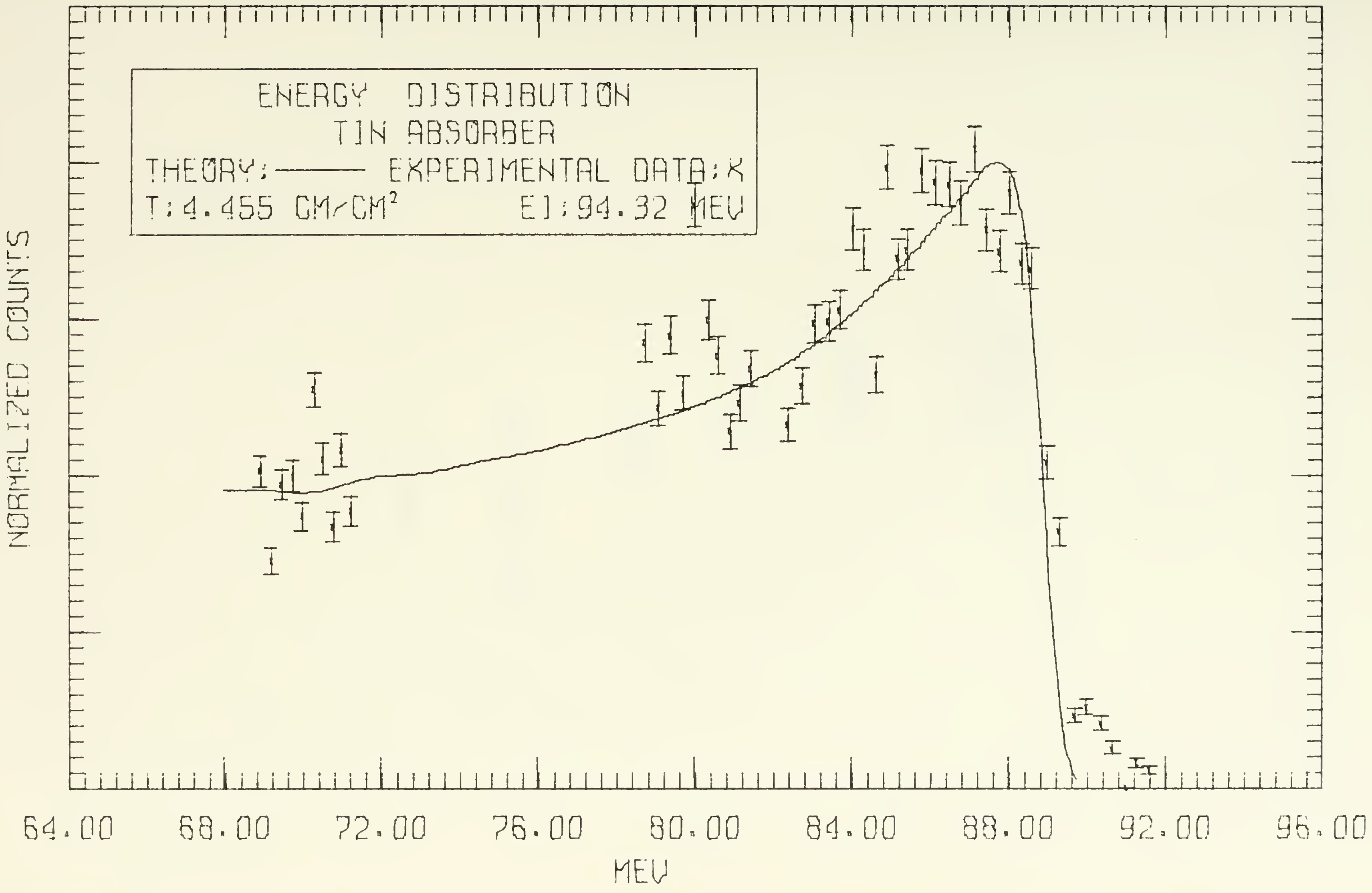
ENERGY DISTRIBUTION
TIN ABSORBER
THEORY: ——— EXPERIMENTAL DATA: K
T: 4.455 GM/CM²
EI: 94.32 MEV
NORMALIZED COUNTS
64.00
68.00
72.00
76.00
80.00
84.00
88.00
92.00
96.00
MEV

Figure 17

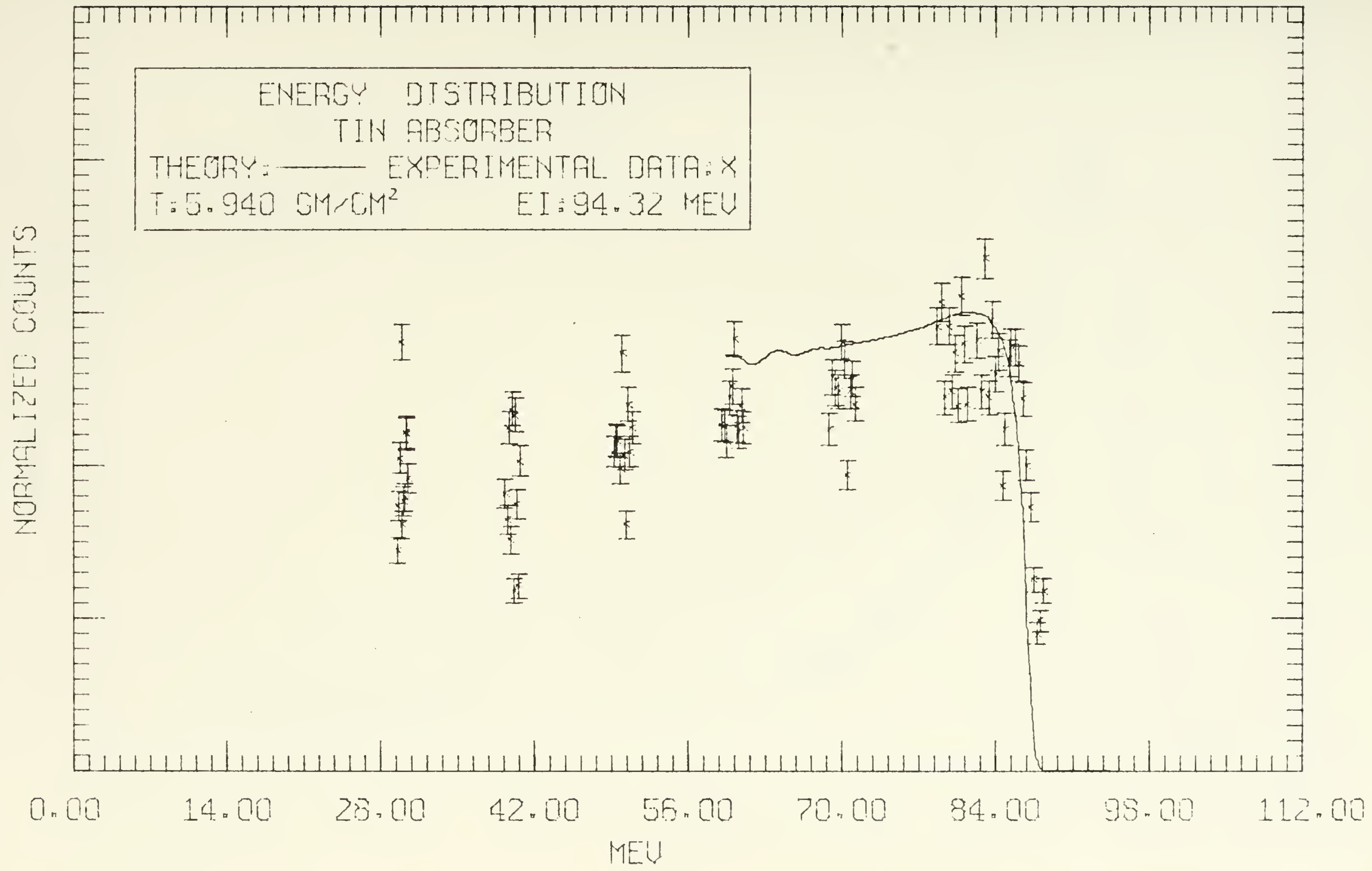
ENERGY DISTRIBUTION
TIN ABSØRBER
THEØRY: ——— EXPERIMENTAL DATA: X
T: 5.940 GM/CM²
EI: 94.32 MEV
NØRMALIZED COUNTS
0.00
14.00
28.00
42.00
56.00
70.00
84.00
98.00
112.00
MEV

Figure 18

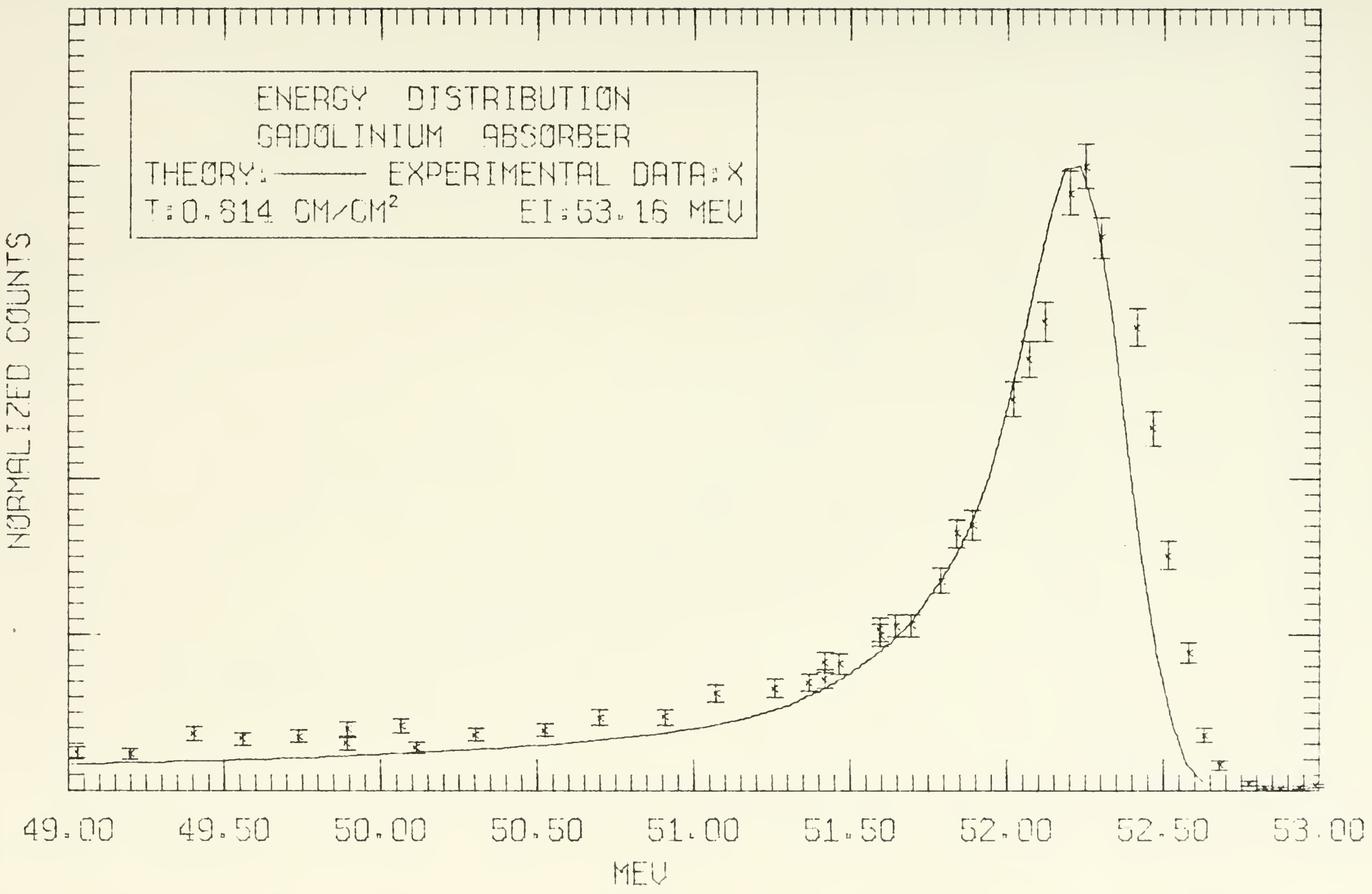
ENERGY DISTRIBUTION
GADOLINIUM ABSORBER
THEORY: ——— EXPERIMENTAL DATA: X
T: 0.814 CM/CM²
EI: 53.16 MEV
NORMALIZED COUNTS
49.00
49.50
50.00
50.50
51.00
51.50
52.00
52.50
53.00
MEV

Figure 19

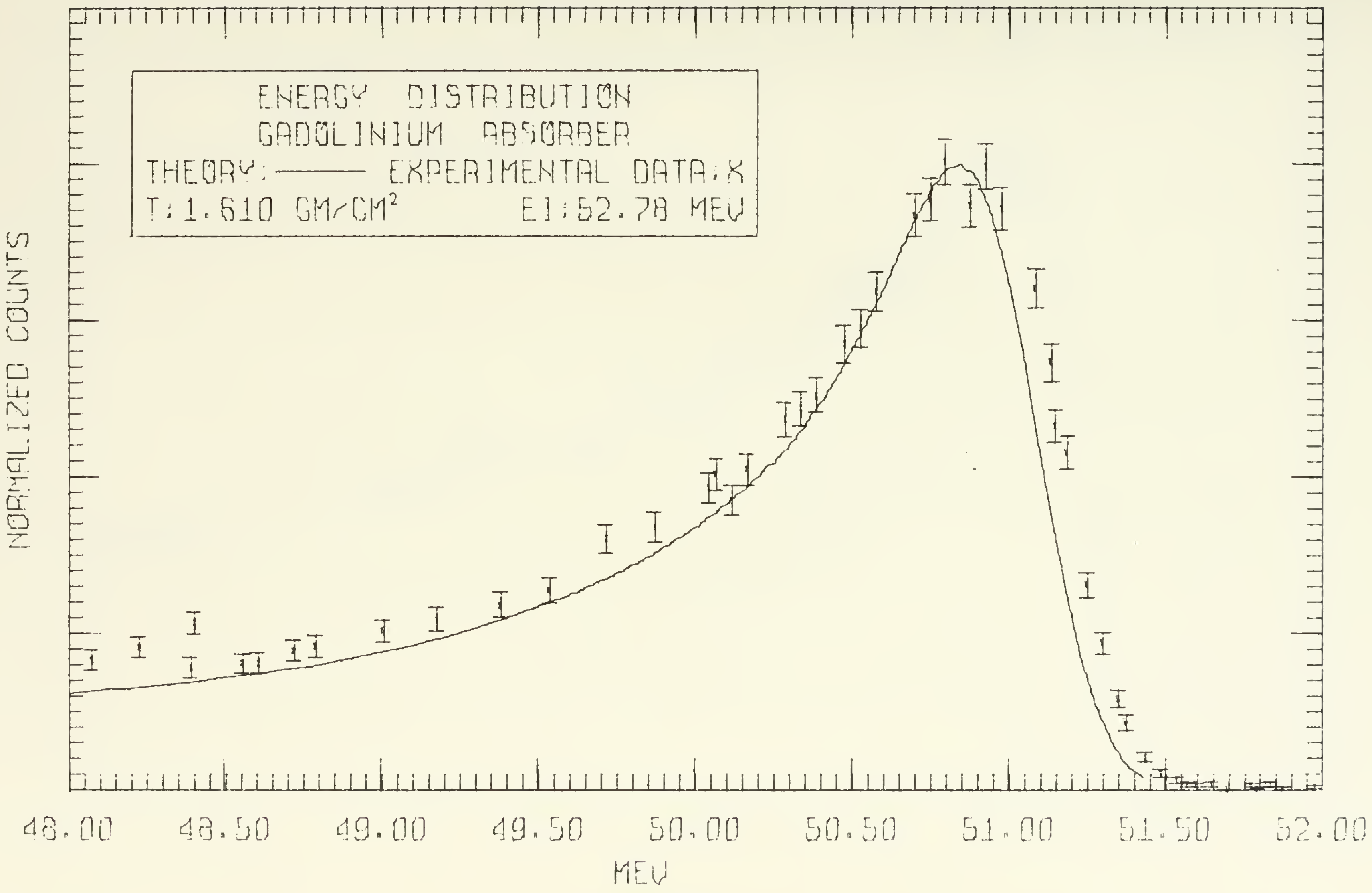
ENERGY DISTRIBUTION
GADOLINIUM ABSORBER
THEORY: ——— EXPERIMENTAL DATA: X
T: 1.610 GM/CM²
E1: 52.78 MEV
NORMALIZED COUNTS
48.00
48.50
49.00
49.50
50.00
50.50
51.00
51.50
52.00
MEV

Figure 20

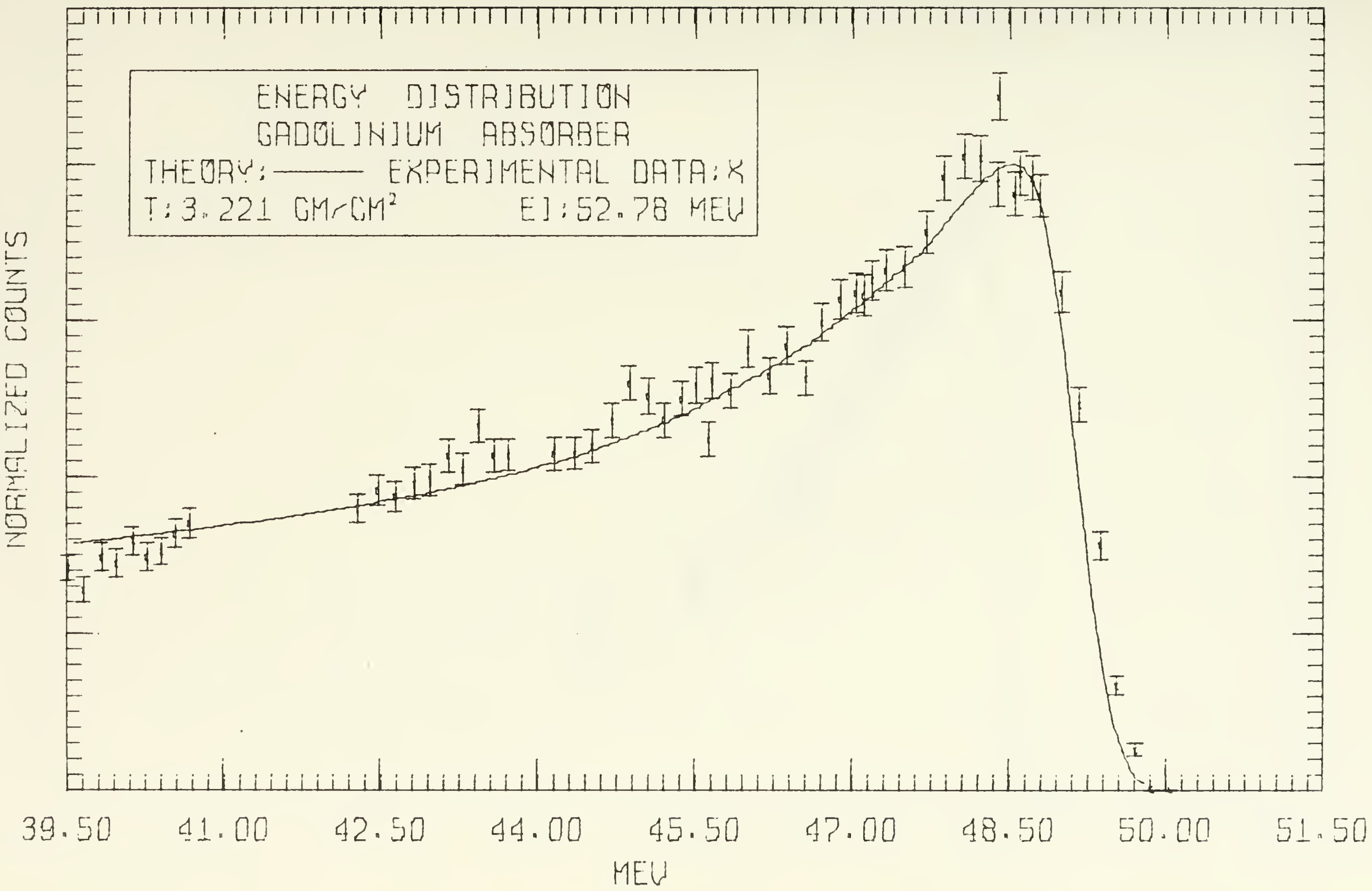
ENERGY DISTRIBUTION
GADOLINIUM ABSORBER
THEORY: ——— EXPERIMENTAL DATA: X
T: 3.221 GM/CM²
EI: 52.78 MEV
NORMALIZED COUNTS
39.50
41.00
42.50
44.00
45.50
47.00
48.50
50.00
51.50
MEV

Figure 21

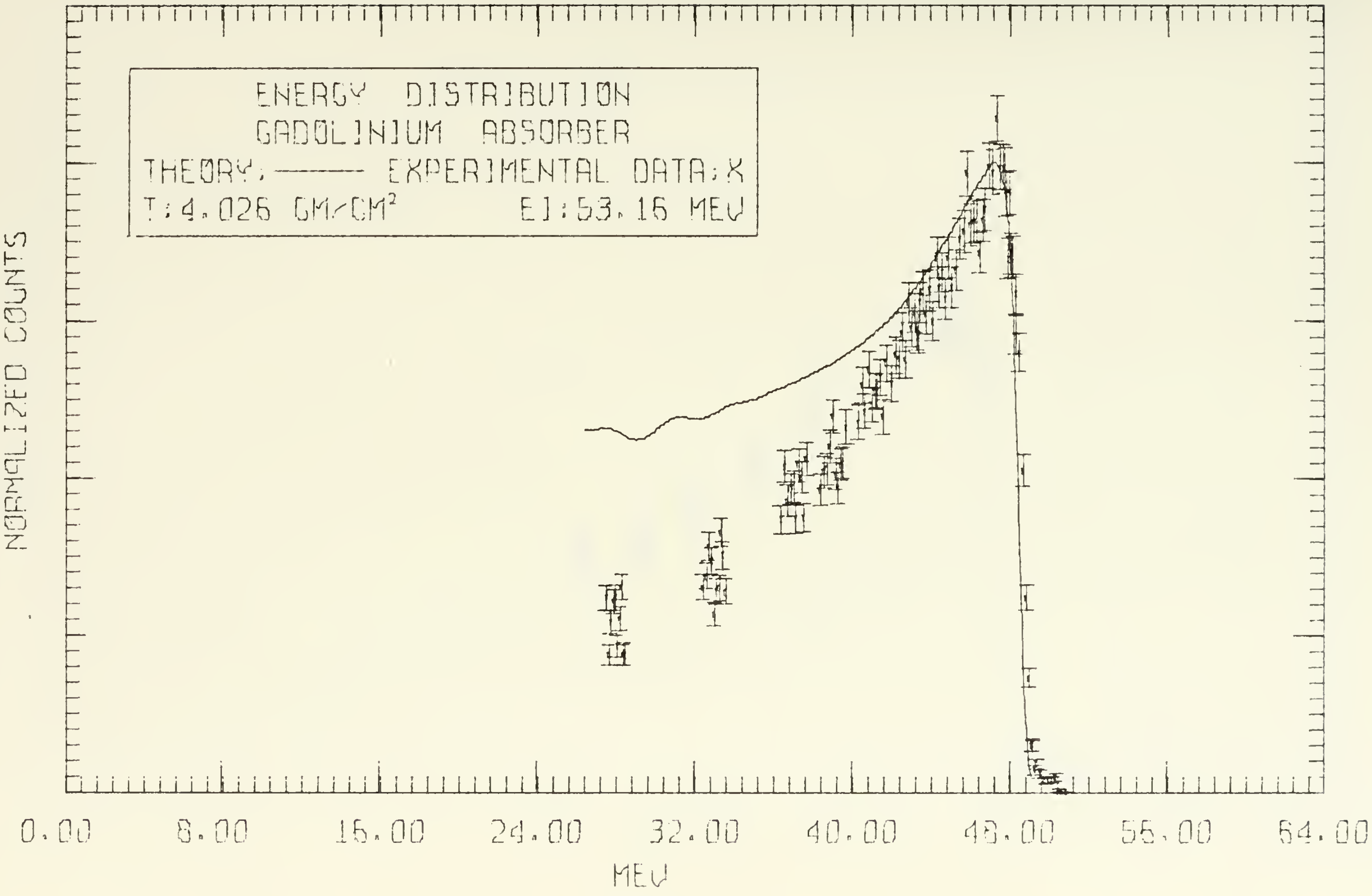
ENERGY DISTRIBUTION
GADOLINIUM ABSORBER
THEORY: ——— EXPERIMENTAL DATA: X
T: 4.026 GM/CM²
EI: 53.16 MEV
NORMALIZED COUNTS
0.00
8.00
16.00
24.00
32.00
40.00
48.00
55.00
64.00
MEV

Figure 22

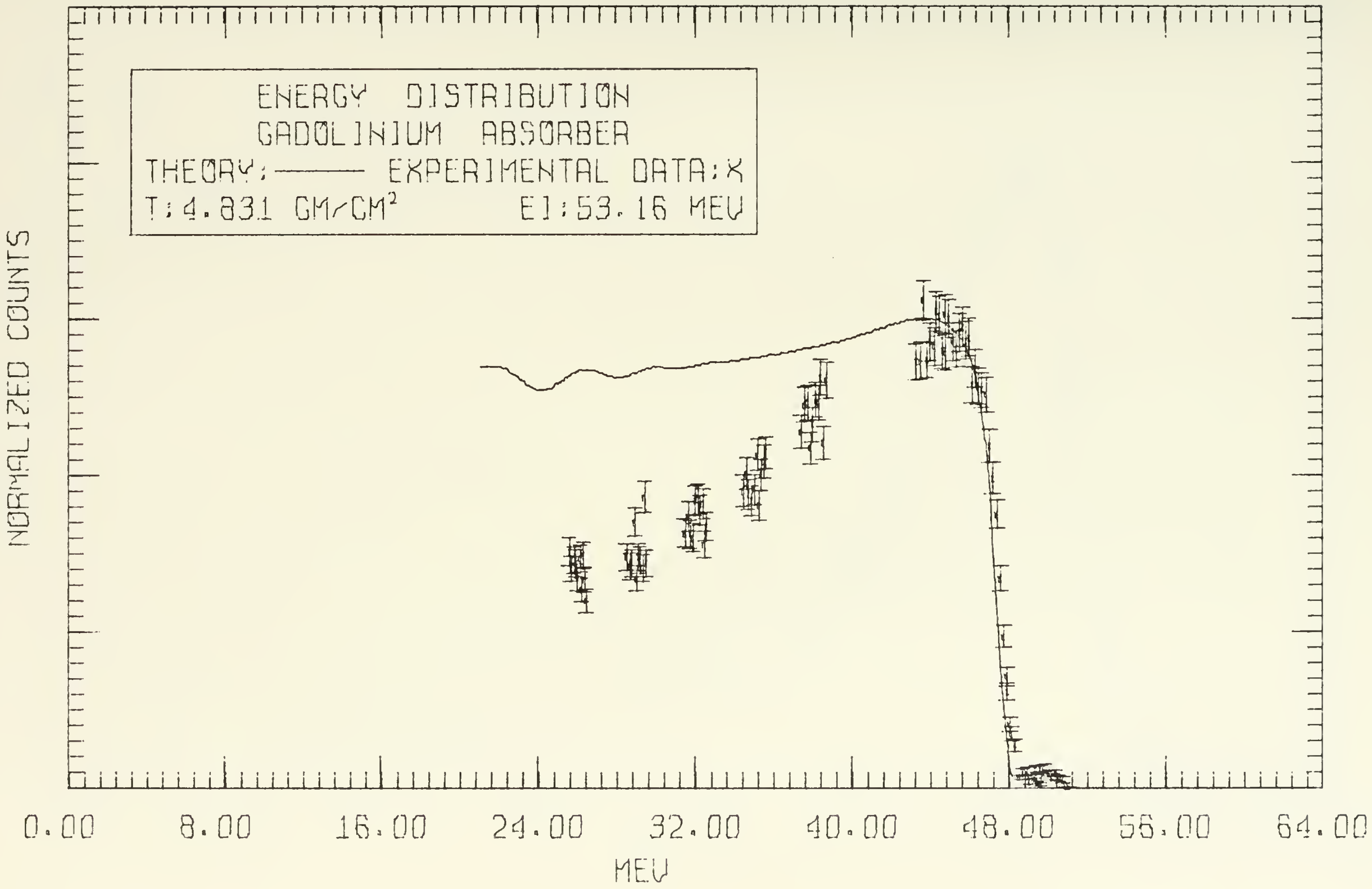
ENERGY DISTRIBUTION
GADOLINIUM ABSORBER
THEORY; ——— EXPERIMENTAL DATA: X
T; 4.831 GM/CM²
E1; 53.16 MEV
NORMALIZED COUNTS
0.00
8.00
16.00
24.00
32.00
40.00
48.00
56.00
64.00
MEV

Figure 23

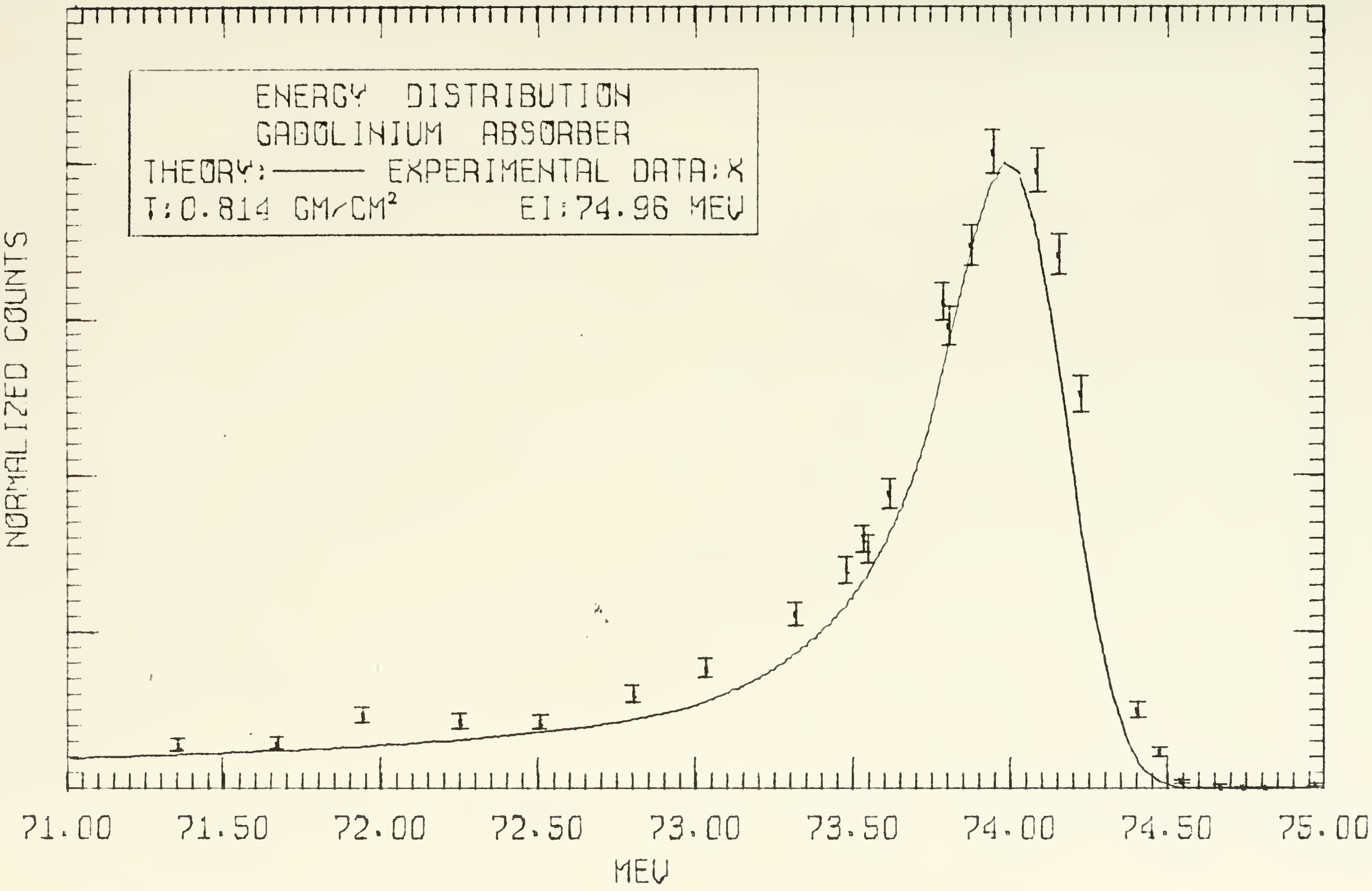
ENERGY DISTRIBUTION
GADOLINIUM ABSORBER
THEORY: —— EXPERIMENTAL DATA: X
T: 0.814 GM/CM²
EI: 74.96 MEV
NORMALIZED COUNTS
71.00
71.50
72.00
72.50
73.00
73.50
74.00
74.50
75.00
MEV

Figure 24

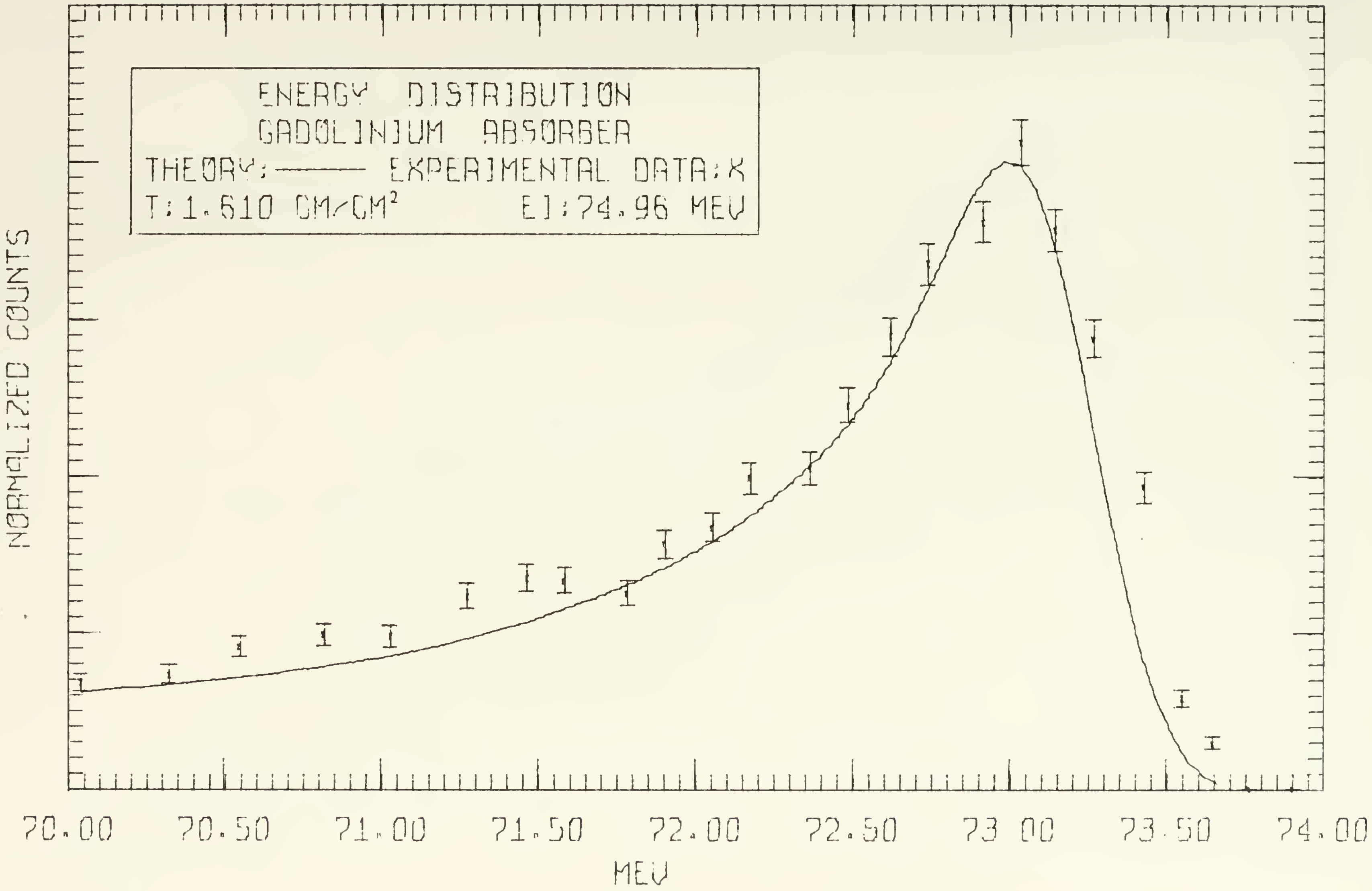
ENERGY DISTRIBUTION
GADOLINIUM ABSORBER
THEORY: ——— EXPERIMENTAL DATA: X
T: 1.610 GM/CM²
EI: 74.96 MEV
NORMALIZED COUNTS
70.00
70.50
71.00
71.50
72.00
72.50
73.00
73.50
74.00
MEV

Figure 25

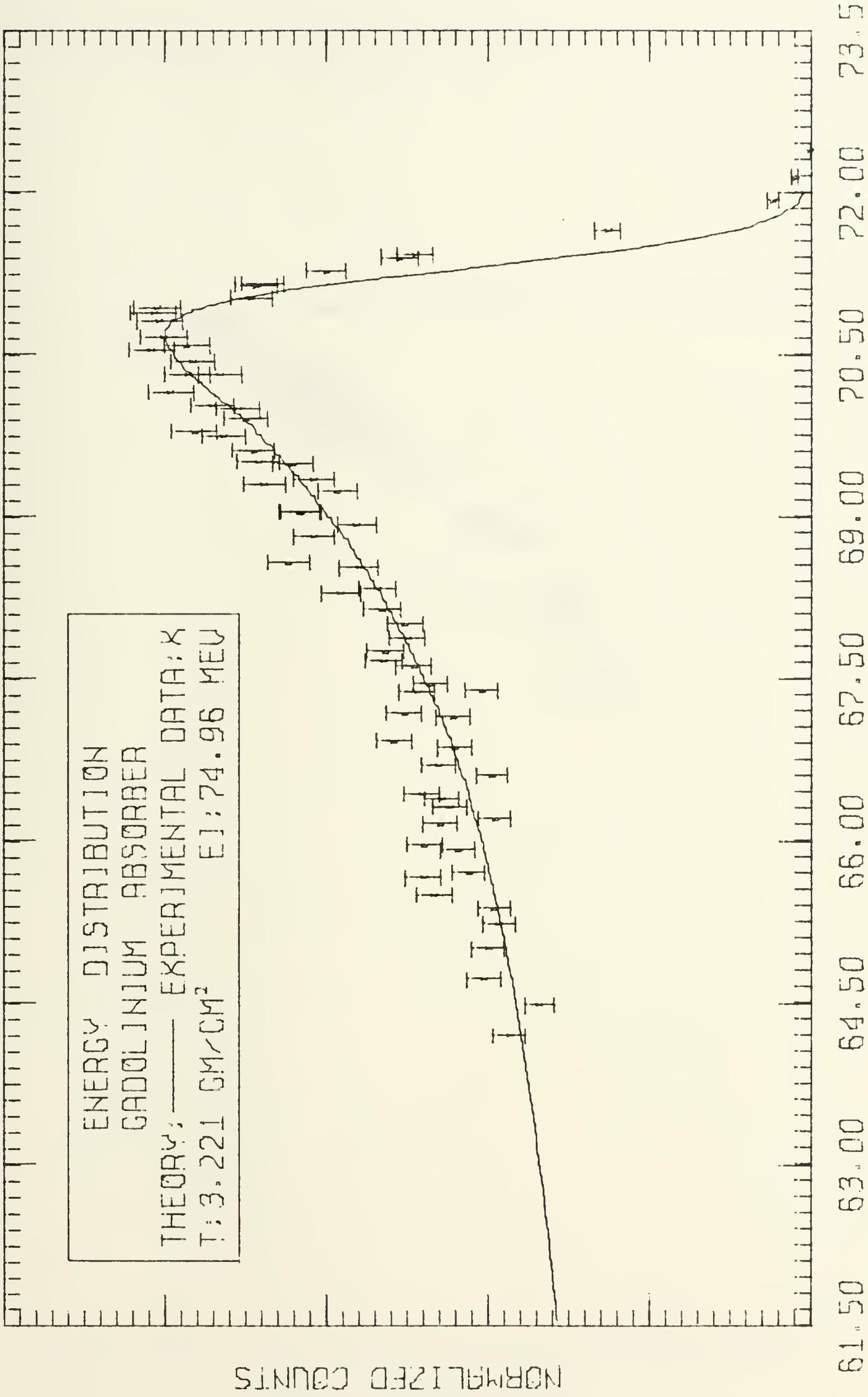
ENERGY DISTRIBUTION
GADOLINIUM ABSORBER
THEORY: ——— EXPERIMENTAL DATA: K
T: 3.221 GM/CM²   EI: 74.96 MEV
NORMALIZED COUNTS
MEV
61.50
63.00
64.50
66.00
67.50
69.00
70.50
72.00
73.50

Figure 26

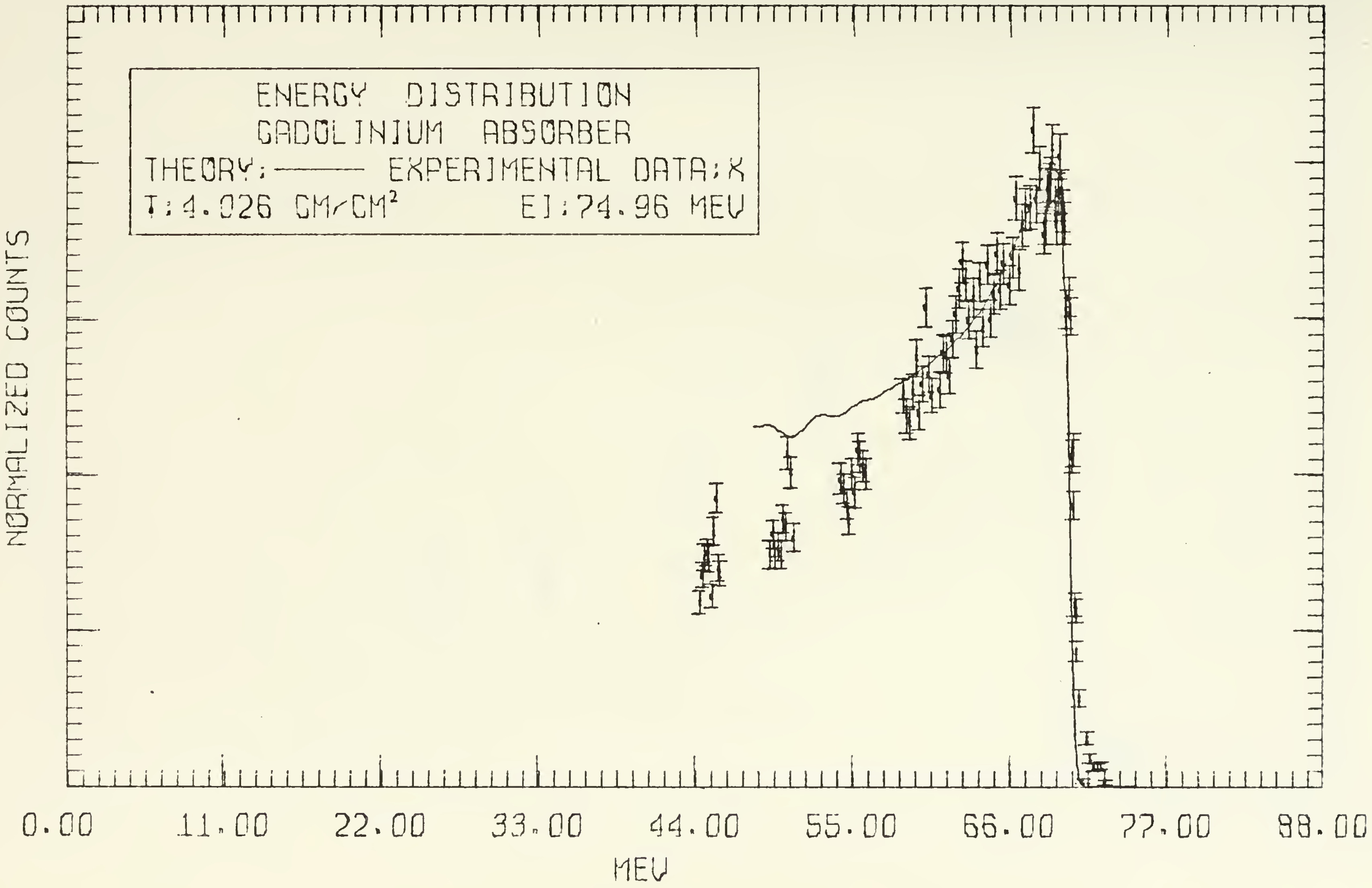
ENERGY DISTRIBUTION
GADOLINIUM ABSORBER
THEORY: ——— EXPERIMENTAL DATA: X
T: 4.026 GM/CM²
EI: 74.96 MEV
NORMALIZED COUNTS
0.00
11.00
22.00
33.00
44.00
55.00
66.00
77.00
88.00
MEV

Figure 27

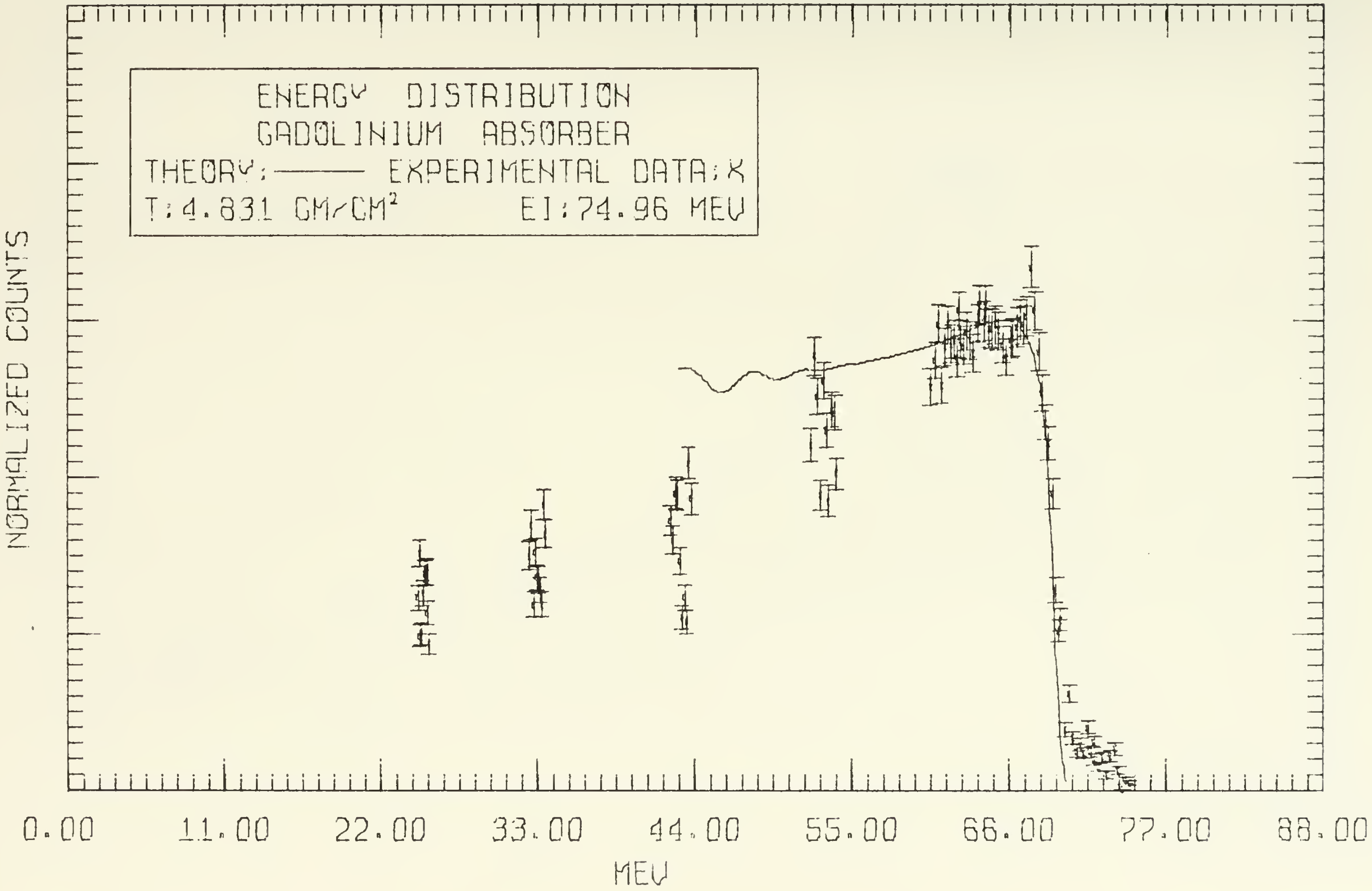
ENERGY DISTRIBUTION
GADOLINIUM ABSORBER
THEORY: ——— EXPERIMENTAL DATA: X
T: 4.831 GM/CM²
EI: 74.96 MEV
NORMALIZED COUNTS
0.00
11.00
22.00
33.00
44.00
55.00
66.00
77.00
88.00
MEV

Figure 28

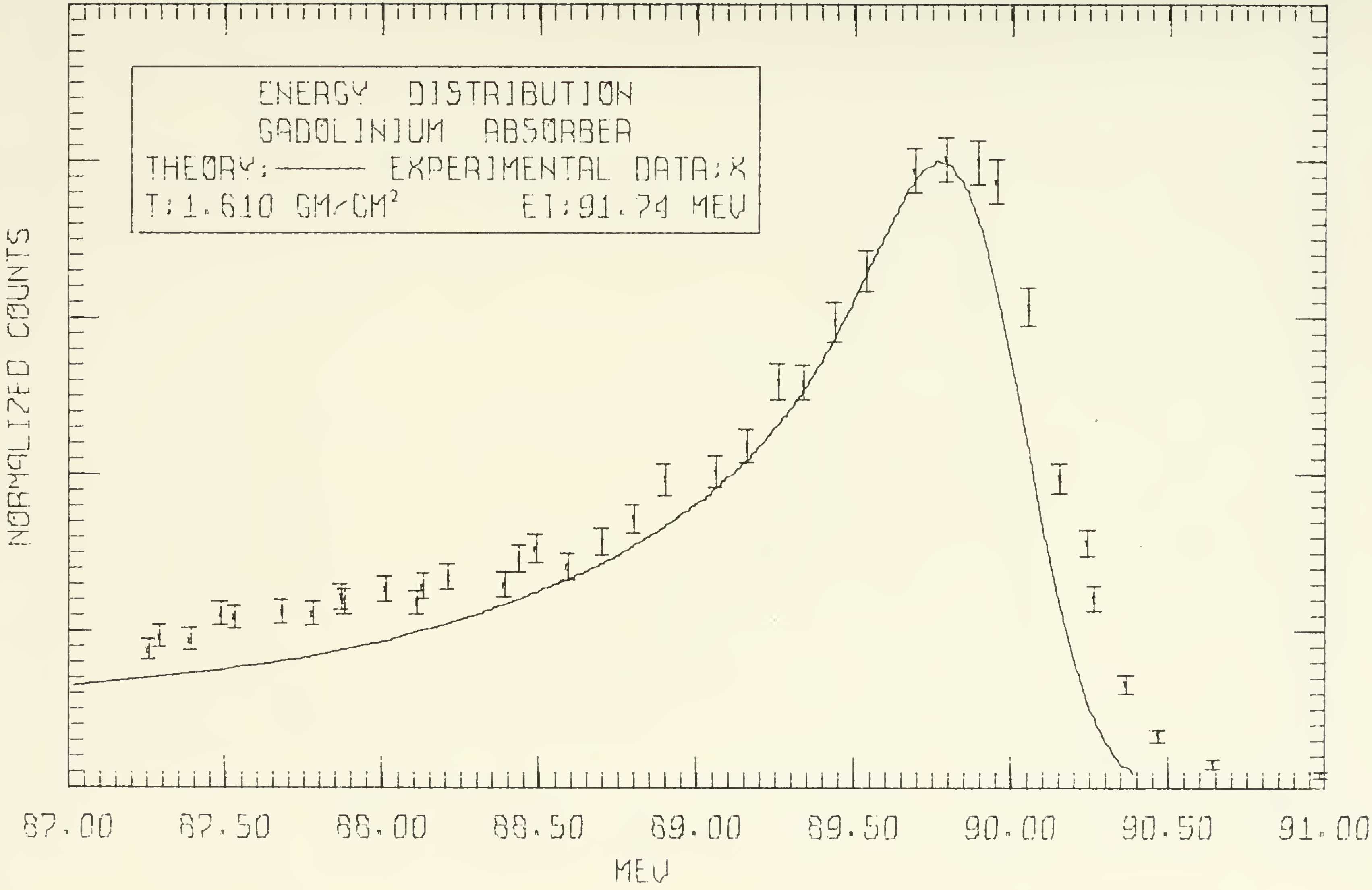
ENERGY DISTRIBUTION
GADOLINIUM ABSORBER
THEORY; ——— EXPERIMENTAL DATA; X
T; 1.610 GM/CM²
EI; 91.74 MEV
NORMALIZED COUNTS
87.00
87.50
88.00
88.50
89.00
89.50
90.00
90.50
91.00
MEV

Figure 29

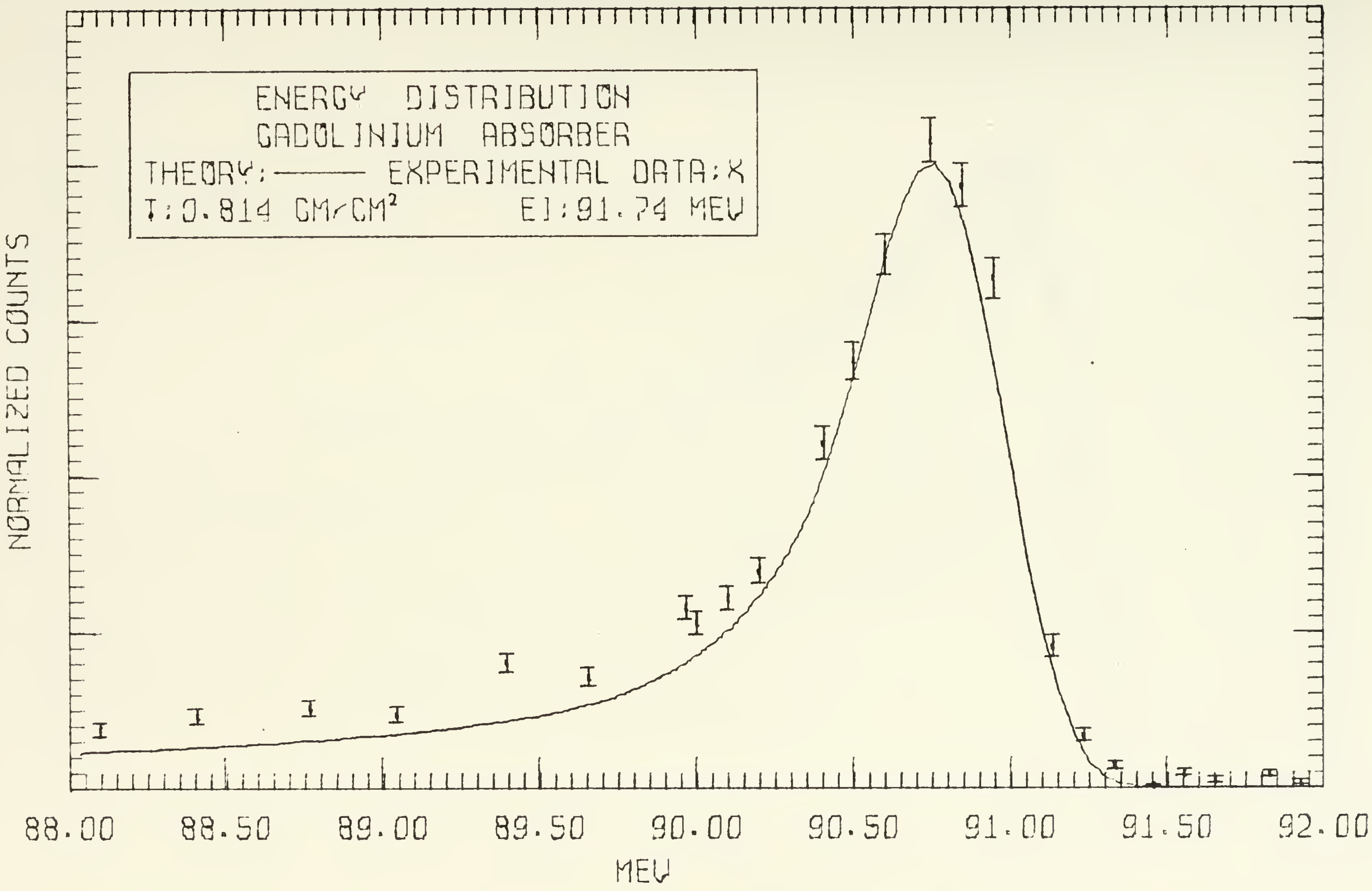
ENERGY DISTRIBUTION
GADOLINIUM ABSORBER
THEORY: ——— EXPERIMENTAL DATA: X
T: 0.814 GM/CM²
EI: 91.74 MEV
NORMALIZED COUNTS
88.00
88.50
89.00
89.50
90.00
90.50
91.00
91.50
92.00
MEV

Figure 30

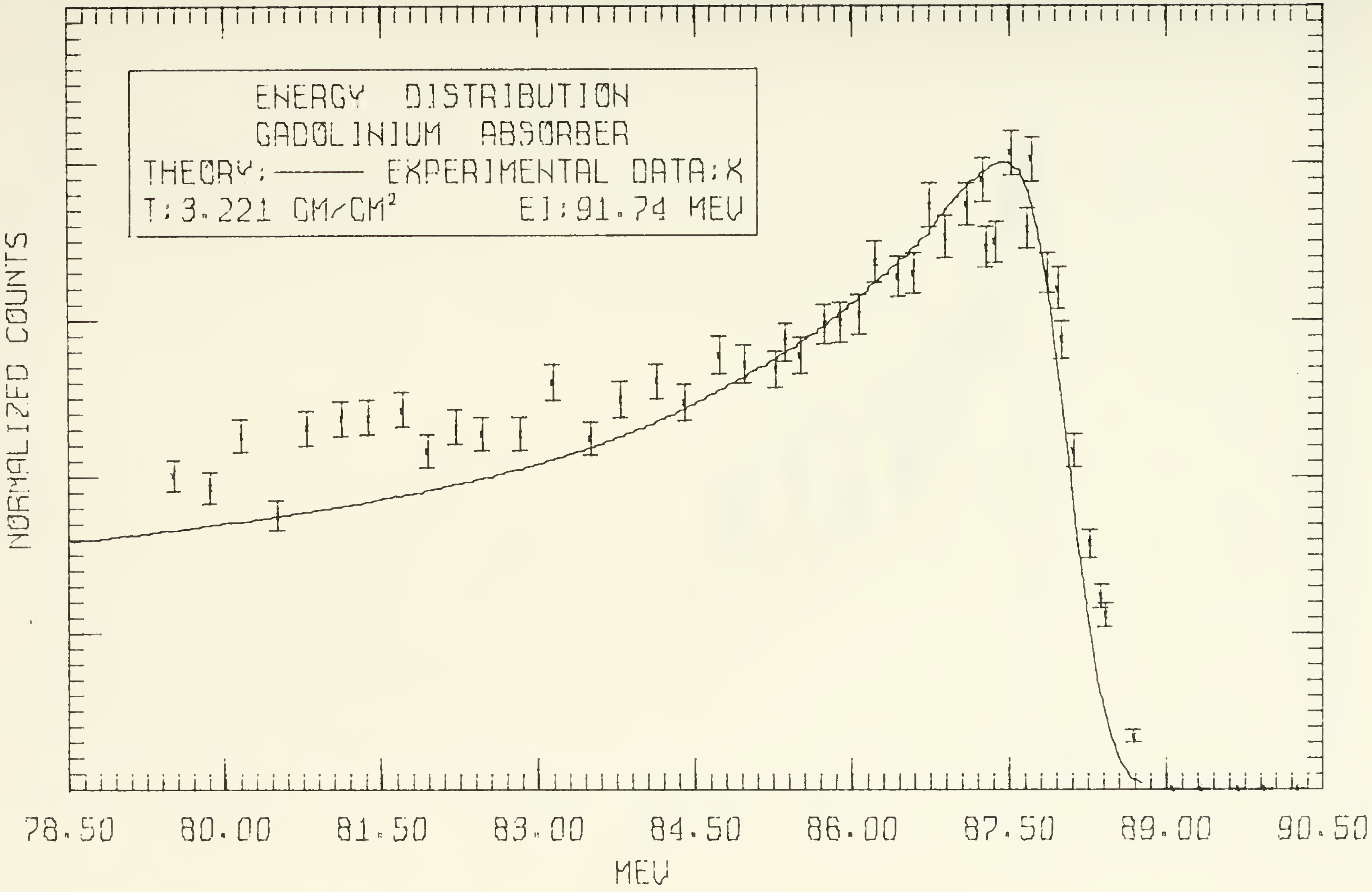
ENERGY DISTRIBUTION
GADOLINIUM ABSORBER
THEORY: ——— EXPERIMENTAL DATA: X
T: 3.221 GM/CM²
EI: 91.74 MEV
NORMALIZED COUNTS
78.50
80.00
81.50
83.00
84.50
86.00
87.50
89.00
90.50
MEV

Figure 31

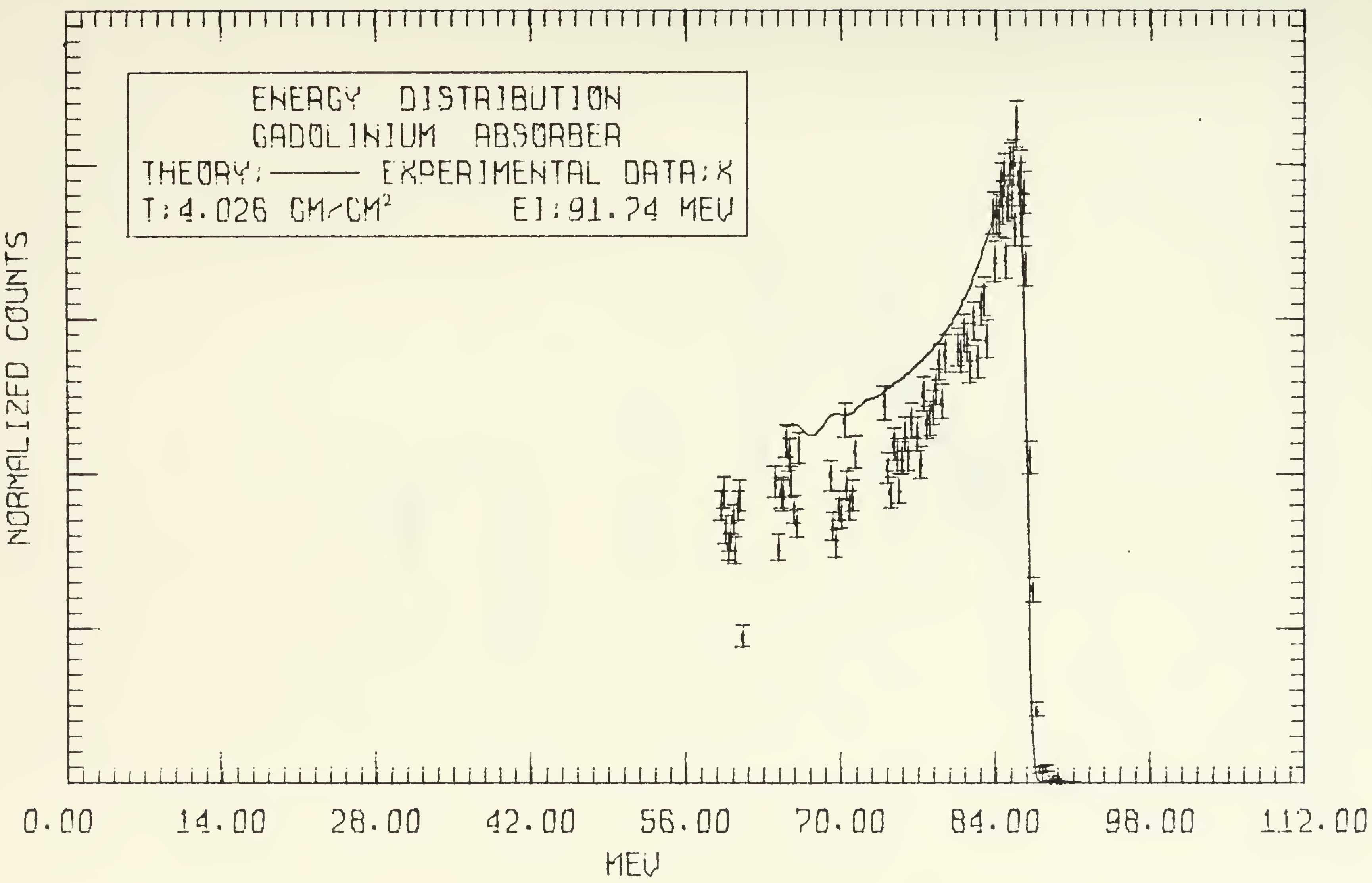
ENERGY DISTRIBUTION
GADOLINIUM ABSORBER
THEORY: ——— EXPERIMENTAL DATA: X
T: 4.026 GM/CM²
E1: 91.74 MEV
NORMALIZED COUNTS
0.00
14.00
28.00
42.00
56.00
70.00
84.00
98.00
112.00
MEV

Figure 32

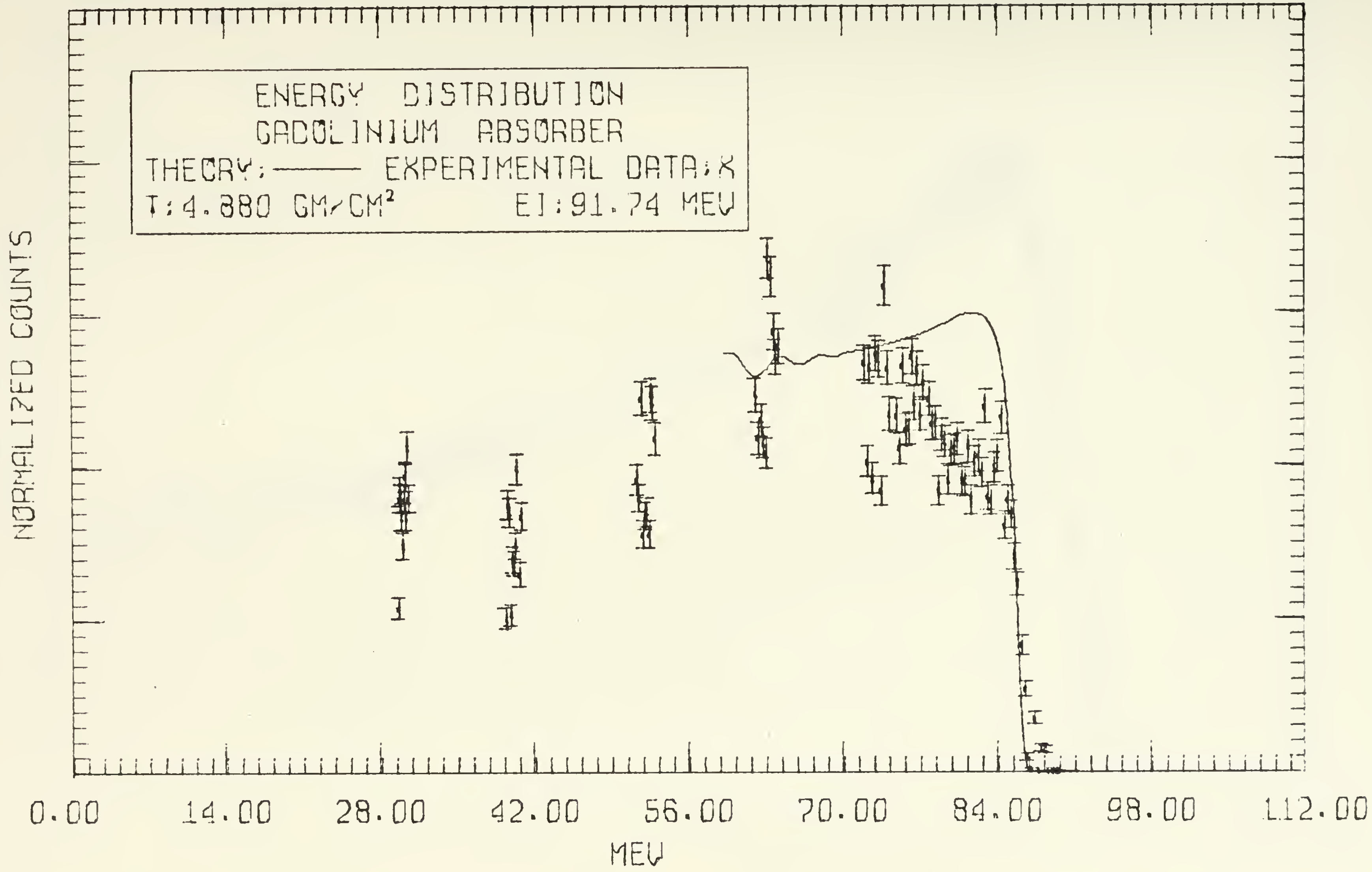
ENERGY DISTRIBUTION
GADOLINIUM ABSORBER
THEORY: ——— EXPERIMENTAL DATA: K
T: 4.880 GM/CM²
EI: 91.74 MEV
NORMALIZED COUNTS
0.00
14.00
28.00
42.00
56.00
70.00
84.00
98.00
112.00
MEV

Figure 33

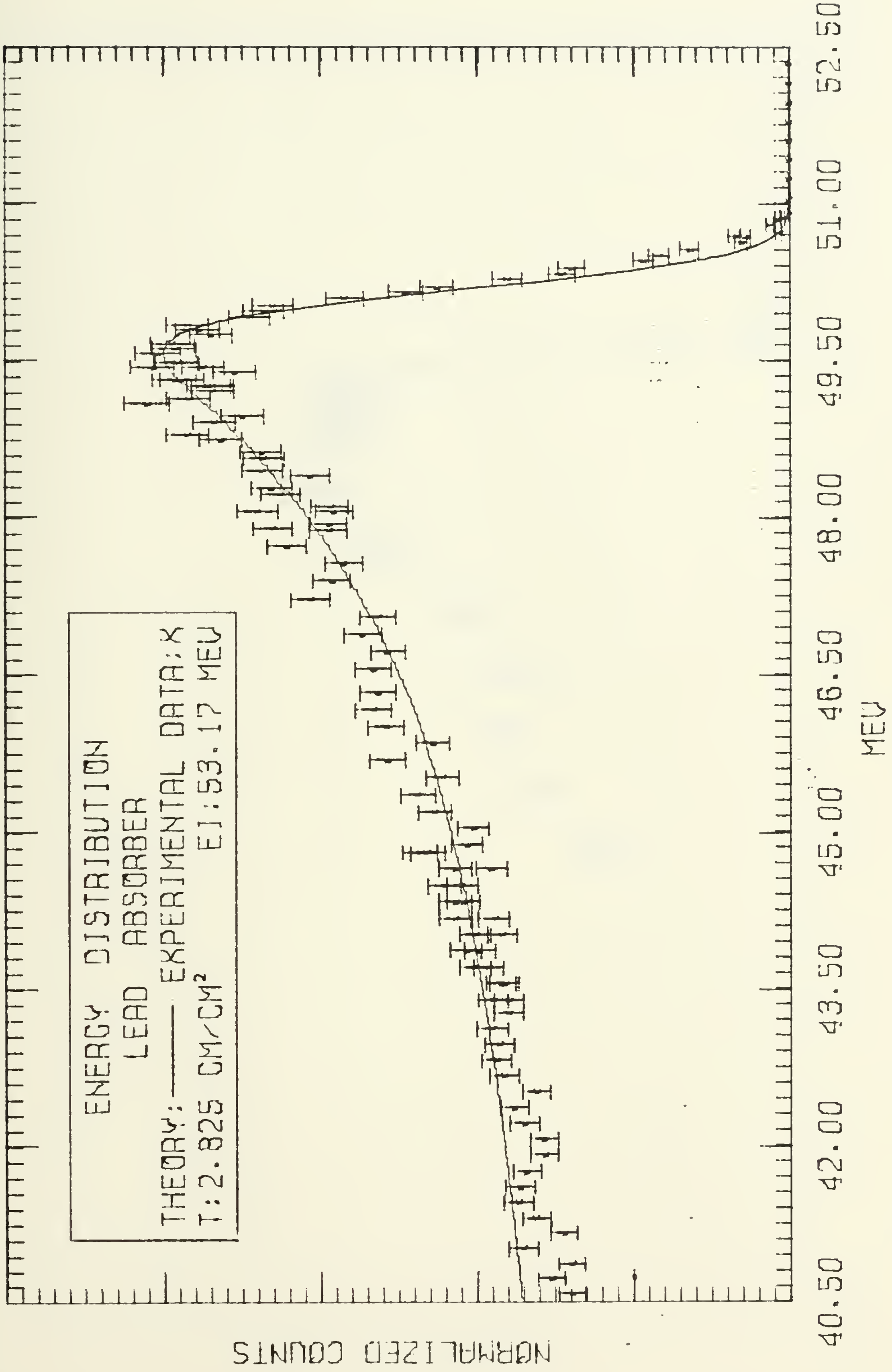
ENERGY DISTRIBUTION
LEAD ABSORBER
THEORY: —— EXPERIMENTAL DATA: X
T: 2.825 GM/CM²
EI: 53.17 MEV
40.50
42.00
43.50
45.00
46.50
48.00
49.50
51.00
52.50
MEV
NORMALIZED COUNTS

Figure 34

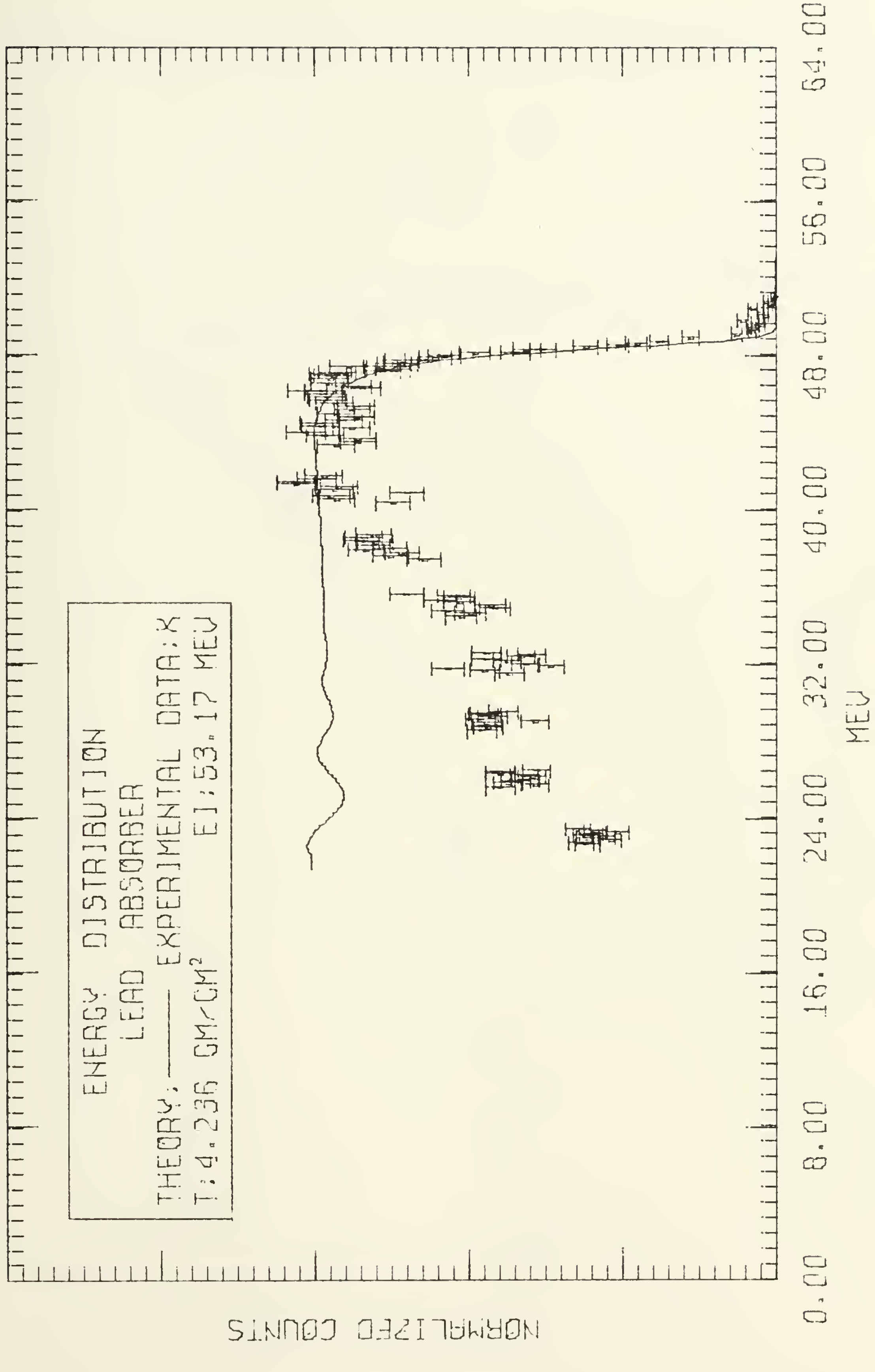
ENERGY DISTRIBUTION
LEAD ABSORBER
THEORY; —— EXPERIMENTAL DATA: X
T: 4.236 GM/CM²
E1: 53.17 MEV
0.00
8.00
16.00
24.00
32.00
40.00
48.00
56.00
64.00
MEV
NORMALIZED COUNTS

Figure 35

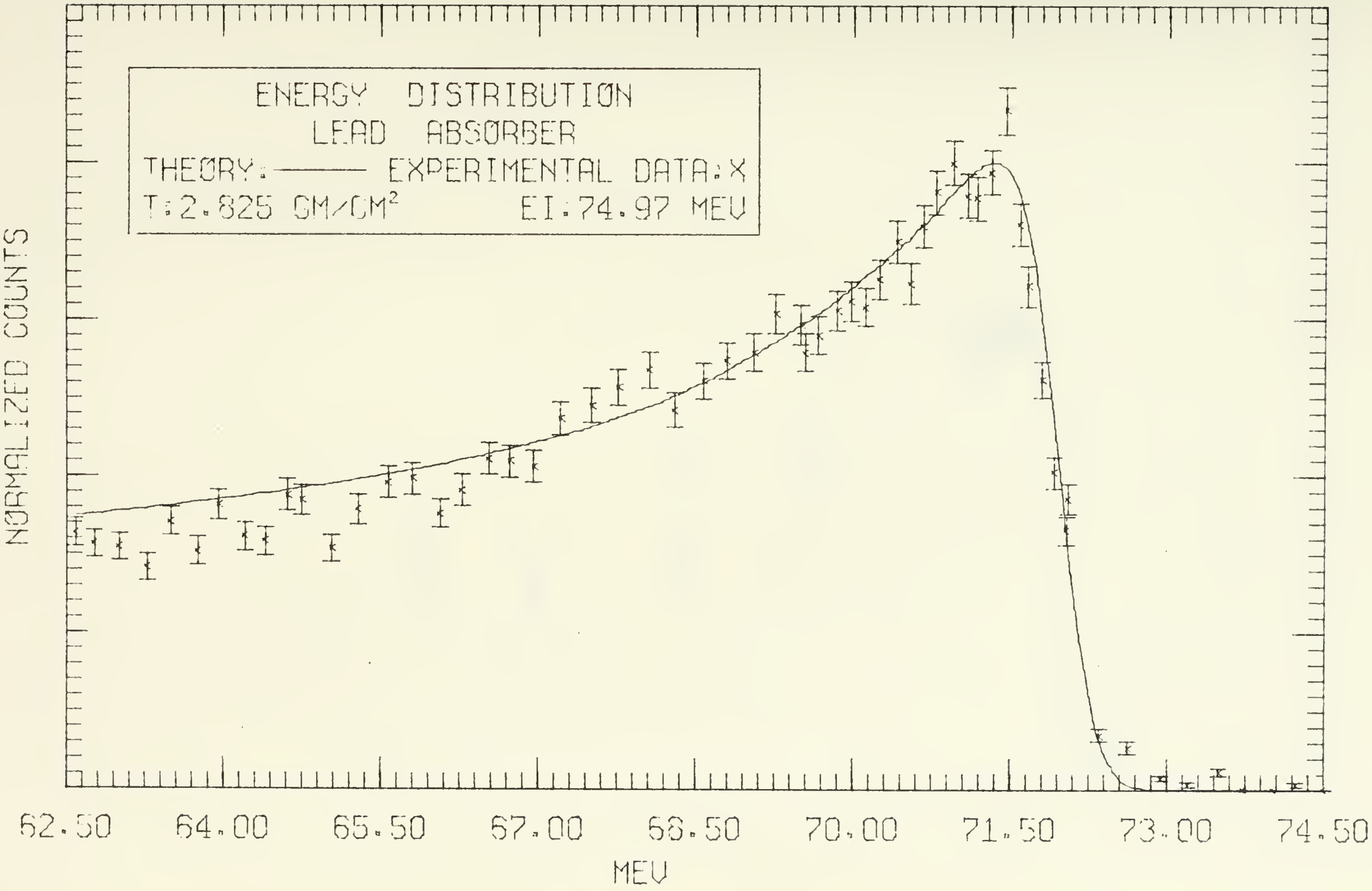
ENERGY DISTRIBUTION
LEAD ABSØRBER
THEØRY: ——— EXPERIMENTAL DATA: X
T: 2.825 GM/CM²
EI: 74.97 MEV
NØRMALIZED COUNTS
62.50
64.00
65.50
67.00
68.50
70.00
71.50
73.00
74.50
MEV

Figure 36

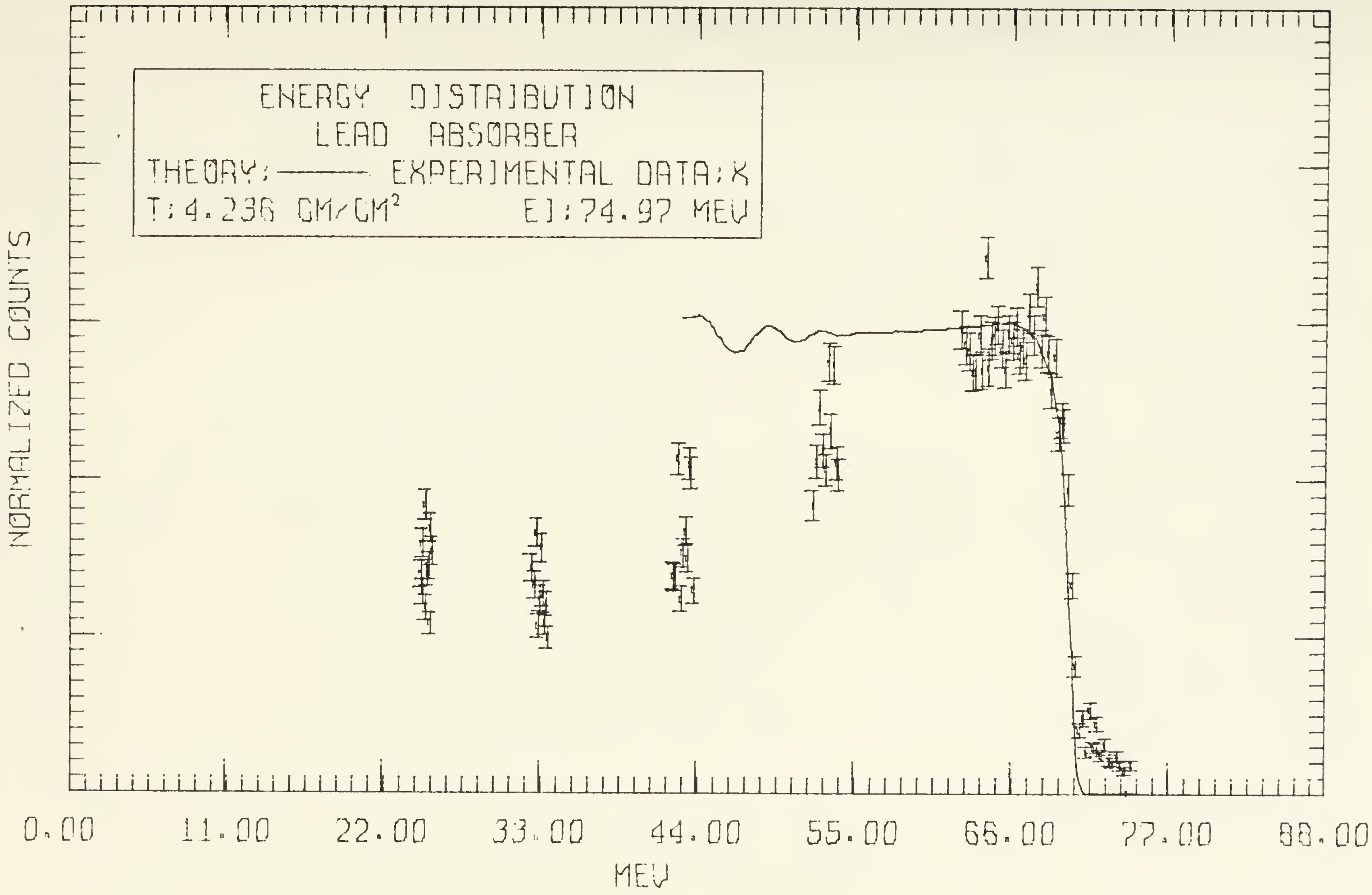
ENERGY DISTRIBUTION
LEAD ABSORBER
THEORY; ——— EXPERIMENTAL DATA; X
T; 4.236 GM/CM²
EI; 74.97 MEV
NORMALIZED COUNTS
0.00
11.00
22.00
33.00
44.00
55.00
66.00
77.00
88.00
MEV

Figure 37

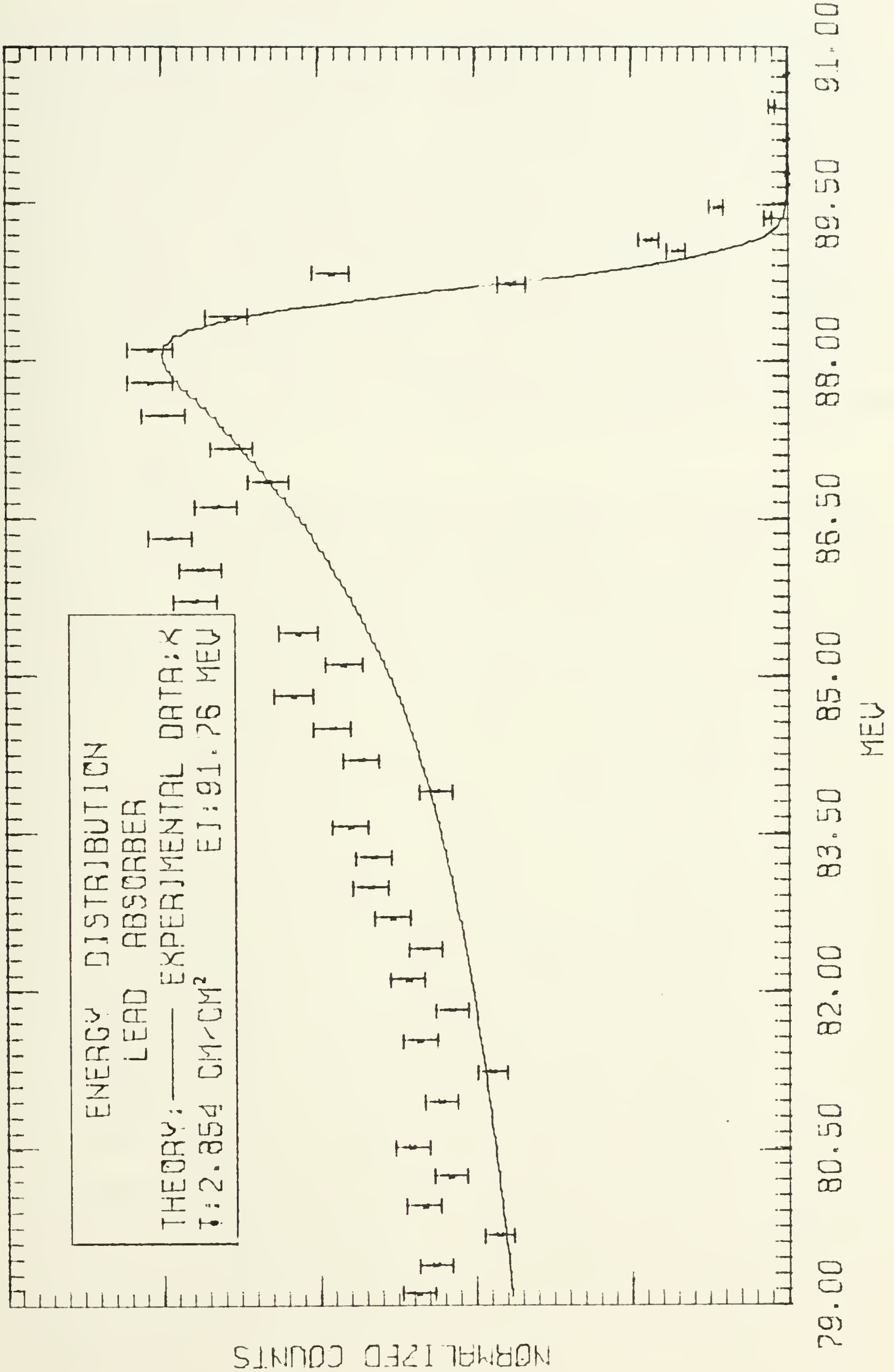
ENERGY DISTRIBUTION
LEAD ABSORBER
THEORY: ——— EXPERIMENTAL DATA: X
T: 2.854 CM/CM²
EJ: 91.76 MEV
79.00
80.50
82.00
83.50
85.00
86.50
88.00
89.50
91.00
MEV
NORMALIZED COUNTS

Figure 38

APPENDIX C - BEAM FOLDING TECHNIQUE

The theory of Blunck and Westphal [1] assumes that the beam of electrons striking the absorber is monoenergetic. The beam of electrons produced by the NPS LINAC, or any other linear accelerator, for that matter, has a finite energy spread about a maximum or most probable energy point. The fact that monoenergetic electrons are not available to strike the absorber must be taken into account in computing theoretical predictions if a meaningful comparison with experimental results is to be made. This has been done here by a technique termed "beam folding".

Beam folding is accomplished by a number of well defined steps. Energy distribution curves may be approximated by histograms. These histograms consist of a series of "bins" of area $W(Q)\Delta Q$, where Q is the energy loss and $W(Q)\Delta Q$ is the probability of loss between Q and $Q + \Delta Q$. Thus, each bin has an "address", Q, on an energy coordinate scale. To accomplish beam folding, the beam distribution must be known. This is observed experimentally and approximated in the computer by a gaussian curve of appropriate half-width. The energy at which the maximum occurs is established by the energy of the beam and the magnitude of energy loss incurred by elastic scattering of the beam as it impinges on the thin aluminum scattering foil prior to striking the absorber. The width ΔQ is then selected for the predicted distribution. This must be a small, but finite number where numerical techniques are to be used. This same width is used to break the beam distribution into a histogram. This is illustrated in figure 1(a) of this appendix. The reason the same width is used for both distributions is to facilitate computer programming.

(a) Beam Distribution

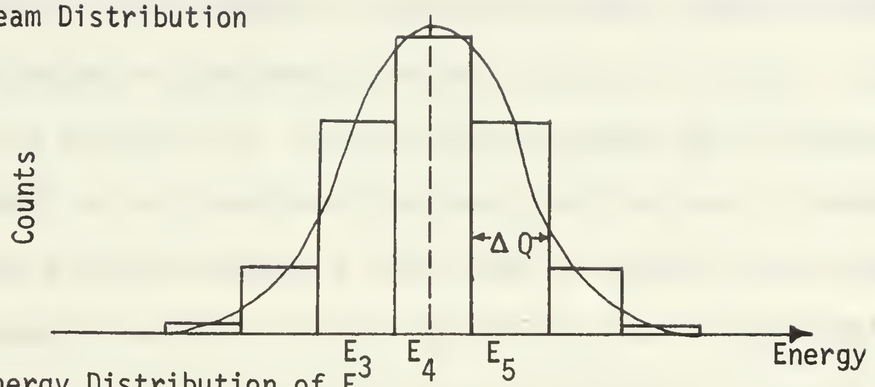

(b) Energy Distribution of E_4

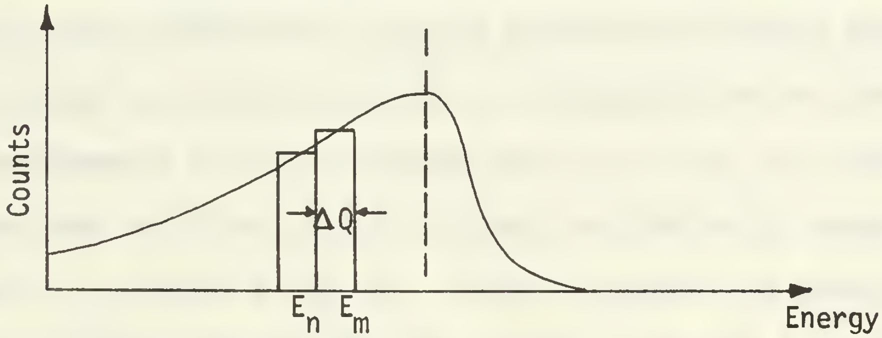

(c) Energy Distribution of E_5

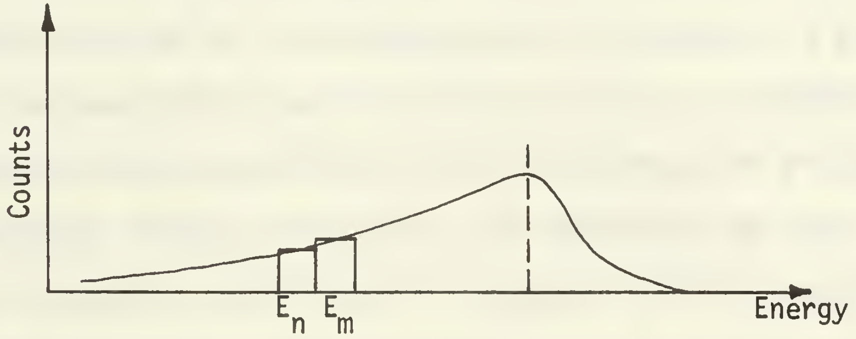

(d) Total energy Distribution

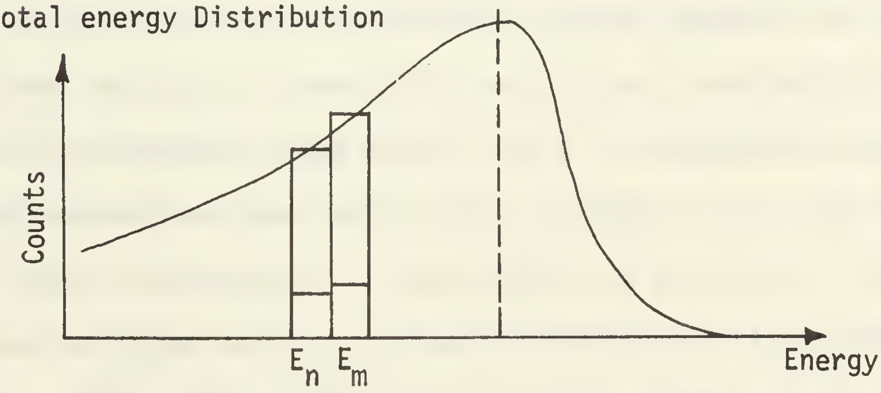

Figure 1

Each bin of the beam distribution is now treated as a monoenergetic beam with energy commensurate with its center location on the energy scale. Each bin also has a definite magnitude, or weight, with the magnitude of the center bin being unity. The formulae of Blunck and Westphal is now applied to each of these beams and an absorber distribution curve results for each, with a maximum amplitude proportional to the height of the appropriate beam distribution histogram. Each of the absorber distribution curves thus obtained may be thought of as being plotted and added to previously determined curves, using the energy of the electrons as a correlation point, as depicted in figures 1 (b), (c), and (d) of this appendix. This is accomplished on the computer by adding the contents of each bin of the same address and plotting the cumulative total. The bin of address E_x is depicted in figures 1 (b), (c), and (d). Note that the beam distribution for histogram E4 is centered over the maximum point of the distribution. This is important as a false picture could easily be presented if the histogram were not symmetrical as the distribution would then appear skewed.

Since the half-width for a particular absorber increases as the thickness (g/cm^2) increases, the beam folding technique is affected in that thick target energy distribution, whose half-width is large, will be affected much less by the finite beam distribution than will the energy distribution of a thin target whose predicted half-width is not more than 2 or 3 times the size of the beam distribution half-width. Thus, in selecting bin width (ΔQ), it is desirable to make the width proportional to the target thickness so as to apply the beam folding technique in greater detail to thin as opposed to thick targets. The computer program (Appendix D) applies the target thickness in direct proportion to establish a bin width for subsequent beam folding calculations. Thus ΔQ is much smaller for the thinner absorbers compared to thick ones.

APPENDIX D. Computer Program

```
C PURPOSE: THIS PROGRAM ACCEPTS PARAMETERS FROM ENERGY LOSS
C    EXPERIMENTS CONDUCTED ON THE LINAC AND WILL COMPUTE
C    THEORETICAL HALFWIDTH AND MOST PROBABLE ENERGY LOSS AND
C    WILL PLOT BOTH THE EXPERIMENTAL AND THEORETICAL ENERGY
C    DISTRIBUTION FOR THE EXPERIMENT.
C
C SCOPE: THE PROGRAM IS SET UP TO MAKE COMPUTATIONS RELATIVE
C    TO EXPERIMENTATION WITH ALUMINUM,COPPER,TIN,GADOLINIUM
C    AND LEAD.
C
C METHOD: THE PROGRAM PLOTS A THEORY CURVE BASED ON THE FIT
C    OF GAUSSIAN CURVES PERFORMED BY BLUNCK AND WESTPHAL FOR
C    THE PREDICTED ENERGY DISTRIBUTION CURVES.  THE INTEGRA-
C    TION OVER ENERGY LOSS INDICATED IN THE AFOREMENTIONED
C    PAPER IS PERFORMED ON THE COMPUTER USING 32 POINT GAUSS
C    QUADRATURE.  TWO GRAPHS ARE PLOTTED: ONE REPRESENTS THE
C    B-W PREDICTION WITH A MONENERGETIC BEAM OF ELECTRONS AND
C    THE OTHER, WHICH ALSO HAS EXPERIMENTAL RESULTS THEREON,
C    REPRESENTS THE SAME THEORY WITH A POLYENERGETIC BEAM
C    DISTRIBUTION FOLDED IN.
C
C THIS PROGRAM IS WRITTEN USING FORTRAN IV LANGUAGE AND THE
C    NPS COMPUTER FACILITY PLOTTING PACKAGE.  TOTAL RUNNING
C    TIME IS ABOUT 25/T MINUTES, WHERE T IS THE ABSORBER
C    THICKNESS IN GM/SQ CM.
C
      IMPLICIT REAL*8(A-H,O-Z)
C
C ESTABLISH TITLES FOR PLOTS.
C
      REAL*8 T1(4)/'          ENERGY  DISTRIBUTION        '/
      REAL*8 T3(4)/'           ALUMINUM  ABSORBER         '/
      REAL*8 T4(4)/'T:          GM/CM        EI:       MEV'/
      REAL*8 T5(4)/'            UNFOLDED  THEORY          '/
      REAL*8 T6(4)/'THEORY:          EXPERIMENTAL DATA:X'/
      REAL*8 T7(4)/'             LEAD  ABSORBER           '/
      REAL*8 T8(4)/'              TIN ABSORBER            '/
      REAL*8 T9(4)/'          GADOLINIUM  ABSORBER        '/
      REAL*8 T10(4)/'            COPPER  ABSORBER          '/
      DIMENSION E(50),WE(50),WOT(300),HW(300),XX(300),
     1WUF(300),XUF(300),EXX(200),EXY(200),IXY(200),T2(4)
      EXTERNAL FCT,BEAM,WION,WRAD
      DO1200 J=1,50
      E(J)=0
 1200 WE(J)=0
      DO1201 J=1,200
      EXX(J)=0
      EXY(J)=0
 1201 IXY(J)=0
      DO1202 J=1,300
      WOT(J)=0
      HW(J)=0
      XX(J)=0
      WUF(J)=0
 1202 XUF(J)=0
C
C READ IN PARAMETERS FOR EXPERIMENT.
C   EB        BEAM ENERGY
C   Z         ATOMIC NUMBER
C   A         ATOMIC WEIGHT
C   T         TARGET THICKNESS: GM/SQ CM
C   QZERO     SPECTROMETER INDICATION OF LOCATION OF BEAM
C                DISTRIBUTION (MEV)
C   CTSNOR    NUMBER TO WHICH EXPERIMENTAL COUNTS WILL BE
C                NORMALIZED
C   HT        HALFWIDTH OF BEAM DISTRIBUTION
```

```
      READ(5,11) EB,Z,A,T,QZERO,CTSNOR,HT
C
C DIVIDE ZERO PEAK INTO "BINS" OF WIDTH DELX.  BIN WIDTH
C   INCREASES WITH TARGET THICKNESS.
C
      DELX=.03*T
      IF(T.LT.1.) DELX=.06*T
C
C QAVE IS THE RECOIL LOSS OF ELECTRONS STRIKING ALUMINUM
C   NUCLEII OF THE SCATTERING FOIL.  IONIZATION LOSS IN
C   SCATTERER IS NEGLECTED.
C
      QAVE=EB*EB/(931.4*A)
C
C CORR IS THE CORRECTION TO BE ADDED TO EXPERIMENTAL ENERGY
C   TO CORRECT FOR SPECTROMETER ERROR.
C
      CORR=QZERO-QAVE
   12 FORMAT(5(1X,F8.3,1X,I6))
C
C READ IN UP TO 200 EXPERIMENTAL POINTS; EXX IS ENERGY (MEV)
C   AND IXY IS COUNTS.  THERE MUST BE 40 DATA CARDS AND THE
C   LAST EXX MUST BE ZERO.
C
      READ(5,12) (EXX(J),IXY(J),J=1,200)
C
C ESTABLISH PARAMETERS FOR SCATTERING FOIL.
C
      FOIL=.024
      ZFOIL=13.
      KSIG=0
      DO 1 J=1,200
    1 EXY(J)=IXY(J)
      M=0
C
C EI IS VALUE OF BEAM ENERGY INCIDENT ON TARGET.
C
      EI=EB-QAVE
      TEMP=EI
C
C THE FOLLOWING PORTION OF THE PROGRAM UNFOLDS BEAM DISTRI-
C   BUTION.  ICENT IS AN INTEGER VALUE ASSIGNED TO THE
C   HISTOGRAM CENTERED OVER THE PEAK OF THE BEAM DISTRIBU-
C   TION.  EACH HISTOGRAM IS DENOTED BY ITS ENERGY E AND
C   MAGNITUDE RELATIVE TO THE PEAK OF THE DISTRIBUTION, WE.
C
      ICENT=(HT+DELX)/DELX
      X=EI-ICENT*DELX
  202 X=X+DELX
      IF(X.GT.(EI+HT)) GOTO 1003
      M=M+1
      E(M)=X
C
C FUNCTION BEAM REPLICATES THE DISTRIBUTION OF BEAM ENERGY
C   AS A SIMPLE GAUSSIAN CURVE BASED ON THE EXPERIMENTALLY
C   OBSERVED HALFWIDTH AND IS LOCATED RELATIVE TO THE BEAM
C   ENERGY BY THE COMPUTED AVERAGE RECOIL LOSS.
C
      WE(M)=BEAM(EI,HT,X)
      GOTO202
 1003 WRITE(6,22) QAVE,HT,FOIL,ZFOIL,EI
      DO 1006 L=1,M
      DX=0
      N=0
 1005 N=N+1
C
C USING EACH HISTOGRAM AS A "BEAM", THE FOLLOWING PORTION OF
C   THE PROGRAM COMPUTES AN ENERGY DISTRIBUTION FOR EACH
C   OF THESE "BEAMS" AND STORES THEM IN "BINS" LABELED BY
C   ENERGY, XX.  THE CUMULATIVE AMOUNT OF ELECTRON COUNTS IN
C   THE BIN IS WQT.  Q IS THE ENERGY LOSS OVER WHICH THE B-W
C   PREDICTION IS INTEGRATED AND DX IS THE AMOUNT BY WHICH
```

```
C    Q CHANGES FOR EACH SUCCESSIVE INTEGRATION.   INTEGRATION
C    IS CARRIED OUT IN SUBROUTINE DQG32.
C
      DX=DX+DELX
      Q=3.0*T*(7/13.)**.50-DX
      IF(Q.LT.EI)GOTO1004
      N=0
      GOTO1005
 1004 IF(Q.LT.0)GOTO1006
      EI=E(L)
      XL=.0000001*Q
      VALIM=.25*Q
      CALL DQG32(0.,XL    ,FCT,ZA,EI,Q,T,A,Z)
      CALL DQG32(XL,VALIM,FCT,ZB,EI,Q,T,A,Z)
      CALL DQG32(VALIM,Q  ,FCT,ZC,EI,Q,T,A,Z)
      WQ=ZA+ZB+ZC
      WQT(L+N-1)=WQT(L+N-1)+WQ*WF(L)
      XX(L+N-1)=E(L)-Q
      J=L+N-1
C
C THE DISTRIBUTION FOR THE HISTOGRAM CORRESPONDING TO THE
C    CENTER OF THE BEAM DISTRIBUTION IS REMOVED AND STORED IN
C    WUF AND XUF AS THE UNFOLDED COUNTS AND ENERGY
C    RESPECTIVELY.
C
      IF(L.NE.ICENT)GOTO1005
      WUF(N)=WQ
      XUF(N)=EI-Q
      K=N
      GOTO 1005
 1006 CONTINUE
      DO 1717 I=1,7
C
C ELIMINATE LOW NUMBERED "BINS" AS THEY ARE ONLY PARTLY FIL-
C    LED AND ARE NOT REPRESENTATIVE OF THE CUMULATIVE
C    DISTRIBUTION.
C
      WUF(I)=WUF(8)
 1717 WQT(I)=WQT(8)
      DO 6 I=1,4
    6 T3(I)=T6(I)
      GOTO 779
  777 DO778 N=1,K
C
C PROCESS THE UNFOLDED THEORY CURVE.  SETTING EXX(1) EQUAL
C    TO ZERO ALLOWS PLOTTING OF THIS THEORY CURVE WITHOUT ANY
C    EXPERIMENTAL DATA.
C
      WQT(N)=WUF(N)
      XX(N)=XUF(N)
      KSIG=1
      J=K
  778 CONTINUE
      EXX(1)=0
      DO 5 I=1,4
    5 T3(I)=T5(I)
  779 WQTMX=0
      DO1007 N=3,J
C
C DETERMINE THE MAXIMUM POINT OF THE DISTRIBUTION, WQTMX,
C    AND THUS ESTABLISH THE MOST PROBABLE ENERGY LOSS, QP.
C
      IF(WQT(N).LE.WQT(N-1).AND.WQT(N-1).GE.WQT(N-2))
     1GOTO1008
      GOTO 1007
 1008 IF(WQT(N-1).LT.WQTMX)GOTO 1007
      WQTMX=WQT(N-1)
      EI=TEMP
      QP=EI-XX(N-1)
 1007 CONTINUE
C
C NORMALIZE ALL POINTS OF DISTRIBUTION AND STORE IN HW.
```

```
      DO 1009 M=1,J
      HW(M)=WQT(M)/WQTMX
 1009 CONTINUE
      J=J-1
      HWI=0
C DETERMINE HALFWIDTH OF THE THEORETICAL DISTRIBUTION, HWA.
      DO 1010 M=1,J
      IF(HW(M+1).GT..5.AND.HW(M).LT..5)HWI=XX(M)+(.5-
     1HW(M))*DELX/(HW(M+1)-HW(M))
      IF(M.EQ.J.AND.HWI.EQ.0)GOTO119
      GOTO121
  119 WRITE(6,20)
      HWA=0
      GOTO1010
   20 FORMAT(/,2X,'NO HALFWIDTH OBTAINED')
  121 IF(HW(M).GT..5.AND.HW(M+1).LT..5)HWA=XX(M)+(HW(M)
     1-.5)*DELX/(HW(M)-HW(M+1))-HWI
 1010 CONTINUE
C
C ESTABLISH CUTOFF SIGNAL FOR PLOTTING SUBROUTINE.
C
      XX(J+1)=0
C
C ESTABLISH CORRECT GRAPH TITLES FOR ABSORBER USED.
C
      IF(Z.GT.13.1)GOTO29
      DO 3 I=1,4
    3 T2(I)=T3(I)
      GOTO1011
   29 IF(Z.GT.29.1)GOTO50
      DO 10I=1,4
   10 T2(I)=T10(I)
      GOTO1011
   50 IF(Z.GT.50.1)GOTO64
      DO 8 I=1,4
    8 T2(I)=T8 (I)
      GOTO1011
   64 IF(Z.GT.64.1)GOTO82
      DO 9 I=1,4
    9 T2(I)=T9 (I)
      GOTO1011
   82 DO 7 I=1,4
    7 T2(I)=T7 (I)
C
C SEND DATA TO PLOTTING SUBROUTINE FOR PROCESSING.
C
 1011 CALL GRAPH(XX,WQT,EXX,EXY,T4,T3,T2,T1,HWA,EI,T,
     1CORR,CTSNOR,QP)
C
C PRINT RESULTS OF COMPUTATIONS IN TABULAR FORM.
C
      WRITE(6,22) QP,HWA,T,Z,EI
      IF(KSIG.EQ.0) GOTO 777
   11 FORMAT(7F10.0)
   22 FORMAT(/,2X,' QP: ',F7.4,' HALF WIDTH: ',F6.3,
     1' T(GM/SQ-CM): ',F6.4,' Z: ',F4.0,' INCIDENT ENERGY: '
     2,F6.2,/)
      STOP
      END
C
C
C
C
C
C
C
C
C
C
C
C
C
```

```
      SUBROUTINE DQG32(XL,XU,FCT,Y,EI,Q,T,D,Z)
C
C PURPOSE: THIS SUBROUTINE PERFORMS THE INTEGRATION REQUIRED
C    IN THE B-W THEORY.
C
      IMPLICIT REAL*8(A-H,O-Z)
      A=.5D0*(XU+XL)
      B=XU-XL
      C=.49863193092474078D0*B
      Y=.35093050047350483D-2*
     1(FCT((A+C),Z,D,T,EI,Q)+FCT((A-C),Z,D,T,EI,Q))
      C=.49280575577263417D0*B
      Y=Y+.8137197365452835D-2*
     1(FCT((A+C),Z,D,T,EI,Q)+FCT((A-C),Z,D,T,EI,Q))
      C=.48238112779375322D0*B
      Y=Y+.12696032654631030D-1*
     1(FCT((A+C),Z,D,T,EI,Q)+FCT((A-C),Z,D,T,EI,Q))
      C=.46745303796886984D0*B
      Y=Y+.17136931456510717D-1*
     1(FCT((A+C),Z,D,T,EI,Q)+FCT((A-C),Z,D,T,EI,Q))
      C=.44816057788302606D0*B
      Y=Y+.21417949011113340D-1*
     1(FCT((A+C),Z,D,T,EI,Q)+FCT((A-C),Z,D,T,EI,Q))
      C=.42468380686628499D0*B
      Y=Y+.25499029631188088D-1*
     1(FCT((A+C),Z,D,T,EI,Q)+FCT((A-C),Z,D,T,EI,Q))
      C=.39724189798397120D0*B
      Y=Y+.29342046739267774D-1*
     1(FCT((A+C),Z,D,T,EI,Q)+FCT((A-C),Z,D,T,EI,Q))
      C=.36609105937014484D0*B
      Y=Y+.32911111388180923D-1*
     1(FCT((A+C),Z,D,T,EI,Q)+FCT((A-C),Z,D,T,EI,Q))
      C=.33152213346510760D0*B
      Y=Y+.36172897054424253D-1*
     1(FCT((A+C),Z,D,T,EI,Q)+FCT((A-C),Z,D,T,EI,Q))
      C=.29385787862038116D0*B
      Y=Y+.39096947893535153D-1*
     1(FCT((A+C),Z,D,T,EI,Q)+FCT((A-C),Z,D,T,EI,Q))
      C=.25344995446611470D0*B
      Y=Y+.41655962113473378D-1*
     1(FCT((A+C),Z,D,T,EI,Q)+FCT((A-C),Z,D,T,EI,Q))
      C=.21067563806531767D0*B
      Y=Y+.43826046502201906D-1*
     1(FCT((A+C),Z,D,T,EI,Q)+FCT((A-C),Z,D,T,EI,Q))
      C=.16593430114106382D0*B
      Y=Y+.45586939347881942D-1*
     1(FCT((A+C),Z,D,T,EI,Q)+FCT((A-C),Z,D,T,EI,Q))
      C=.11964368112606854D0*B
      Y=Y+.46922199540402283D-1*
     1(FCT((A+C),Z,D,T,EI,Q)+FCT((A-C),Z,D,T,EI,Q))
      C=.7223598079139825D-1*B
      Y=Y+.47819360039637430D-1*
     1(FCT((A+C),Z,D,T,EI,Q)+FCT((A-C),Z,D,T,EI,Q))
      C=.24153832843869158D-1*B
      Y=B*(Y+.48270044257363900D-1*
     1(FCT((A+C),Z,D,T,EI,Q)+FCT((A-C),Z,D,T,EI,Q)))
      RETURN
      END
C
C
C
C
C
C
C
C
C
C
C
C
```

```
      REAL FUNCTION WION*8(X,EI,T,Z,A,Q )
C
C PURPOSE: THIS FUNCTION CALCULATES THAT PART OF THE ENERGY
C   DISTRIBUTION OF AN ELECTRON DUE TO LOSS OF ENERGY BY
C   IONIZATION WHILE PASSING THROUGH AN ABSORBER.
C
      IMPLICIT REAL*8(A-H,O-Z)
C
C IL ARE THE AVERAGE IONIZATION POTENTIALS PER ELECTRON FOR
C   LEAD FOR EACH SHELL, BEGINNING WITH THE K SHELL.
C
C NPOTL IS THE NUMBER OF IONIZATION POTENTIALS USED FOR LEAD
C
C IN THIS CONTEXT, L=LEAD, G=GADOLINIUM, S=TIN, C=COPPER,
C   AND A=ALUMINUM.
C
      REAL*8 IL(6)/.088000,.014700,.003200,.000490,
     1.000076,.000002/
      REAL*8 NL(6)/2.,8.,18.,32.,18.,4./
      REAL*8 IG(5)/.05024,.00795,.00189,.00024,.000025/
      REAL*8 NG(5)/2.,8.,18.,25.,9./
      REAL*8 IS(5)/.0292,.0044,.00072,.000062,.000001/
      REAL*8 NS(5)/2.,8.,18.,18.,4./
      REAL*8 IC(3)/.00898,.00099,.000068/
      REAL*8 NC(3)/2.,8.,18./
      REAL*8 IA(2)/.00156,.000088/
      REAL*8 NA(2)/2.,8./
      NPOTL=6
      NPOTG=5
      NPOTS=5
      NPOTC=3
      NPOTA=2
C
C SB IS THE SUMMATION OF IONIZATION POTENTIALS FOR THE
C   EXPERIMENTAL ATOM.
C
      SB=0.
C
C XMASE IS THE REST MASS OF AN ELECTRON IN MEV.
C
      XMASE=.511006
C
C BETA IS THE NORMAL V/C USED IN RELATIVISTIC CALCULATIONS.
C
C GAMMA IS THE NORMAL TERM USED IN RELATIVISTIC CALCULATIONS
C
      BETA=DSQRT((EI*EI+2.*EI*XMASE)/(EI*EI+2.*EI*XMASE
     1+XMASE*XMASE))
      GAMMA=1./(1.-BETA**2)**(1./2.)
C
C AT THIS POINT, THE PROGRAM MUST COMPUTE THE PROPER CON-
C   STANTS FOR THE EXPERIMENTAL Z.  A SERIES OF LOGIC STATE-
C   MENTS SELECT THE CORRECT FORMULAE.
C
   13 IF(Z.GT.13.1)GOTO29
C
C COMPUTE SB FOR EXPERIMENTAL Z.  B IS THE IONIZATION POTEN-
C   TIAL FROM ONE SHELL.
C
      DO 71 I=1,NPOTA
      B=IA(I)*NA(I)*DLOG(2.*EI/(IA(I)*(1.-BETA**2)))
   71 SB=SB+B
C
C ESTABLISH VALUES FOR B2 AND A1.  THESE ARE MATERIAL DE-
C   PENDENT CONSTANTS USED TO COMPUTE THE AVERAGE ENERGY
C   LOSS BY IONIZATION AND ARE SUPPLIED BY THE STERNHEIMER
C   PAPER.  THESE ARE B AND A, RESPECTIVELY, FROM HIS PAPER.
C
      B2=16.77
      A1=.0740
C
C DELT IS A PART OF THE EXPRESSION BY STERNHEIMER FOR THE
```

```
C    AVERAGE ENERGY LOSS DUE TO IONIZATION.  NUMBERS HEREIN
C    REPRESENT OTHER STERNHEIMER CONSTANTS AS FOLLOWS:
C        SMALL A    .0906
C        SMALL M    3.510
C        X1         3.000
C        -C         4.210
C
        DELT=4.606*DLOG10(BETA*GAMMA)-4.21+.0906*
      1(3.-DLOG10(BETA*GAMMA))**3.51
        GO TO 111
   29   IF(Z.GT.29.1)GOTO50
        DO 72 I=1,NPOTC
        B=IC(I)*NC(I)*DLOG(2.*EI/(IC(I)*(1.-BETA**2)))
   72   SB=SB+B
        B2=15.09
        A1=.0701
        DELT=4.606*DLOG10(BETA*GAMMA)-4.74+.1190*
      1(3.-DLOG10(BETA*GAMMA))**3.38
        GO TO 111
   50   IF(Z.GT.50.1)GOTO64
        DO 73 I=1,NPOTS
        B=IS(I)*NS(I)*DLOG(2.*EI/(IS(I)*(1.-BETA**2)))
   73   SB=SB+B
        B2=13.83
        A1=.0647
        DELT=4.606*DLOG10(BETA*GAMMA)-6.28+.404*(3.-
      1DLOG10(BETA*GAMMA))
      1**2.52
        GO TO 111
   64   IF(Z.GT.64.1)GOTO82
        DO 74 I=1,NPOTG
        B=IG(I)*NG(I)*DLOG(2.*EI/(IG(I)*(1.-BETA**2)))
   74   SB=SB+B
        B2=13.3
        A1=.0624
        DELT=4.606*DLOG10(BETA*GAMMA)-6.8+.418*(3.-
      1DLOG10(BETA*GAMMA))
      1**2.10
        GO TO 111
   82   IF(Z.GT.82.1)GOTO800
        DO 75 I=1,NPOTL
        B=IL(I)*NL(I)*DLOG(2.*EI/(IL(I)*(1.-BETA**2)))
   75   SB=SB+B
        B2=12.81
        A1=.0608
        DELT=4.606*DLOG10(BETA*GAMMA)-6.93+.0652*
      1(4.-DLOG10(BETA*GAMMA))**3.41
        GO TO 111
C
C  AR IS THE QUANTITY SMALL A, FROM BLUNCK AND WESTPHAL,
C    MULTIPLIED BY R, THE TARGET THICKNESS IN CENTIMETERS.
C
  111   AR=0.154*Z*T/A/BETA/BETA
C
C  COMPUTE BS2, THE SMALL B SQUARED FROM THE BLUNCK AND
C    LEISEGANG PAPER.
C
        BS2=3.*SB/(Z*AR)
C
C  VAR1, VAR2, AND VAR3 ARE CONVENIENCE STORAGE LOCATIONS
C    USED TO STORE COMPUTED PORTIONS OF STERNHEIMER'S AVERAGE
C    ENERGY LOSS.
C
        VAR1=A1*T/BETA**2
        VAR2=B2+.43+2.*DLOG(BETA*GAMMA)
        VAR3=DLOG(EI)-BETA**2
C
C  QAVE IS THE FINAL VALUE FOR THE AVERAGE ENERGY LOSS.
        QAVE=VAR1*(VAR2+VAR3-DELT)
        B1=DSQRT(BS2)
C
C  X IS THE PORTION OF SOME TOTAL ENERGY LOSS Q DUE TO
```

```
      REAL FUNCTION WRAD*8(X,EI,T,Z,A,Q)
C
C PURPOSE: THIS FUNCTION CALCULATES THAT PART OF THE ENERGY
C    DISTRIBUTION OF AN ELECTRON DUE TO LOSS OF ENERGY BY
C    RADIATION WHILE PASSING THROUGH AN ABSORBER.
C
      IMPLICIT REAL*8(A-H,O-Z)
C
C U IS AN INTERMEDIATE STORAGE LOCATION USED IN COMPUTING
C    ALPHA.
C
      U=183.0/Z**(1./3.0)
C
C COMPUTE VALUE OF ALPHA*R FOR TARGET THICKNESS, ATOMIC
C    NUMBER AND ATOMIC WEIGHT OF EXPERIMENTAL ABSORBER.  R IS
C    THE TARGET THICKNESS EXPRESSED IN CENTIMETERS.
C
      ALPHR=0.0014*T*Z*Z/A*(4.0/3.0*DLOG(U)+1.0/9.0)
C
C COMPUTE VALUE FOR B, A NORMALIZING CONSTANT.
C
      B=1./DGAMMA(ALPHR+1.)
C
C COMPUTE WRAD, THE NUMBER OF COUNTS EXPECTED AS A RESULT OF
C    RADIATION ENERGY LOSSES.  X REPRESENTS THAT PORTION OF
C    SOME TOTAL ENERGY LOSS Q WHICH IS NOT LOST BY IONIZATION
C
      WRAD=(B*ALPHR*(X**ALPHR)/(EI**ALPHR))/X
      RETURN
      END
C
C
C
C
C
C
C
C
C
C
C
C
      REAL FUNCTION BEAM*8(EI,HW,X)
      IMPLICIT REAL*8(A-H,O-Z)
      Y=2.
      ALFA=4.*DLOG(Y )/(HW*HW)
      BEAM=DEXP(-((X-EI)**2)*ALFA)
      RETURN
      END
C
C
C
C
C
C
C
C
C
C
C
C
C
      REAL FUNCTION FCT*8(X,Z,A,T,EI,Q)
C
C PURPOSE: THIS FUNCTION MULTIPLICATIVELY JOINS TOGETHER THE
C    PREDICTION OF ENERGY LOSS DUE TO IONIZATION AND THE LOSS
C    DUE TO RADIATION.
C
      IMPLICIT REAL*8(A-H,O-Z)
      FCT=WRAD(X,EI,T,Z,A,Q )*WION(X,EI,T,Z,A,Q )
      RETURN
      END
```

```
      SUBROUTINE GRAPH(THX,THY,EXX,EXY,T1,T2,T3,T4,HW,EI,T,
     1CORR,CTSNOR,QP)
C
C PURPOSE: THIS SUBROUTINE PLOTS THE RESULTS OF THEORY CAL-
C    CULATIONS AND EXPERIMENTAL RESULTS.
C
      IMPLICIT REAL*8(A-H,O-Z)
      REAL*8 TITLEX(1)/'MEV      '/
      REAL*8 TITLEY(3)/'NORMALIZED COUNTS       '/
      REAL*8 TITLEQ(2)/'BOX 13, EGY LOSS'/
      DIMENSION T1(4),T2(4),T3(4),T4(4),THX(200),THY(200),
     1EXX(200),EXY(200),CTSUP(200),CTSDN(200)
C
C DETERMINE SCALING FACTORS AND CHANGE DATA TO DISPLACEMENT
C
      X=8.
      Y=5.
      SIXIN=(EI-QP)*2.
      ISIXIN=SIXIN+.5
      SIXIN2=ISIXIN
      SIXIN=SIXIN2/2.
      IF(HW.EQ.0)GOTO90
      XNCR2=.5*HW
      INCR2=XNCR2+.5
      IF(INCR2.LT.1)INCR2=1
      XINCR2=INCR2
      XINCR=XINCR2/2.
      SP=SIXIN-6.*XINCR
      IF(SP.LT.0)GOTO90
      GOTO91
   90 SP=0
      INCR=(EI-1.5*T)/6.+.5
      XINCR=INCR
   91 N=0
      I=0
   20 I=I+1
      IF(EXX(I).GT.1.) GOTO21
      GOTO22
   21 N=N+1
      GOTO 20
   22 IF(N.EQ.0)GOTO100
      DO 23 J=1,N
      EXX(J)=(EXX(J)-SP)/XINCR+CORR/XINCR
      IF(J.EQ.N)GOTO23
   23 CONTINUE
  100 I=0
      M=0
   30 I=I+1
      IF(THX(I).GT.1.) GOTO 31
      GOTO32
   31 M=M+1
      GOTO30
   32 DO 33 J=1,M
      THX(J)=(THX(J)-SP)/XINCR
      IF(J.EQ.M)GOTO33
      IF(THY(J+1).GT.THY(J))THYMAX=THY(J+1)
   33 CONTINUE
      IF(N.EQ.0)GOTO101
      SCALE=4.
      IF(T.GT.4.8) SCALE=3.
      DO 40 J=1,N
      EXY(J)=EXY(J)/CTSNOR*SCALE
   40 CONTINUE
  101 DO 50 J=1,M
      SCALE=4.
      IF(T.GT.4.8) SCALE=3.
      THY(J)=THY(J)/THYMAX*SCALE
   50 CONTINUE
C
C SORT EXX AND ELIMINATE VALUES OFF GRAPH
```

```
      IF(N.EQ.0)GOTO102
      K=N-1
      DO 60 I=1,K
      IP1=I+1
      DO 60 J=IP1,N
      IF(EXX(I).LE.EXX(J)) GOTO 60
      TEMP=EXX(I)
      TEM=EXY(I)
      EXX(I)=EXX(J)
      EXY(I)=EXY(J)
      EXX(J)=TEMP
      EXY(J)=TEM
   60 CONTINUE
      J=0
      KK=0
      K=N
      DO 61 I=1,K
      IF(KK.EQ.1)GOTO61
      IF(EXX(I).LT.0)GOTO61
      J=J+1
      N=J
      EXX(J)=EXX(I)
      EXY(J)=EXY(I)
      IF(EXX(J).GT.X)GOTO62
      GOTO 61
   62 N=J-1
      KK=1
   61 CONTINUE
  102 KK=0
      J=0
      K=M
      DO 71 I=1,K
      IF(KK.EQ.1)GOTO71
      IF(THX(I).LT.0)GOTO71
      J=J+1
      M=J
      THX(J)=THX(I)
      THY(J)=THY(I)
      IF(THX(I).GT.X)GOTO72
      GOTO71
   72 M=J-1
      KK=1
   71 CONTINUE
C
C DETERMINE ERROR BAR MAGNITUDE
C
      IF(N.EQ.0)GOTO103
      DO 700 I=1,N
      CTSDN(I)=EXY(I)-DSQRT(EXY(I)*200.)/200.
      CTSUP(I)=EXY(I)+DSQRT(EXY(I)*200.)/200.
  700 CONTINUE
C
C INITIALIZE PLOT AND WRITE IDENTIFICATION
C
  103 CALL PLOTS
      CALL SYMBOL(0.,0.,.28,TITLE0,0.,16)
      CALL PLOT(0.,2.,-3)
C
C DRAW OUTLINE OF GRAPH
C
      Z=0
      CALL PLOT(Z,Y,2)
      CALL PLOT(X,Y,2)
      CALL PLOT(X,Z,2)
      CALL PLOT(Z,Z,2)
C
C DRAW OUTLINE OF TITLE BOX
C
      B1=.4
      B2=4.4
      B3=3.54
      B4=4.6
```

```
      B5=B1+.1
      B6=B3+.1
      CALL PLOT(B1,B3,3)
      CALL PLOT(B2,B3,2)
      CALL PLOT(B2,B4,2)
      CALL PLOT(B1,B4,2)
      CALL PLOT(B1,B3,2)
      CALL SYMBOL(B5,B6,.14,     T1,0.0,32)
      B5=B5+.24
      CALL NUMBER(B5,B6,.14,T,0.0,3)
      B5=B5+1.32
      B6=B6+.1
      EXP=2.
      CALL NUMBER(B5,B6,.07,EXP,0.0,-1)
      B5=B5+1.20
      B6=B6-.1
      CALL NUMBER(B5,B6,.14,FI,0.0,2)
      B5=B5-2.76
      B6=B6+.24
      CALL SYMBOL(B5,B6,.14,     T2,0.0,32)
      IF(N.EQ.0)GOTO701
      B6=B6+.07
      B5=B5+.82
      B7=B5+.58
      CALL PLOT (B5,B6,3)
      CALL PLOT (B7,B6,2)
      B6=B6-.07
      B5=B5-.82
  701 B6=B6+.24
      CALL SYMBOL(B5,B6,.14,     T3,0.0,32)
      B6=B6+.24
      CALL SYMBOL(B5,B6,.14,     T4,0.0,32)
C
C PLOT TIC MARKS
C
      G=.1
      H=Y-.1
 1570 CALL PLOT(G,Y,3)
      CALL PLOT(G,H,2)
      G=G+.1
      IF (G.LE.X)GO TO 1570
      G=X-.1
      H=.1
 1580 CALL PLOT(G,H,3)
      CALL PLOT(G,0.,2)
      G=G-.1
      IF(G.GT.0.)GO TO 1580
      G=1.
      H=.2
 1670 CALL PLOT(G,H,3)
      CALL PLOT(G,0,2)
      G=G+1.
      IF(G.LT.X) GO TO 1670
      H=Y-.2
 1680 CALL PLOT(G,H,3)
      CALL PLOT(G,Y,2)
      G=G-1.
      IF(G.GT.0.) GO TO 1680
      G=.1
      H=Y-.1
 1571 CALL PLOT(G,H,3)
      CALL PLOT(0.,H,2)
      H=H-.1
      IF(H.GT.0.) GO TO 1571
      G=X-.1
      H=.1
 1581 CALL PLOT(G,H,3)
      CALL PLOT(X,H,2)
      H=H+.1
      IF(H.LT.Y) GO TO 1581
      G=X-.2
      H=Y-1.
```

```
 1671 CALL PLOT(G,H,3)
      CALL PLOT(X,H,2)
      H=H-1.
      IF(H.GT.0) GO TO 1671
      G=.2
      H=1.
 1681 CALL PLOT(G,H,3)
      CALL PLOT(0,H,2)
      H=H+1.
      IF(H.LT.Y) GO TO 1681
C
C LABEL AXIS
C
      CALL SYMBOL(3.5,-.6,.14,TITLEX,0,4)
      CALL SYMBOL(-.25,1.56,.14,TITLEY,90.,24)
C
C NUMBER ENERGY AXIS
C
 1050 G=-.28
      H=-.32
      FLO=SP
 1060 CALL NUMBER(G,H,.14,FLO,0,2)
      G=G+1.
      IF(G.GT.X) GO TO 1070
      FLO=FLO+XINCR
      GO TO 1060
C
C PLOT EXPERIMENTAL DATA
C
 1070 IF(N.EQ.0)GOTO104
      CALL LINE(EXX,EXY,N,2,-6)
C
C PLOT ERROR FLAGS
C
      DO 1010 I=1,N
      ES1=EXX(I)-.05
      ES2=EXX(I)+.05
      CALL PLOT(ES1,CTSUP(I),3)
      CALL PLOT(ES2,CTSUP(I),2)
      CALL PLOT(EXX(I),CTSUP(I),3)
      CALL PLOT(EXX(I),CTSDN(I),2)
      CALL PLOT(ES1,CTSDN(I),3)
      CALL PLOT(ES2,CTSDN(I),2)
 1010 CONTINUE
C
C PLOT THEORY CURVE
C
  104 CALL LINE(THX,THY,M,2,1)
C
C FINALIZE PLOT
C
      CALL PLOT(0.,8.,-3)
      CALL PLOTE
      RETURN
      END
```

BIBLIOGRAPHY

1. Blunck, O., and K. Westphal, Zeitschrift fur Physik, Vol. 130, page 641, (1951).
2. Landau, L., Journal of Physics, USSR, Vol. 8, page 201, (1944).
3. Eyges, L., Physical Review, Vol. 76, page 264, (1949); Vol. 77, page 81, (1950).
4. Bethe, H., and W. Heitler, Proc. Roy. Soc., London, Series A, Vol. 146, page 83, (1934).
5. Blunck, O., and S. Leisegang, Zeitschrift fur Physik, Vol. 128, page 500, (1950).
6. Breuer, H., Zeitschrift fur Physik, Vol. 180, page 209, (1964).
7. Bumiller, F. A., F. R. Buskirk, J. N. Dyer, and R. D. Miller, Zeitschrift fur Physik, Vol. 223, page 415, (1969).
8. Miller, R. D., Energy Loss of High Energy Electrons in Aluminum, Master's Thesis, Naval Postgraduate School, (1968).
9. Goodwin, J. C., Energy Loss of High Energy Electrons in Aluminum and Copper, Master's Thesis, Naval Postgraduate School, (1968).
10. DeLeuil, W. R., and J. B. Raynis, Energy Loss of High Energy Electrons in Aluminum, Copper, and Lead, Master's Thesis, Naval Postgraduate School, (1969).
11. Steinheimer, R. M., Physical Review, Vol. 88, page 851, (1952).
12. Steinheimer, R. M., Physical Review, Vol. 91, page 156, (1953).
13. Steinheimer, R. M., Physical Review, Vol. 109, page 511, (1956).
14. Kenaston, G. W., C. T. Luke, Jr., and W. C. Sones, A Multichannel Electron Detection System for Use in a Stabilized Magnetic Spectrometer, Master's Thesis, Naval Postgraduate School, (1965).

INITIAL DISTRIBUTION LIST

		No. Copies
1.	Defense Documentation Center Cameron Station Alexandria, Virginia 22314	2
2.	Library Naval Postgraduate School Monterey, California 93940	2
3.	Professor John N. Dyer Department of Physics, Code 61 Naval Postgraduate School Monterey, California 93940	10
4.	Major Michael L. Mosbrooker 16944 Hartland Street Van Nuys, California 91406	1
5.	Major David L. Sandquist 1019 Hacker Avenue Joliet, Illinois 60432	1

DOCUMENT CONTROL DATA - R & D

(Security classification of title, body of abstract and indexing annotation must be entered when the overall report is classified)

1. ORIGINATING ACTIVITY *(Corporate author)* Naval Postgraduate School Monterey, California 93940	2a. REPORT SECURITY CLASSIFICATION Unclassified 2b. GROUP

3. REPORT TITLE
Energy Loss of High Energy Electrons in Tin, Lead, and Gadolinium

4. DESCRIPTIVE NOTES *(Type of report and, inclusive dates)*
Master's Thesis, June 1970

5. AUTHOR(S) *(First name, middle initial, last name)*
Michael L. Mosbrooker
David L. Sandquist

6. REPORT DATE June 1970	7a. TOTAL NO. OF PAGES 81	7b. NO. OF REFS 14

8a. CONTRACT OR GRANT NO. N/A	9a. ORIGINATOR'S REPORT NUMBER(S) N/A
b. PROJECT NO. N/A	
c.	9b. OTHER REPORT NO(S) *(Any other numbers that may be assigned this report)* N/A
d.	

10. DISTRIBUTION STATEMENT
This document has been approved for public release and sale; its distribution is unlimited.

11. SUPPLEMENTARY NOTES	12. SPONSORING MILITARY ACTIVITY Naval Postgraduate School Monterey, California 93940

13. ABSTRACT

The LINAC at the Naval Postgraduate School, Monterey, was used to accelerate electrons to energies ranging from 52 to 92 MeV in order to study the energy distributions of high energy electrons before and after passing through layers of tin, gadolinium, and lead. The thickness of these materials ranged from 0.8 to 5.9 g/cm^2.

The most probable energy losses agreed with the theory of Blunck and Westphal for all materials used, while distribution half-widths agreed only for absorbers of thickness less than 3.0 g/cm^2. The thickness at which theory and experiment began to exhibit a noticeable discrepancy was found to be dependent on the atomic number of the material.

Where comparison was possible, results of this experiment generally agreed with the findings of similar works concluded previously.

KEY WORDS	LINK A		LINK B		LINK C	
	ROLE	WT	ROLE	WT	ROLE	WT
Energy loss in tin, lead, and gadolinium						
Half-width						
Energy distribution						
Most probable energy losses						

27 AUG 74 22483

Thesis 121629
M8405 Mosbrooker
c.1 Energy loss of high energy electrons in tin, lead, and gadolinium.
27 AUG 74 22483

Thesis 121629
M8405 Mosbrooker
c.1 Energy loss of high energy electrons in tin, lead, and gadolinium.

thesM8405
Energy loss of high energy electrons in
3 2768 001 91740 4
DUDLEY KNOX LIBRARY